

Abishana Saravani

# Rheological Characterization of Alginate- Based Hydrogels for Tissue Engineering Applications

Master's thesis in Chemical Engineering and Biotechnology

Supervisor: Berit L. Strand

Co-supervisor: Catherine T. Nordgård

June 2023



Abishana Saravani

# **Rheological Characterization of Alginate- Based Hydrogels for Tissue Engineering Applications**

Master's thesis in Chemical Engineering and Biotechnology  
Supervisor: Berit L. Strand  
Co-supervisor: Catherine T. Nordgård  
June 2023

Norwegian University of Science and Technology  
Faculty of Natural Sciences  
Department of Biotechnology and Food Science





Abishana Saravani

# **Rheological Characterization of Alginate-Based Hydrogels for Tissue Engineering Applications**

A Study on Characterizing the Viscoelastic Properties in Alginate, Alginate/Sulfated Alginate and Alginate/Fucoidan Hydrogels

Master's thesis in Chemical Engineering and Biotechnology  
Supervisor: Berit L. Strand  
Co-supervisor: Catherine T. Nordgård  
June 2023

Norwegian University of Science and Technology  
Faculty of Natural Sciences  
Department of Biotechnology and Food Science





## ABSTRACT

The field of tissue engineering is aiming to combine scaffolds, cells, and biologically active molecules into functional tissues. In recent years, there has been a growing interest in the use of hydrogels for tissue engineering due to their tunable physical and biochemical properties. Alginate is a linear co-polymer consisting of two monosaccharides,  $\beta$ -D-mannuronic acid (M) and  $\alpha$ -L-guluronic acid (G) and form a hydrogel under mild conditions. Alginate hydrogels also meets the requirements for a scaffold, in terms of mechanical strength and being biocompatible. On the downside, the inability to interact with cells and proteins poses a disadvantage when alginate is used in tissue engineering. A way of functionalizing alginate toward cell interactions, is chemically modifying the structure with sulfate groups to produce sulfate alginate. Sulfated alginate have structural and functional similarities to sulfated glycosaminoglycans (GAGs) found in the extracellular matrix (ECM). Fucoidan is a sulfated polysaccharide that could also provide a structural and functional similarity to the sulfated GAGs.

This study aims to evaluate the mechanical properties of alginate, alginate/sulfated alginate and alginate/fucoidan gels for tissue engineering applications, in terms of elastic modulus and Young's modulus. Subjecting LF200S and UP-MVG alginate to formamide and  $\text{HClSO}_3$  yielded sulfated alginate with a degree of sulfation (DS) of 0.71 and 0.55, respectively. SEC-MALLS analysis of the sulfated alginates revealed that depolymerization had occurred, resulting in  $M_w$  of 68.8 kDa and 119.9 kDa, respectively. Initial rheological measurements with alginate gel gelled and stored with  $\text{CaCl}_2$ -solution indicated that when excess  $\text{Ca}^{2+}$ -ions are present, the elastic modulus is altered significantly with reducing gap. This hampers the quality of the data produced from these measurements. To limit the alteration  $G'$ , due to additional  $\text{Ca}^{2+}$  cross-links, NaCl was utilized as the storing solution. The rheological data obtained for 80/20 alginate/sulfated alginate gel and 80/20 alginate/fucoidan gel revealed to obtain a realistic value for elastic modulus for samples with  $\text{CaCl}_2$  as gelling solution and NaCl as storing solution. The rheological data for alginate gels under the same condition, demonstrated that the normal force acted as an artifact causing a steep increase in elastic modulus with reducing gap. To counteract the effect of induced stiffness in alginate gels, the hold time increased, which resulted in a more realistic value for the elastic modulus. The elastic modulus was determined to be 5441 Pa for alginate gels,  $5702 \pm 1218$  Pa for 80/20 alginate/sulfated alginate gels and  $4314 \pm 1274$  Pa for 80/20 alginate/fucoidan gels. The Young's modulus was calculated to be 11191 Pa for alginate gel,  $26572 \pm 3420$  Pa for alginate/sulfated alginate gels and  $28389 \pm 6934$  Pa for alginate/fucoidan gels. The findings of this study highlight that dependable rheological data is obtained for alginate gels with a smaller sample volume. This bears significance for accurately characterizing the rheological properties of hydrogels containing valuable materials.

## SAMMENDRAG

Feltet vevsteknikk har som mål å erstatte eller reparere skadet vev eller organer, ved å kombinere materialer, celler og biologisk aktive molekyler for å danne funksjonelle vev. De siste årene har det vært en økende interesse for bruk av hydrogeler i vevsteknikk på grunn av deres justerbare fysiske og biokjemiske egenskaper. Alginat er et lineært polymer bestående av to monosakkarider,  $\beta$ -D-mannuronsyre (M) og  $\alpha$ -L-guluronsyre (G), som danner en hydrogel under fysiologiske forhold. Alginat hydrogeler oppfyller kravene til materialer som brukes i vevsteknikk med hensyn til mekanisk styrke og biokompatibilitet. Imidlertid, en ulempe med bruk av alginat i vevsteknikk er mangelen på interaksjon med celler og proteiner. En måte å funksjonalisere alginat for å fremme celleinteraksjoner, er å kjemisk modifisere strukturen for å danne sulfatert alginat. Sulfatert alginat har strukturelle og funksjonelle likheter som sulfaterte glykosaminoglykaner (GAGer) som finnes i den ekstracellulære matrisen (ECM). Fukoidan er en sulfatert polymer som kan potensielt ha samme funksjon som sulfatert proteiner funnet i ECM.

Målet for dette studie er å evaluere de mekaniske egenskapene til alginat, alginat/sulfatert alginat og alginat/fukoidan-geler for anvendelser innen vevsteknikk, med hensyn til elastisk modulus og Young's modulus. I tillegg evaluere kvaliteten på dataene som produseres når målingene utføres på et betydelig lavt volum. Ved å behandle LF200S- og UP-MVG-alginat med formamid og  $\text{HClSO}_3$  ble det dannet sulfatert alginat med en sulfateringsgrad (DS) på henholdsvis 0,71 og 0,55. SEC-MALLS-analyse av de sulfaterte alginatene antydte til en høyere grad av depolymerisering i LF200S alginat, i forhold til UP-MVG alginat, med resulterende  $M_w$  på 68,8 kDa og 119,9 kDa, henholdsvis. Reologiske målinger av alginatgeler lagret i  $\text{CaCl}_2$  løsning viste tydelige endringer i den elastiske modulusen når det var et overskudd av  $\text{Ca}^{2+}$ -ioner til stede med minkende gap mellom platene. For å motvirke effekten av ytterligere  $\text{Ca}^{2+}$ -kryss bindinger ble NaCl løsning brukt som lagringsløsning. Dataene for 80/20 alginat/sulfatert alginat gel og 80/20 alginat/fukoidan lagret i NaCl løsning gel viste til at en realistisk verdi for elastisk modulus kunne oppnås, og at dataene kunne reproduseres. Når samme målinger ble utført på alginat gel under de samme forholdene, ble det observert at normalkraften fungerte som en artifakt som forårsaket en tydelig økning i den elastiske modulusen, med minkende gap mellom platene. For å motvirke effekten av indusert stivhet i alginat geler ble tiden mellom hver frekvenssveip økt. Dataen hentet fra disse målingene viste til en mer realistisk verdi for elastisk modulus. Elastisk modulus for alginatgeler ble bestemt til å være 5441 Pa, for 80/20 alginat/sulfatert alginat  $5702 \pm 1218$  Pa og  $4314 \pm 1274$  Pa for 80/20 alginat/fukoidan-geler. Youngs modulus ble beregnet til å være 11191 Pa for alginat gel,  $26572 \pm 3420$  Pa for 80/20 alginat/sulfatert alginat geller og  $28389 \pm 6934$  Pa for alginat/fukoidan geller.



## PREFACE

The work described in this project was carried out at the Department of Biotechnology and Food Science at the Norwegian University of Science and Technology.

I express my gratitude towards Professor Berit Løkensgard Strand and Associate Professor Catherine Taylor Nordgård, my supervisors, for providing me with the chance to work on this master thesis and for their invaluable guidance throughout the research and writing process. Further, I want to thank Postdoctoral fellow Joachim S. Kjesbu for his help in preparation and characterizing of sulfated alginate. A great thanks goes to Senior Engineers Olav Andreas Aarstad for running the SEC-MALLS analysis and Wenche I. Strand for all their technical support. Lastly, I want to thank my family for all their love and support.

NTNU, Trondheim  
Abishana Saravani

# CONTENTS

<b>Abstract</b>	<b>i</b>
<b>Abstract</b>	<b>i</b>
<b>Preface</b>	<b>ii</b>
<b>Contents</b>	<b>v</b>
<b>List of Figures</b>	<b>v</b>
<b>List of Tables</b>	<b>ix</b>
<b>Abbreviations</b>	<b>xi</b>
<b>1 Introduction</b>	<b>1</b>
1.1 Background . . . . .	1
1.2 The aims of the study . . . . .	2
<b>2 Theory</b>	<b>3</b>
2.1 Tissue engineering . . . . .	3
2.1.1 Cell encapsulation . . . . .	4
2.2 Alginate . . . . .	4
2.2.1 Gelling of alginate . . . . .	5
2.3 Sulfated alginate . . . . .	6
2.4 Fucoidan . . . . .	7
2.5 Rheology . . . . .	8
2.5.1 Viscoelasticity . . . . .	9
2.5.2 Rheometer . . . . .	10
2.5.3 Young's modulus . . . . .	11
2.6 Structural Characterization . . . . .	11
2.6.1 ICP-MS . . . . .	11
2.6.2 SEC-MALLS . . . . .	12
<b>3 Materials &amp; Methods</b>	<b>13</b>
3.1 Alginate . . . . .	13
3.2 Fucoidan . . . . .	13
3.3 Preparation of Sulfated Alginate . . . . .	13

3.4	Characterization of sulfated alginate . . . . .	14
3.5	Preparation of samples for gels . . . . .	14
3.6	Rheology . . . . .	15
3.6.1	Sequence 1: Alginate-based gels stored in $\text{CaCl}_2$ - solution . . . . .	16
3.6.2	Sequence 2: Alginate-based gels stored in NaCl solution . . . . .	16
3.6.3	Sequence 3: Alginate-based gels stored in NaCl solution with increased hold time . . . . .	17
<b>4</b>	<b>Results &amp; discussion</b>	<b>19</b>
4.1	Sulfatation of Alginate . . . . .	19
4.2	Rheological analysis of alginate gels stored in $\text{CaCl}_2$ -solution . . . . .	20
4.2.1	Evaluating syneresis in Alginate gels stored with $\text{CaCl}_2$ -solution . . . . .	20
4.2.2	Reproducibility of rheological data obtained for alginate gels in $\text{CaCl}_2$ -solution . . . . .	23
4.2.3	Dependence of elastic modulus in alginate gel stored in $\text{CaCl}_2$ on measuring height . . . . .	27
4.3	Rheological analysis of alginate/fucoidan gel in $\text{CaCl}_2$ -solution . . . . .	28
4.3.1	Evaluating syneresis in alginate/fucoidan gel . . . . .	29
4.3.2	Dependence of elastic modulus in alginate/fucoidan gel on measuring height . . . . .	33
4.4	Inhibiting additional $\text{Ca}^{2+}$ -crosslinks during reduction in measuring height: altering the storage solution . . . . .	34
4.4.1	Dependence of elastic modulus in alginate gels in alternative storing solution on measuring height . . . . .	36
4.5	Rheological analysis of alginate gels in NaCl solution . . . . .	37
4.5.1	Evaluating syneresis in alginate gels stored with NaCl solution . . . . .	37
4.5.2	Reproducibility of rheological data obtained for alginate gels in NaCl solution . . . . .	38
4.5.3	Dependence of elastic modulus in alginate gel stored in NaCl solution on measuring height. . . . .	42
4.6	Rheological analysis of alginate/sulfated alginate gels in NaCl solution . . . . .	44
4.6.1	Evaluating syneresis in alginate/sulfated alginate gels . . . . .	44
4.6.2	Reproducibility of the rheological data obtained for alginate/sulfated alginate gels stored with NaCl solution . . . . .	45
4.6.3	Dependence of elastic modulus in alginate/sulfated alginate gels stored in NaCl-solution on measuring height . . . . .	48
4.7	Rheological analysis of alginate/fucoidan gels stored in NaCl-solution . . . . .	49
4.7.1	Evaluating syneresis in alginate/fucoidan gel stored with NaCl-solution . . . . .	49
4.7.2	Reproducibility of the rheological data obtained for alginate/fucoidan gels . . . . .	52
4.7.3	Dependence of elastic modulus in alginate/fucoidan on measuring height . . . . .	55
4.8	Effective concentration . . . . .	57
4.9	Measuring height normal force relation . . . . .	59
4.10	Rheological analysis of alginate gels with increased hold time . . . . .	62
4.10.1	Evaluating syneresis in alginate gel with increased hold time . . . . .	62

4.10.2	Dependence of elastic modulus in alginate gel with increasing hold time On measuring height . . . . .	65
4.10.3	Driving factors for the rheological behavior in alginate gels . . . . .	65
4.11	Rheological analysis of alginate/sulfated alginate and alginate/fucoidan gels, with increased hold time . . . . .	67
4.12	Mechanical characterization of alginate-based gels . . . . .	70
4.12.1	Rheological characterization of alginate-based gels and calculation of Young's modulus . . . . .	70
4.13	Future work . . . . .	76
<b>5</b>	<b>Conclusions</b>	<b>79</b>
	<b>References</b>	<b>81</b>
A	Calculation of the degree of sulfation from elemental analysis data . . . . .	87
B	SEC-MALLS analysis of sulfated alginate . . . . .	88
C	Mechanical spectra for alginate-based gels . . . . .	89
C.1	Mechanical spectra for alginate gels in $\text{CaCl}_2$ -solution . . . . .	89
C.2	Mechanical spectra for Alginate/fucoidan gels in $\text{CaCl}_2$ -solution . . . . .	90
C.3	Mechanical spectra for alginate gels with alternative storing solution . . . . .	91
C.4	Mechanical spectra for alginate gels in $\text{Na}^+$ -solution . . . . .	92
C.5	Mechanical spectra for alginate/sulfated alginate gels in $\text{NaCl}$ -solution . . . . .	92
C.6	Mechanical spectra for alginate/fucoidan gels in $\text{NaCl}$ -solution . . . . .	94
D	Microdamage in Alginate Gels Stored with $\text{NaCl}$ -solution . . . . .	95
E	Young's modulus . . . . .	97

## LIST OF FIGURES

2.2.1 Structural characteristics of alginate: (a) alginate monomers: $\beta$ - D- manuronate (M) and $\alpha$ -L- guluronate (G). (b) The conformation of $\beta$ -D- mannuronic and $\alpha$ -L-guluronic acid residues in an alginate chain, showing how neighbouring G-residues form a cavity between them because of their diaxial linkage. (c) Sequential arrangement of M and G residues arranged in blockwise pattern. Retrieved from [4] . . . . .	5
2.2.2 Illustration of the "egg box model" gelation of alginate. Junction zones are formed by two facing G-sequences that each cross-links a ion e.g $\text{Ca}^{2+}$ that interacts with two adjacent G-residues, in addition to two G-residues in the opposing chain. Retrieved from [24] . . . . .	6
2.3.1 Published methods for chemical sulfation of alginate using different reagents. Retrieved from [7] . . . . .	7
2.4.1 The structural backbone of fucoidan, dominating of 1 $\rightarrow$ 3 (left) and 1 $\rightarrow$ 4 (right) glycosidic linkages. Retrieved from: [39] . . . . .	8
2.5.1 A parallel plate rheometer with two parallel plates. The bottom plate is stationary, while the top plate is moveable and cant exert a controlled force or displacement of the sample. Retrieved from [43]. . . . .	10
2.5.2 The difference between stress and strain during sinusoidal oscillation relays on the phase angle values, which is a measure of the amount of liquid and solid properties in a sample. Retrieved from [44] . . . . .	11
3.6.1 A schematic presentation of the experimental setup for the parallel rheometer. Sample (60 $\mu\text{L}$ ) was loaded to the lower geometry. The gap between the plates was adjusted to 1 mm. Gelling solution (2 mL) was added to the lower geometry. One hour of gelation occurred, before the gap between the plates was reduced by 0.01 mm stepwise. . . . .	15
4.2.1 Normal force as a function of measuring height for Alg-Ca(1) gel. 1.8 % (w/v) alginate solution (60 $\mu\text{L}$ ) was loaded to the lower geometry and the distance between the plates was set to 1 mm. 50 mM $\text{CaCl}_2$ (2mL) was added to the lower geometry for gelling. One hour of gelation occurred before the gap was reduced by 0.01 mm stepwise to a total reduction to 0.80 mm. . . . .	21

4.2.5	Frequency sweeps of Alg-Ca(3) gel at 0.91 mm. Elastic modulus (blue), viscous modulus (red) and phase angle (green) is plotted on y-axis against the frequency range on the x-axis for 1.8 % (w/v) alginate gel gelled with (50 mM) CaCl <sub>2</sub> -solution. All values are obtained from frequency sweeps (1-0.05 Hz) performed at 20°C, a constant shear strain at 0.1 % and 10 measurements per decade. . . . .	27
4.2.6	G' at 1 Hz (Pa) plotted against the gap height for Alg-Ca (1) gel (red), Alg-Ca(2) gel (blue) and Alg-Ca (3) gel (orange). Values for G' before establishing contact point is noted with a cross. . . . .	28
4.3.3	G' at 1 Hz (Pa) plotted against the gap height for Alg-Ca (1) gel (red), Alg-Ca(2) gel (blue) and Alg-Ca (3) gel (orange). Values for G' before establishing contact point is noted with a cross. . . . .	33
4.4.2	G' at 1 Hz (Pa) plotted against the gap height for Alg-Na (1) gel (red) and Alg-no solution gel (purple). . . . .	36
4.5.1	Frequency sweeps of Alg-Na (1) at 0.95 mm. Elastic modulus (blue), viscous modulus (red) and phase angle (green) is plotted on y-axis against the frequency on the x-axis for 1.8 % (w/v) alginate gel gelled with (50 mM) CaCl <sub>2</sub> solution and stored in NaCl solution. All values are obtained from frequency sweeps (1-0.05 Hz) performed at 20°C with 0.1 % constant shear strain and 10 measurements per decade . . . . .	37
4.5.4	Frequency sweeps of Alg-Na(2) at 0.94 mm. Elastic modulus (blue), viscous modulus (red) and phase angle (green) is plotted on y-axis against the frequency on the x-axis. For 1.8 % (w/v) alginate gel gelled with (50 mM) CaCl <sub>2</sub> solution. All values are obtained from frequency sweeps (1-0.05 Hz) performed at 20°C with 0.1 % constant shear strain, with 10 measurements per decade. . . . .	42
4.5.5	G' at 1 Hz (Pa) plotted against the gap height for Alg-Na (1) gel (red), Alg-Na(2) gel (blue) and Alg-Na (3) gel (orange). The values are from the first contact point with the gel and the measured G'-value, any value measured before that is noted with a cross. . . . .	43
4.6.1	Normal force as a function of measuring height for Alg/SA-Na(1) gel. Measurement was performed on 1.8 % (w/v) 80/20 alginate/sulfated alginate solution (60 μL) was loaded to the lower geometry and the distance between the plates was set to 1 mm. 50 mM CaCl <sub>2</sub> (2mL) was added to the lower geometry for gelling. One hour of gelation occurred before removing CaCl <sub>2</sub> solution and adding NaCl solution (2 mL) was added. The gap was reduced by 0.01 mm stepwise to a total reduction to 0.80 mm. . . . .	44
4.6.2	Frequency sweeps of Alg/SA-Na(1) gel at 0.96 mm. Elastic modulus (blue), viscous modulus (red) and phase angle (green) is plotted on y-axis against the frequency on the x-axis. Values are obtained for 1.8 % (w/v) 80/20 alginate/sulfated gelled with 50 (mM) CaCl <sub>2</sub> solution and stored in NaCl solution. Frequency sweep (1-0.05 Hz) was performed at 20°C with a constant shear strain at 0.1 %, with 10 measurements per decade. . . . .	45
4.6.5	G' at 1 Hz (Pa) plotted against the gap height for Alg/SA-Na (1) gel (red), Alg/SA-Na(2) gel (blue) and Alg/SA-Na (3) gel (orange). The values are from the first contact point with the gel and the measured G'-value, any value measured before that is noted with a cross. . . . .	48

4.7.1	Normal force as a function of measuring height for Alg/FD-Na(1) gel. Measurement was performed by loading 1.8 % (w/v) 80/20 alginate/sulfated alginate solution (60 $\mu$ L) the lower geometry and the distance between the plates was set to 1 mm. 50 mM $\text{CaCl}_2$ (2mL) was added to the lower geometry for gelling. One hour of gelation occurred before $\text{CaCl}_2$ solution was removed and NaCl solution (2 mL) was added. The gap was reduced by 0.01 mm stepwise to a total reduction to 0.80 mm. . . . .	50
4.7.5	Frequency sweeps of Alg/FD-Na(3) gel at 0.95 mm. Elastic modulus (blue), viscous modulus (red) and phase angle (green) is plotted on y-axis against the frequency on the x-axis, for 1.8 % (w/v) 80/20 alginate/sulfated gelled with 50 (mM) $\text{CaCl}_2$ solution and stored in NaCl solution (2 mL). Frequency sweeps (1-0.05 Hz) were performed at 20°C with a constant shear strain at 0.1 % and 10 measurements per decade. . . . .	55
4.7.6	$G'$ at 1 Hz (Pa) plotted against the gap height for Alg/FD-Na (1) gel (red), Alg/FD-Na(2) gel (blue) and Alg/FD-Na (3) gel (orange). The values are from the first contact point with the gel and the measured $G'$ -value, any value measured before that is noted with a cross. . . . .	56
4.9.2	A overview of normal force values at the start point of each measuring height plotted against the gap height (mm) for Alg-Na gels, Alg/SA-Na gels and Alg/FD-Na gels relative to each other. . . . .	61
4.10.1	Normal force as a function of measuring height for Alg/-Na(1 h). Measurements was performed on 1.8 % (w/v) alginate solution (60 $\mu$ L) was loaded to the lower geometry and the distance between the plates was set to 1 mm. 50 mM $\text{CaCl}_2$ (2mL) was added to the lower geometry for gelling. One hour of gelation occurred before $\text{CaCl}_2$ (2 mL) solution was removed and NaCl solution was added (2 mL). The gap was reduced by 0.01 mm stepwise, where one hour was waited before a new height reduction to a total reduction to 0.90 mm. . . . .	63
4.10.3	$G'$ obtained at 1 Hz at each height was plotted against the reducing gap for alginate gel with increased hold time. . . . .	65
4.12.1	The individual $G'$ values at 1 Hz for each measurements and the calculated mean and standard deviation for alginate gel, 80/20 alginate/sulfated alginate gels and 80/20 alginate/fucoidan gels, relative to each other. The values are obtained from frequency sweep (1-0.05 Hz) at 0.95 mm. . . . .	72
4.12.2	The individual calculated Young's modulus values for each measurements and the calculated mean and standard deviation for alginate gel, 80/20 alginate/sulfated alginate gels and 80/20 alginate/fucoidan gels, relative to each other. The values are obtained by performing a linear regression on the initial slope of the stress-strain curve at 0.95 mm.. . . .	73
A.1	Second degree polynomial curve for LF200S alginate. % S plotted against theoretical obtained DS values to estimate DS for the sample. . . . .	87
B.1	Molecular weight averages and dispersity of the UPV-MVG alginate and LFS200S alginate after sulfation and LF10/60 alginate strand used as standard. Green: LF10/60 Alginate standard, brown: UP-MVG sulfated and pink: LF200S sulfated. . . . .	88

E.1 Stress-strain curve for Alg-Na (1h) when the gap was reduced from 0.95 to 0.94. The stress (y-axis) is calculated by dividing the normal force/ area of the probe and is plotted against the strain (x-axis). . . . . 97



## LIST OF TABLES

3.1.1	Sequence characteristics and average molecular weight ( $M_w$ ) of alginates used in this project. . . . .	13
3.2.1	Type, source, composition, molecular weight ( $M_w$ ), and degree of sulfation (DS) for the fucoidan materials. . . . .	13
3.5.1	Final concentration (% (w/v)) of alginate hydrogels mixed with sulfated alginate or fucoidan. Total polymer concentration was 1.8 % (v/w) for all samples. . . . .	15
4.1.1	Calculated degree of sulfation (D.S) of sulfated alginates (LF200S & UP-MVG). . . . .	19
4.1.2	Number average molecular weight ( $M_n$ ), Molecular weight averages ( $M_w$ ) and polydispersity index for sulfated LF200S alginate and sulfated UP-MVG alginate after sulfation. . . . .	19
4.12.1	The individual $G'$ values at 1 Hz for each measurement and the calculated mean and standard deviation for alginate gel, 80/20 alginate/sulfated alginate gels and 80/20 alginate/fucoidan gels. The values are obtained from frequency sweep (1-0.05 Hz) at 0.95 mm. . . . .	71
4.12.2	The individual calculated Young's modulus for each measurements and the calculated mean and standard deviation for alginate gel, 80/20 alginate/sulfated alginate gels and 80/20 alginate/fucoidan gels. The values are obtained by performing a linear regression on the initial slope of the stress-strain curve at 0.95 mm. . . . .	73
E.1	Elastic modulus ( $G'$ ) obtained at 1 Hz by performing frequency sweep. In addition Young's modulus (E) was obtained by plotting the stress-strain relationship at 5 % gap reduction. . . . .	99
E.2	Elastic modulus ( $G'$ ) obtained at 1 Hz by performing frequency sweep. In addition Young's modulus (E) was obtained by plotting the stress-strain relationship at 5 % gap reduction. . . . .	100

## SYMBOLS & ABBREVIATIONS

$\delta$  Phase angle

$\epsilon$  Strain

$\sigma$  Stress

$\eta$  Viscosity

**Alg** Alginate

**DS** Degree of substitution

**E** The Young's modulus

**FD** Fucoidan

$G^*$  Complex modulus

$G'$  The elastic modulus

$G''$  The viscous modulus

**GAGs** Glycosaminoglycans

**G-unit**  $\alpha$ -L-Guluronic acid

**HA** Heparin Sulfate

$F_G$  Guluronic acid frequency

$F_M$  Mannuronic acid frequency

**ICP-MS** Inductively coupled plasma mass spectrometry

**M-unit**  $\beta$ -D-Mannuronic acid

$N_{G>1}$  Average length of G-blocks

**PFO** Pericapsular fibrotic overgrowth

**SA** Sulfated Alginate

**SEC-MALLS** Size exclusion chromatography coupled with multiangle laser light scattering

**% (w/v)** Weight/volume percentage – 1g / 100 mL



## INTRODUCTION

### 1.1 Background

In the last decade, modern techniques of transplanting tissue and organs from one individual into another have been revolutionary and lifesaving [1]. Transplantation from one individual into another, although very successful, has severe constraints. A significant challenge lies in obtaining sufficient amounts of tissue and organs to meet the needs of all patients requiring them. It is within this context that the field of tissue engineering has emerged [1]. The idea of tissue engineering is that new and functional tissue can be fabricated using living cells associated with a scaffolds guiding tissue development [2]. Over the past few years, there has been growing interest in the use of hydrogels for tissue engineering application due to their tunable physical and biochemical properties [2]. Hydrogels have several characteristic that are similar to those of the extracellular matrix (ECM) such as high water content and rapid diffusion of nutrients, oxygen and waste products [3].

Alginate is an attractive material for tissue engineering, because of its biocompatibility and the possibility of forming hydrogels under physiological conditions, in addition to exhibit a low immunogenic profile and being a nontoxic material [4] [5]. Cell anchorage is critical for the survival of many cell types and is also involved in cell migration proliferation, differentiation and apoptosis [6]. The hydrophilic surface of alginate hydrogels does not encourage cell adhesion. One way to improve the ability of alginate to interact biologically is by coupling cellular adhesion molecules such as fibronectin, collagen or laminin to the alginate [6]. Peptides such as the fibronectin-derived peptide arginin-glycine-aspartic acid (RGD) from ECM proteins coupled with alginate can also obtain biological activity [6]. An alternative approach to promote cell interaction is by chemically modifying alginate by sulfation. The ECM is rich in sulfated glycosaminoglycans (GAGs) that have vital roles in cell signaling and tissue homeostasis [7]. Heparin, a sulfated glycosaminoglycans, binds directly to several adhesion proteins and may thus indirectly provide anchor points for cell attachment [7] [8]. Sulfated alginate exhibit structural and functional similarities to sulfated glycosaminoglycans and may functionalize alginate toward cell- and protein interactions characteristics of sulfated GAGs [7]. There is a prospect that fucoidan from brown seed incorporated with alginate could have the same effect as sulfated alginate, in terms of functionalizing alginate towards cell interactions.

Natural ECMs are viscoelastic and ability of a substrate to either store (purely elastic)

or dissipate (viscoelastic) cellular forces could provide a powerful cue to interacting cells [9]. The ideal mechanical strength of the scaffold mimicking the ECM, should match the desired tissue as the mechanical properties of a hydrogel may effect the cellular mechanotransduction [2]. Which is the conversion of mechanical information from the microenvironment into biochemical signaling [10]. Cells can recognize and respond to mechanical forces of the surrounding environment, gradients of ligands and the topography of the tissues in which they reside [10]. Hydrogel mechanical properties are characterized by the elastic modulus ( $G'$ ) or Young's modulus ( $E$ ) [10]. The mechanical and rheological behavior of hydrogels has long been recognized as fundamentally important to understand the effect of using these materials for tissue engineering [10].

## 1.2 The aims of the study

The main objective for this thesis is to investigate the rheological properties of pure alginate gels and alginate gels when a part is substituted with sulfated alginate and fucoidan, with respect to its suitability as a tissue engineering material. This thesis has two main objectives which are outlined below.

First objective is to chemically modify alginate with chlorosulfonic acid to produce sulfated alginate, and characterize the material based of degree of sulfation and molecular weight.

Second objective is to understand factors that contribute to the rheological behavior in alginate-based gels. Understanding the driving factors for the rheological behavior of a gel is crucial for determining a realistic value for its elastic modulus. The obtained values will characterize the rheological properties of alginate, and the effect of substituting a fraction of alginate with sulfated alginate or fucoidan. The mechanical properties of alginate-based hydrogels, can be characterized by evaluating the elastic modulus and Young's modulus. The reliability of the rheological data obtained from measurements performed on a smaller sample volume should be evaluated. Being able to measure the rheological data on small volume sample is important for valuable material e.g. peptide grafted alginate.

## 2.1 Tissue engineering

Tissue engineering offers the potential to create functional tissues and organs in the laboratory, reducing the reliance on donor organs and providing a viable solution to meet the growing demand of organs and tissue[1]. New functional tissue can be fabricated using living cells associated with a scaffold guiding tissue development [1]. A scaffold create a three-dimensional structure or framework that serves as a support system for cells to grow, adhere, and organize themselves into functional tissues [11]. The materials used as scaffold must be biocompatible and accommodate for cell adhesion. Porosity and permeability of the material is important to allow for the diffusion of oxygen, nutrients and waste products [11]. In addition, the material should have suitable mechanical strength and stiffness to withstand physiological forces and provide mechanical cues for cells to align, differentiate and form functional tissue [1] [12].

There is a growing interest in utilizing hydrogels for tissue engineering applications [10]. This is due to their unique properties and versatility. A hydrogel is a three-dimensional network of hydrophilic polymers that can absorb and retain large amounts of water or biological fluids, resulting in a gel-like structure [10]. In addition, hydrogels are hydrophilic solid materials that do not dissolve in aqueous or physiological medium making them stable in physiological conditions, making hydrogels an attractive material in the field of tissue engineering as they have physical properties similar to many tissues [10]. Alginate is one of the natural polymers used to create hydrogels in tissue engineering. Alginate possesses some interesting features like gelation, film formation and thickening ability of solutions [13]. Where the ability to form a gentle hydrogel under physiological conditions makes it suitable for application in tissue engineering, to facilitate the development of new tissue growth. However, despite such unique characteristics, alginate has some limitations to develop the scaffold system [13]. The hydrophilic surface and lack of cell interaction limit cell attachment, differentiation and proliferation [13]. Hence scaffold alginate mixed with other natural polymer like collagen or chitosan, or synthetic peptides or any cellular materials is often used to promote cell interaction [13].

### 2.1.1 Cell encapsulation

This part is retrived from my specialization project [14].

Hydrogels provide a suitable environment for cell encapsulation [10]. Cells can be embedded within the hydrogel matrix, protecting them from mechanical stresses and immune responses [15]. This encapsulation can enhance cell survival, promote their differentiation, and facilitate the formation of tissue-like structures [16]. Cell encapsulation have been proposed as an alternative approach to treat diseases, since they allow localized and controlled delivery of therapeutic cells to specific physiological sites to restore the lost function and protection from potential hazardous processes in a physiological environment[17] [16]. The cells are immobilized within a semipermeable membrane that forms a three-dimensional hydrogel environment to enhance cell-cell interaction and maintain cell function [17]. Diabetes type 1 is a autoimmune disease where the immune system attacks the body's own beta-cells that produces insulin needed to regulate the blood glucose. Cell encapsulation is a functional way to cure autoimmune diseases like diabetes type 1 [18], by enveloping the cell in artificial, partially permeable membrane that potentially allows the grafting of the cells without using immunosuppressant drugs [17].

## 2.2 Alginate

Alginate is an unbranched anionic biopolymer consisting of 1,4- $\beta$ -D-mannuronic acid (M) and 1,4- $\alpha$ -L-guluronic acid (G) monomers [19]. Alginate is synthesized as a homopolymer of mannuronic acid before conversion of M residues to G residues occurs, by mannuronan C-5 epimerases inverting the stereocenter at C-5 [4]. Alginate do not consist of regular repeating unit, and it is described as a binary copolymer of 1 $\rightarrow$ 4-linked M and G residues arranged in blockwise pattern. The sequential arrangement of M and G, together with the molecular weight, determines to a great extent the properties of the alginate [20] [15]. M-blocks follows a ribbonlike chain conformation due to the diequatorial linkages connecting mannuronic acid residues. G-blocks have a buckled and rigid structure, due to the diaxially linked guluronic acid residues. The diaxially linked residues originate for specific ion binding and gel formation [21]. The MG-block consist of alternating axial-equatorial and equatorial-axial glycosidic bonds connecting residues. The variation between the bond leads to greater flexibility of the MG-block compared to other sequences [22]. Figure 2.2.1 present the structure of alginate with the monomer units, fragment of the polysaccharide chain with different MG sequences and M and G blocks distribution in the alginate chain.





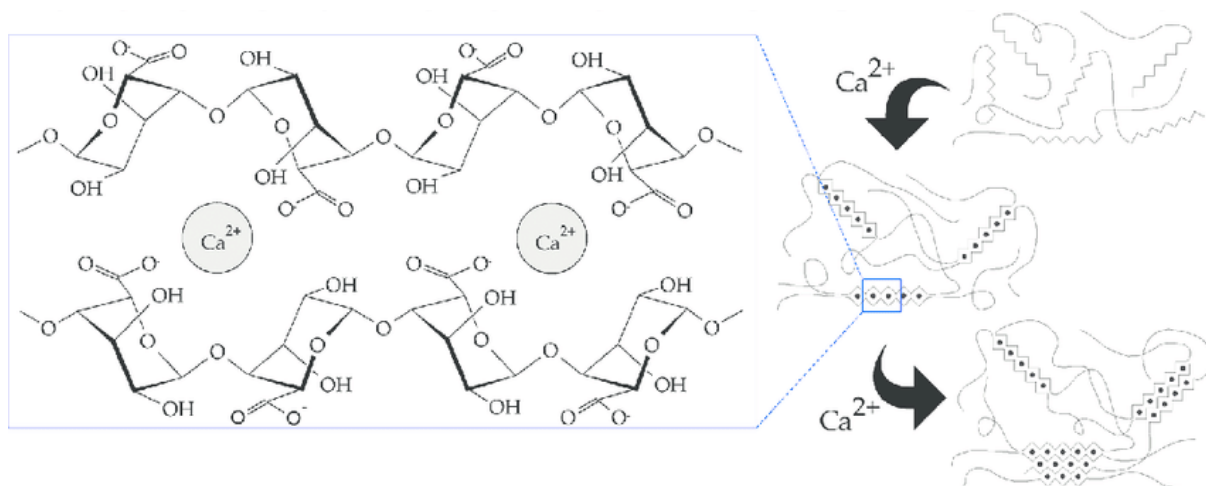


Figure 2.2.2: Illustration of the "egg box model" gelation of alginate. Junction zones are formed by two facing G-sequences that each cross-links a ion e.g  $\text{Ca}^{2+}$  that interacts with two adjacent G-residues, in addition to two G-residues in the opposing chain. Retrieved from [24]

Two different approaches are used to obtain calcium-alginate gels. The diffusion method is characterized by allowing a cross-linking ion (e.g  $\text{Ca}^{2+}$ ) to diffuse into the alginate solution from a larger external reservoir [25]. When divalent metal ions diffuse into an alginate solution, the rapid ion binding and formation of a network produce an inwardly moving gelling zone. Alginate will diffuse towards this gelling zone from the center of the gel [20]. Diffusion setting is characterized by rapid gelling kinetics, and is utilized for immobilization purposes [25]. While an external gelation is the preferred method for immobilization purposes, internal gelation can be used to obtain a more homogenous gel when this is desirable [26] [27]. In internal gelation, complexed calcium or calcium-salts, like  $\text{CaCO}_3$  of low solubility is mixed into the alginate solution with glucono- $\delta$ -lactone (GDL). GDL is a slow hydrolyzing acid that allows a slow and controlled release of  $\text{Ca}^{2+}$ -ions which results in gelation [28]. When  $\text{CaCO}_3$  and GDL is used for internal gelation, homogenous alginate gels are formed over a wide range of pH, leaving the non-toxic by-products  $\text{CO}_2$  and D-gluconic acid behind [28].

Syneresis refers to the process where a gel undergoes contraction and releases liquid [29]. Previous research demonstrate that alginate gels gelled with  $\text{Ca}^{2+}$ -ions are prone to syneresis. During gel formation of alginate hydrogel, negatively charged carboxylate groups ( $\text{COO}^-$ ) of alginate interacts with cations (e.g  $\text{Ca}^{2+}$ ) that results in shrinkage of the hydrogel [30], as a consequence of the electrostatic attraction. This may result in exudation of water from the gel network, leading to a higher concentration of alginate in the gels.

## 2.3 Sulfated alginate

The free hydroxyl group of alginate can be chemically sulfated to facilitate electrostatic interaction with a range of proteins and other cationic surfaces in a manner similar to sulfated glycosaminoglycans (GAGs) such as heparin sulfate (HS) and heparin [7]. Methods for chemically modifying alginate is presented in Figure 2.3.1. Sulfated alginate exhibit

biological properties like anticoagulation and particularly influence the intrinsic pathway, compared to unmodified alginate [8]. These properties are analogous to naturally occurring highly negatively charged linear glycosaminoglycan heparin, that is widely used as an anticoagulant [31].

Sulfated polysaccharides generally have more complex interactions with the immune system, resulting in a variety of interlinked pro- and anti-inflammatory responses. Introduction of charged and relatively bulky substituent, will notably alter the chemical structure of alginate that may alter inherent properties such as solubility or gelation [7]. Sulfation of alginate has a declining effect on the gelling ability of alginates; where the resulting gels have a lower stiffness and increased rate of swelling and destabilization compared with unmodified alginate [7]. Negatively charged sulfate groups do associate with divalent cations through electrostatic interactions, but disrupt the long G-blocks that are responsible for the cooperative binding of ions and forming of cross-linking junction zones in the gel network [31][7].

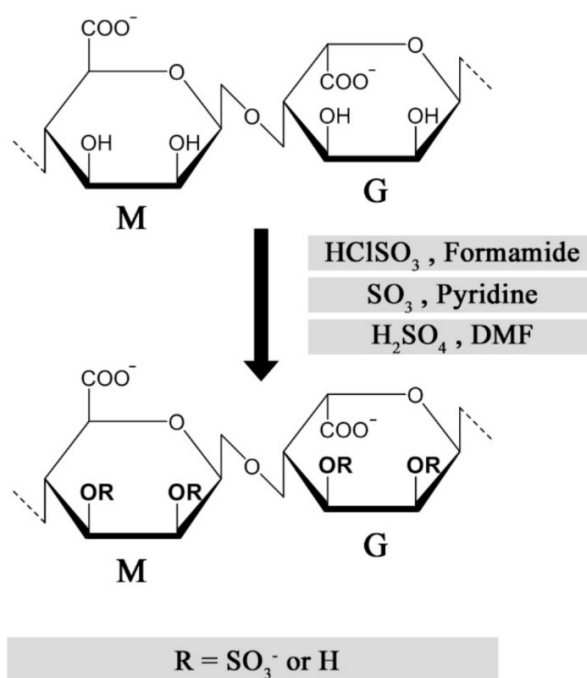


Figure 2.3.1: Published methods for chemical sulfation of alginate using different reagents. Retrieved from [7]

## 2.4 Fucoidan

Fucoidans are a diverse class of sulfated polysaccharides integral to the cell wall of brown algae [32]. Depending on the species, the structure of fucoidan varies in terms of composition, glycosidic linkages, branching and degree of sulfation and acetylation [33] [34]. Fucoidans are therefore classified into homofucans and heterofucans. Homofucans have a backbone of  $\alpha$ -1,3 L-fucose with sulfate groups mainly at C2 and C4. Heterofucans have an alternating  $\alpha$ -1,3/ $\alpha$ -1,4 linked L-fucose sulfated at C2 or C3 [32] [34]. Homofucans have branches of fucose and/or galactose, glucuronic acids, xylose, mannose and acetate.

While heterofucans have a non-fucose backbone with galactose or glucuronic acid with a side branches of sulfated fucose [35] [33]. The structural backbone of fucoidan is presented in Figure 2.4.1.

Fucoidan are of high pharmaceutical interest as they display anticoagulant, antiviral, antitumor and immune-inflammatory bioactivtites [32] [36]. For instance the activated partial thromoplastin time (APTT) assay showed that fucoidan induced anticoagulant activity in a dose dependent manner [37], making fucoidan a promising candidate for pharmacological use. Fucoidans are generally a water-soluble molecule with lower viscosity relative to alginate. In addition, fucoidan lack gelling properties and do not form hydrogels with divalent ions on its own [38].

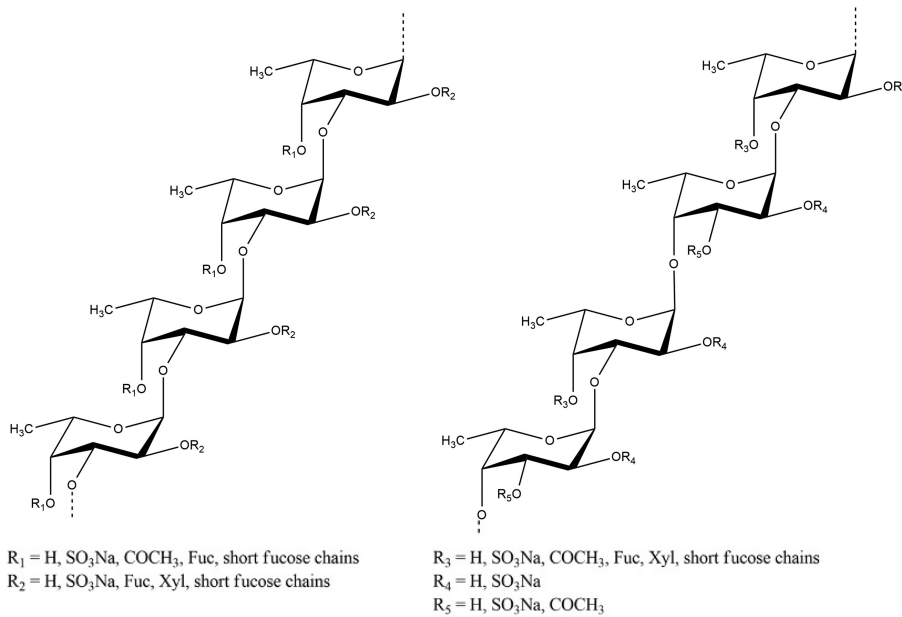


Figure 2.4.1: The structural backbone of fucoidan, dominating of 1→3 (left) and 1→4 (right) glycosidic linkages. Retrieved from: [39]

## 2.5 Rheology

Rheology is the study of how materials deform when forces are applied to them [40]. The amount of deformation will depend upon the area over which the force acts and is defined as stress. Stress is the measure of an external force acting over the cross sectional area of an object.

$$\sigma = \frac{F}{A} \quad (2.1)$$

Stress has units of force per area, such as newtons per square meter (N/m<sup>2</sup>) or pascal (Pa) [40].

The amount of deformation is measured as strain induced. Strain represents the

displacement between particles in the body relative to a reference length [41].

$$\epsilon = \frac{\delta}{l} \quad (2.2)$$

A material can deform in two ideal ways depending on their properties [42]. The differentiation between liquids and solids can be determined based on the behavior exhibited by the material when stress is applied [40]. Ideal materials exhibit purely elastic deformation. This implies that when stress is applied, the material will deform and remain in that state until the force is removed and return to its native state once the stress is removed [40]. This kind of perfectly recoverable deformation is called elastic, as the energy or work that was done to produce the deformation is stored within the deformed material and is recoverable once the force is removed [41].

When a force is applied, an ideal liquid will deform without limit for as long as the force is applied and remain in the deformed state after the force is removed. The extent of deformation is not limited and the rate at which the liquid will deform and flow is determined by the magnitude of the force [42]. Viscosity ( $\eta$ ) is the primary property that dictate the deformation of liquid and is defined as the ratio of force to rate of deformation [40].

### 2.5.1 Viscoelasticity

Real materials exhibit both elastic and viscous responses when deformation is applied and are therefore categorized as viscoelastic materials [41]. They are also often highly anisotropic meaning that the material exhibit different viscoelastic properties in different directions. Viscoelastic properties of a material could be quantified with rheological experiments. Rheological information for viscoelastic systems is often obtained by applying small amplitude oscillatory strains or stresses to the sample. When a material is exposed to a harmonic, oscillating force/deformation with an angular velocity/frequency ( $\omega/f$ ), the response is measured. The resulting data is used to calculate various rheological parameters, such as storage modulus ( $G'$ ), loss modulus ( $G''$ ), complex modulus ( $G^*$ ), phase angle ( $\delta$ ) and viscosity ( $\eta$ ) that provide a insight to the material's viscoelastic property [42].

$G'$  (storage modulus) represents the elastic or solid-like component of a viscoelastic material. It quantifies the ability of the material to store under deformation.  $G''$  (loss modulus) represents the viscous or liquid-like component of a viscoelastic material. This parameter quantifies the energy dissipation of loss that occurs when deformation is applied on the material. The phase angle indicate the degree of viscoelasticity or the balance between the elastic and viscous properties of the material [40]. A phase angle of  $0^\circ$  corresponds to a material with purely elastic behavior, while a phase angle of  $90^\circ$  indicates a purely viscous behavior [42]. The viscoelastic character at any given frequency of oscillation is characterized by storage/elastic modulus ( $G'$ ) and the loss/viscous modulus ( $G''$ ) which quantify the solid-like and liquid-like contribution to the measured stress response, respectively.

## 2.5.2 Rheometer

A rheometer is any instrument that enables the determination of rheological properties by measuring the stress-strain relationship to understand the flow/deformation properties of the material. This allows researchers to determine properties such as viscosity, elasticity, and shear stress, which are important in understanding the behavior of materials under different conditions [42] [40]. Rheometers that are rotational type use either cone and plate, parallel plate or concentric cylinder geometrics. A parallel plate rheometer is presented in Figure 2.5.1.

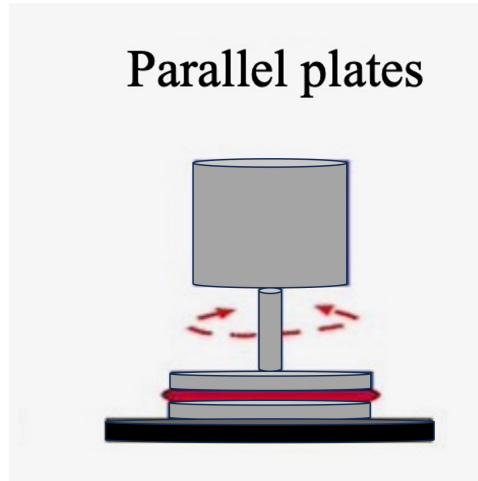


Figure 2.5.1: A parallel plate rheometer with two parallel plates. The bottom plate is stationary, while the top plate is moveable and can exert a controlled force or displacement of the sample. Retrieved from [43].

Strain and stress are computed from two signals, the angular position and the torque, obtained from the rotational rheometer. The maximum strain is obtained at the perimeter of the measuring plate, where the strain is zero at the rotational axis. The angle of rotation,  $\phi$ , is proportional to the strain and the proportionality constant depends on gap size and geometry [40]. An oscillatory rheometer applies a sinusoidal deformation to the sample and measures the resulting stress. When an oscillatory test is performed, the computer monitors both the position and torque signals as a function of time. The stress and strain amplitude and the phase shift are fitted to sine waves and  $G'$  and  $G''$  are calculated from the fits.  $G'$  and  $G''$  are only defined in the linear range where both strains and stresses are simple sinusoidal curves [42] [17]. Figure 2.5.2 presents the difference between stress and strain during sinusoidal oscillation.

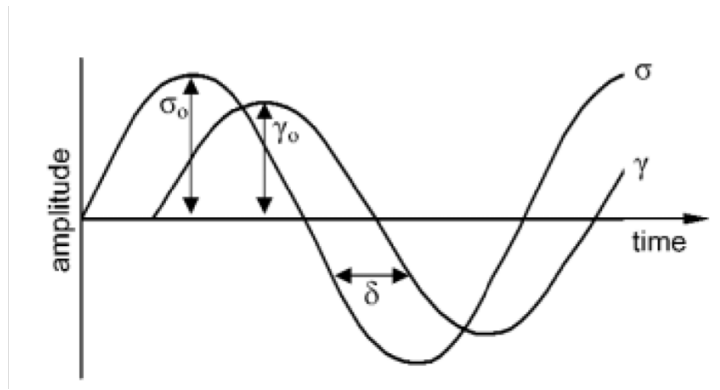


Figure 2.5.2: The difference between stress and strain during sinusoidal oscillation relays on the phase angle values, which is a measure of the amount of liquid and solid properties in a sample. Retrieved from [44]

### 2.5.3 Young's modulus

Young's modulus is a measure of a material's stiffness or rigidity and is another way to quantify how much a material deforms when subjected to an external force (stress). Young's modulus ( $E$ ) is the ratio of principal stress in one direction to corresponding strain in the elastic range in the same direction.

$$E = \frac{\sigma}{\epsilon} \quad (2.3)$$

Stress ( $\sigma$ ) is defined as a force acting per unit area of an object, while strain ( $\epsilon$ ) is stated as the amount of relative deformation caused by the force acting on an object [42] [45]. Hence, the Young's modulus is normally obtained as the initial slope of a stress-strain curve.

## 2.6 Structural Characterization

### 2.6.1 ICP-MS

This part of is retrieved from my specialization project [14].

Inductively coupled plasma mass spectroscopy (**ICP-MS**) is an analytical technique that is utilized to measure elements at trace levels in biological fluids. A plasma is an ionized gas consisting of positively-charged ions and free electrons, and argon plasma is the most used [46] [47]. A 1-2.5 kW plasma is generated by radiofrequency (rf) magnetic fields induced by a coil wound around the end of quartz torch through which argon flows. A high-voltage spark is used to seed the argon with electrons, which collide with argon atoms, ultimately causing ionization and plasma ignition [46]. The motion of electrons and ions are continuously induced by oscillating magnetic field. When the sample reaches the high-temperature plasma, the sample is desolvated, vaporized, atomized and ionized [46]. Most elements have a first ionization potential much lower than argon, and therefore efficiently ionized in the plasma. The ionized entities are transferred through a quadruple mass analyzer, a mass filter that separates the ions on the basis of their mass-to-charge ( $m/z$ ) ratio. By pre-configuring the system with respect to  $m/z$  ratio, their type and relative abundance can be recorded [46]. In this study, ICP-MS analysis was conducted

to determine the sulfate content in alginate after sulfation, to determine the degree of substitution [47].

### 2.6.2 SEC-MALLS

Size exclusion chromatography (SEC) is a convenient method to determine the average molecular weight and the molecular weight distribution in a sample [48]. With SEC the polymers are separated based on hydrodynamic column or size [19]. This method consist of a solid phase of porous particles with a known pore size packed in a column and a mobile phase. The sample is dissolved in a solvent, usually the same solvent as the mobile phase and is injected into a column. Particles that are too large to enter the pores are eluded from the column first. While the smaller molecules will spend time getting through the column due to the pores and will elude lastly. This will give a size based separation of the molecule. [48]

Multiangle laser light scattering (MALLS) is used to determine the molecular weight of the samples from the SEC column. The basic principle behind MALLS is that when a beam of laser light passes through a sample, it interacts with the particles or molecules present in the solution [49]. As the light scatters off these particles at various angles, detectors positioned at different angles collect the scattered light. By measuring the intensity of scattered light at different angles, MALLS provides information about the size distribution and molecular weight of the particles or molecules in the solution. Larger particles scatter light more intensely at low angles, while smaller particles scatter light more intensely at high angles. By analyzing the scattering pattern at multiple angles, MALLS can generate a complete size distribution profile [49].

## MATERIALS & METHODS

### 3.1 Alginate

Two different alginates were used in this project. One being the commercial sodium alginate LF200S S21483 acquired from *DuPont* (Sandvika, Norway) and the other one is a high molecular weight, ultrapure sodium alginate (UP-MVG) with medium viscosity provided by *NovaMatrix* (Sandvika, Norway). The sequence characteristics and average molecular weight of alginates used in the project is given in Table 3.1.1.

Table 3.1.1: Sequence characteristics and average molecular weight ( $M_w$ ) of alginates used in this project.

Alginate	$F_G$	$F_M$	$F_{GG}$	$F_{GM}$	$F_{MM}$	$F_{GGM}$	$F_{MGM}$	$F_{GGG}$	$N_{G>1}$	$M_w$ [kDa]
UP-MVG	0.66	0.34	0.55	0.22	0.12	0.05	0.09	0.50	13	162
LF200S	0.68	0.32	0.57	0.11	0.21	0.04	0.007	0.53	16	298

### 3.2 Fucoidan

The fucoidan used in this project is obtained from the brown algae *L.hyperborea*. Fucoidan sample was provided by prof. Finn L. Aachmann at *The Department of Biotechnology and Food Science*. The source, composition, molecular weight and degree of substitution for the fucoidan is given in Table 3.2.1.

Table 3.2.1: Type, source, composition, molecular weight ( $M_w$ ), and degree of sulfation (DS) for the fucoidan materials.

Fucoidan type	Source	Fucose cont. [%](w/w)	Galactose cont. [%](w/w)	DS	$M_w$ [kDa]
FD	<i>L.hyperborea</i>	97.8	2.2	1.7	1547

### 3.3 Preparation of Sulfated Alginate

Alginate LF200S and Alginate UP-MVG was subjected to sulfation by adding formamide (200 mL) to dried alginate (5000 mg) to a final concentration of 2.5 % (w/v). Chlorosul-



fonic acid (6 mL) was added dropwise to the suspension to a approximate final concentration of 3 % (w/v). The reaction mixture was incubated at 60 °C at constant agitation for 2.5 h. The alginate was transferred to a centrifuge tube (50 mL) and precipitated with acetone (2x reaction volume). Further, the solution was centrifuged at 4700 rpm for 7 minutes at 10 °C. The precipitated alginate was then redissolved in deionized water and the pH neutralized by 1M NaOH. All solution was dialyzed with NaCl (0.1M) then with ionized water until the conductivity was below 2 microS/cm and freeze dried. The sulfur content was measured by ICP-MS by the NTNU Dept. of Chemistry, Trondheim, Norway. The sulfation degree was then estimated from mass balance equation provided in Appendix A.

### 3.4 Characterization of sulfated alginate

The sulfur content in the samples was measured by high-resolution inductively coupled plasma mass spectromy (**ICP-MS**) at the NTNU department of Chemistry, Trondheim, Norway. Estimated theoretical degree of sulfation was calculated.

Size-exclusion chromatography (SEC) with online multi-angle static laser light scattering (MALS) were performed at ambient temperature on an Agilent 1260 Infinity II system consisting of a solvent reservoir, isocratic pump, automatic sample injector, OHPak LB-G 6B guard and OHPak LB 806M main column. The column outlet was connected to a Dawn HELEOS-II multi-angle laser light scattering photometer (Wyatt, U.S.A.) ( $\lambda_0=663.8$  nm) followed by a RI-501 refractive index detector (Shodex). The eluent was 0.15M NaNO<sub>3</sub>, pH 6.0 with 10mM EDTA and the flow rate was 0.5 mL/min. The sample was dissolved over night in mobile phase (0.5 mg/ml) and filtered (pore size 0.45 $\mu$ m) before injection. The sample was analyzed two times, injection volume was 50-100  $\mu$ L. Data were collected and processed (with  $dn/dc = 0.150$  mL/g) for unmodified and 0.130 for sulfated alginate.  $A_2 = 5 \cdot 10^{-3}$  ml  $\cdot$  mol/ g<sup>2</sup> using the Astra (v. 7.3.21) software (Wyatt, U.S.A.).

### 3.5 Preparation of samples for gels

Alginate solution (1.8% (w/v)) was prepared by dissolving alginate LF200S (90 mg) to deionized water (2.5 mL). NaCl (100mM, 2.5 mL) was added to alginate solution mixture to achieve a more homogeneous gel. The solution was stirred with a magnet overnight. Fucoidan solution (1.8% (w/v)) was made by weighing fucoidan (54.0 mg) and adding deionized water (3.0 mL). Sulfated alginate (36 mg) was dissolved in deionized water (2.0 mL) to a sulfated alginate solution (1.8%(w/v)). The different compositions of alginate/fucoidan and alginate/sulfated-alginate samples were prepared by weighing the required volumes of alginate and fucoidan and then mixed for a few minutes with a magnet. It was assumed that the alginate solution had a density of 1 g/mL, due to the solution being too viscous and a accurate pipetting of the volume was not possible. The final ratio between the alginate and fucoidan, as well as for sulfated-alginate and alginate for the different samples are given in Table 3.5.1.

Table 3.5.1: Final concentration (% (w/v)) of alginate hydrogels mixed with sulfated alginate or fucoidan. Total polymer concentration was 1.8 % (w/v) for all samples.

Type of gel	[%(w/v)] final concentration
Alg	1.8
80/20 Alg/FD	1.44/0.36
80/20 Alg/SA	1.44/0.36

### 3.6 Rheology

All rheological measurements were carried out using *Malvern Kinexus ultra+ Rheometer*. A 8 mm roughened/texture (to prevent slip) parallel upper geometry and a lower geometry were used for all measurements. Measurements were carried out at 20°C. To prevent the samples from drying during the measurements, a plastic cover was fitted round the sample. rSpace version 2.0.0 was used for instrument control and data analysis. A relevant volume between a 8 mm probe and lower geometry was determined to be 60  $\mu\text{L}$ . A 8 mm probe was used for the experiments to establish procedures for rheological characterization of small alginate gel volumes. The purpose of using a smaller probe diameter will allow for future characterization of valuable samples of e.g enzymatically or chemically modified alginates. The sample (60  $\mu\text{L}$ ) was loaded to the lower geometry. The gap between the plates was adjusted to 1 mm, to ensure proper loading of the sample. (50 mM)  $\text{CaCl}_2$  solution (2mL) was added to lower geometry and gelation occurred for one hour, before the height between the plates were reduced by 0.01 mm stepwise. A schematic presentation of the experimental setup is presented in Figure 3.6.1.

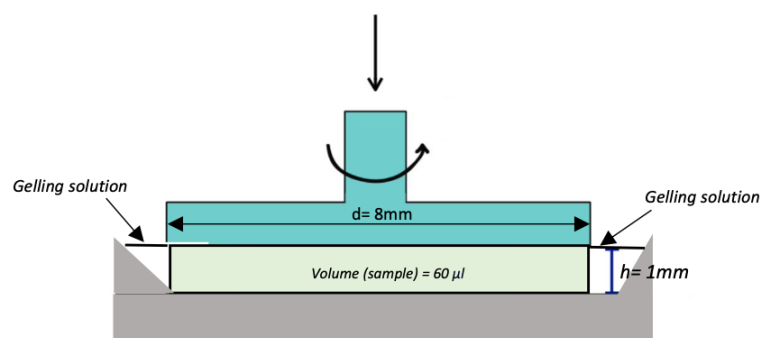


Figure 3.6.1: A schematic presentation of the experimental setup for the parallel rheometer. Sample (60  $\mu\text{L}$ ) was loaded to the lower geometry. The gap between the plates was adjusted to 1 mm. Gelling solution (2 mL) was added to the lower geometry. One hour of gelation occurred, before the gap between the plates was reduced by 0.01 mm stepwise.

Further, the sequence used for the measurements was developed throughout the course of the thesis. This was a consequence of working with alginate gels, that are known to

be prone to syneresis, that made it challenging to get accurate data which characterized the different gels. Therefore, the sequence was changed as the results were analyzed to improve the resulting data. The different sequence used in this thesis are given in chronological order relative to when the changes occurred.

### 3.6.1 Sequence 1: Alginate-based gels stored in $\text{CaCl}_2$ - solution

- Set temperature to 20°C.
- Load sample (60  $\mu\text{L}$ ) with reverse pipetting.
- Adjust gap and distance between the plates to 1 mm to ensure proper loading.
- Add  $\text{CaCl}_2$  solution (50mM, 2 mL) to the lower geometry to allow for gelation upon diffusion of  $\text{Ca}^{2+}$ -ions into the sample.
- Gelling for one hour.
- Frequency sweep (1-0.05 Hz, 0.1 % shear strain, 10 samples per decade)
- Probe height reduction by 1 % hold (120 s).
- Loop (20)
  - Frequency sweep (1-0.05 Hz, 0.1 % shear strain, 10 samples per decade).
  - Probe height reduction by 1% hold (120 s).
  - Oscillation frequency sweep was measured until probe height was reduced by 20 % in total.

### 3.6.2 Sequence 2: Alginate-based gels stored in NaCl solution

- Set temperature to 20°C.
- Load sample (60  $\mu\text{L}$ ) with reverse pipetting.
- Adjust gap and distance between the plates to 1 mm to ensure proper loading.
- Add  $\text{CaCl}_2$  solution (50mM, 2 mL) to the lower geometry to allow for gelation upon diffusion of  $\text{Ca}^{2+}$ -ions into the sample.
- Gelling for one hour.
- Remove  $\text{CaCl}_2$  solution from lower geometry and add NaCl-solution (150 mM, 2 mL).
- Frequency sweep (1-0.05 Hz, 0.1 % shear strain, 10 samples per decade)
- Probe height reduction by 1 % hold (120 s).
- Loop (20)
  - Frequency sweep (1-0.05 Hz, 0.1 % shear strain, 10 samples per decade).
  - Probe height reduction by 1% hold (120 s).
  - Oscillation frequency sweep was measured until probe height was reduced by 20 % in total.

### 3.6.3 Sequence 3: Alginate-based gels stored in NaCl solution with increased hold time

- Set temperature to 20°C.
- Load sample (60  $\mu\text{L}$ ) with reverse pipetting.
- Adjust gap and distance between the plates to 1 mm to ensure proper loading.
- Add  $\text{CaCl}_2$  solution (50mM, 2 mL) to the lower geometry to allow for gelation upon diffusion of  $\text{Ca}^{2+}$ -ions into the sample.
- Gelling for one hour.
- Remove  $\text{CaCl}_2$  solution from lower geometry and add NaCl-solution (150 mM, 2 mL).
- Frequency sweep (1-0.05 Hz, 0.1 % shear strain, 10 samples per decade)
- Probe height reduction by 1 % hold (120 s).
- Loop (10)
  - Frequency sweep (1-0.05 Hz, 0.1 % shear strain, 10 samples per decade).
  - Probe height reduction by 1% hold (120 s).
  - Oscillation frequency sweep was measured until probe height was reduced by 10 % in total.



## RESULTS & DISCUSSION

### 4.1 Sulfatation of Alginate

The sulfur content in the samples after sulfation of alginates, was measured by performing ICP-MS analysis. The results from the analysis was then used to calculate the theoretical degree of sulfation (DS), as presented in Appendix A. The DS value for the alginates are given in Table 4.1.1.

Table 4.1.1: Calculated degree of sulfation (D.S) of sulfated alginates (LF200S & UP-MVG).

Alginate	Sulphur concentration [ $\mu\text{g/g}$ ]	Estimated D.S-value
LF200S	77634.46	0.71
UP-MVG	62144.01	0.55

Molecular weight averages and dispersity were determined with size exclusion chromatography with multi-angle laser light scattering (SEC-MALLS). Table 4.1.2 present Number average molecular weight ( $M_n$ ), Molecular weight averages ( $M_w$ ) and polydispersity index for LF10/60, sulfated LF200S alginate and sulfated UP-MVG alginate after sulfation.

Table 4.1.2: Number average molecular weight ( $M_n$ ), Molecular weight averages ( $M_w$ ) and polydispersity index for sulfated LF200S alginate and sulfated UP-MVG alginate after sulfation.

Alginate	$M_n$ [kDa]	$M_w$ [kDa]	$\frac{M_w}{M_n}$
Sulfated LS200S	30.9	68.6	2.2
Sulfated UP-MVG	66.2	119.9	1.8

The sulfation of the alginate has been using methodology described in Section (3.3). The degree of sulfation per alginate monomer is dependent on the concentration of chlorosulfonic acid in formamide utilized during the preparation [8]. In this study, the degree

of sulfation was estimated to be 0.71 for LF200S alginate and 0.55 for UP-MVG alginate. This indicates that approximately 71 % and 55 % of the monomer units in the alginate have substituted hydroxyl-group with sulfate on the C2 or C3 [50]. Previous studies with the same methodology on sulfation of alginate, resulted in a DS value of 0.76 and 0.83, where the sulfation was performed on ultra-pure alginates with varying viscosity [18]. The difference in DS value could be due to the batch size used in this study being larger. It is reasonable to expect a change in conformation and orientation of the alginate when sulphate groups are introduced, as the sulfate group is charged and relatively bulky. This could lead to limitation for the number and position of the sulfates to various extents in different monosaccharide sequences, that results in a lower D.S value than expected [8]. Moreover, during the preparation the solution was placed in a shaking water bath for 2.5 h, however it was discovered that the bath had been turned off for the last 10-15 minutes leading to a decrease in temperature for both alginate samples. As the temperature acts as the catalyst for the sulfation reaction, the decrease in temperature could have led to a lower sulfation degree, compared to previous research [18].

The samples were analyzed by performing SEC-MALLS analysis. The results revealed that the molecular weight of LF200S alginate was 68.6 kDa, while UP-MVG had a molecular weight of 119.9 kDa after sulfation. LF200S had a considerable reduction in  $M_w$  indicating that depolymerization in the sample, as presented in Table 4.1.2. Further, there was some reduction in  $M_w$  for UP-MVG alginate, indicating some depolymerization. Depolymerization of alginates as a result of sulfation has previously been reported [51], for experiments for alginates above 100 000 Da. The methodology used in this study have previously proven to that the DS can be systematically tuned under conditions mild enough to ensure good reproducibility while minimizing depolymerization and unwanted side reactions [8]. However, the findings of the current study contradict those of the previous study. One possible explanation could be that alginate, in the aforementioned study, was subjected to hydrolysis to reduce the molecular weight to  $\sim 14$  000 Da prior to sulfation [8]. In the current study acid hydrolysis did not take place. This could explain the depolymerization of both alginates in the current study.

## 4.2 Rheological analysis of alginate gels stored in $\text{CaCl}_2$ -solution

The aim for this section is to characterize the rheological properties of alginate gels. For all measurements 1.8 % (w/v) alginate solution (60  $\mu\text{L}$ ) was loaded to the lower geometry. Gap between the measuring plates were adjusted by lowering the upper geometry to a gap distance of 1 mm between the plates, to ensure proper loading of sample. (50 mM)  $\text{CaCl}_2$  solution (2mL) was added for gelation and one hour of gelation occurred, before the gap was reduced by 0.01 mm stepwise.

### 4.2.1 Evaluating syneresis in Alginate gels stored with $\text{CaCl}_2$ -solution

Over time various systems undergoing a solution-gel transition often results in exudation of liquid, known as syneresis, it is macroscopically characterized by a slow, time-dependent de-swelling of a gel [29] [52]. This phenomena often represent a challenge when measuring

the rheological properties of a hydrogels, as syneresis lead to changes in main parameters that effect the accuracy of measured modulus. Alginate hydrogels are known to be susceptible to syneresis [13]. Establishing a contact point between the instrument and the gel is crucial for accurately characterizing the rheological properties of the gel. Normal force was therefore monitored through gap reduction to assist determining the contact point. Initial increase in normal force is an indication for reaching a contact point between the instrument and gel.

Gap was reduced by 0.01 mm stepwise and a frequency sweep was performed on the gel at each measuring height, in order to get a comprehensive understanding of the gel's response to the mechanical deformation. The values for the measured normal force was plotted against gap height, resulting in Figure 4.2.1.

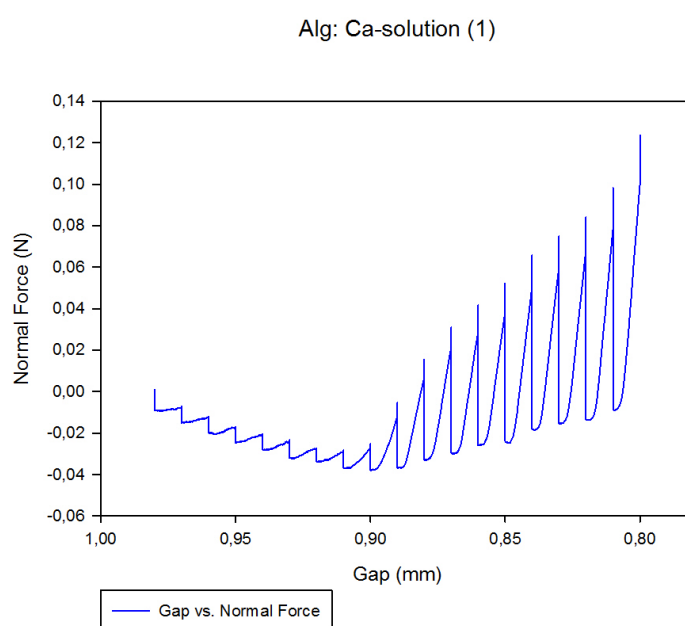


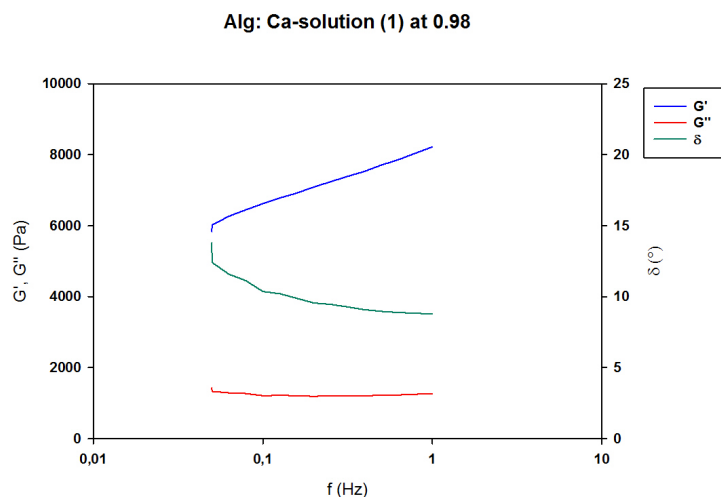
Figure 4.2.1: Normal force as a function of measuring height for Alg-Ca(1) gel. 1.8 % (w/v) alginate solution ( $60 \mu\text{L}$ ) was loaded to the lower geometry and the distance between the plates was set to 1 mm. 50 mM  $\text{CaCl}_2$  (2mL) was added to the lower geometry for gelling. One hour of gelation occurred before the gap was reduced by 0.01 mm stepwise to a total reduction to 0.80 mm.

Figure 4.2.1 present the normal force measured at each gap reduction. A increase in measured normal force was measured at 0.98 mm, indicating a contact point between the probe and gel could have occurred. The corresponding y-value ( $x= 0.98$  mm) was set to zero and the remaining value for normal force measured at each height was adjusted to match the respective y-value. After a contact point had been established, the gap was further reduced. As the height kept reducing the normal force was measured to be decreasing to 0.90 mm. The decrease in normal force initially might be attributed to the lack of sufficient contact between the probe and the gel or possibly caused by a degree of slip, which can be due to by the syneretic nature of alginate gel. At 0.90 mm the instrument has sufficient contact with the gel, as the normal force is measured to be increasing rapidly subsequently. The rapid increase in normal force suggests that the gel is undergoing compression for decreasing height. Moreover, after each height reduction a

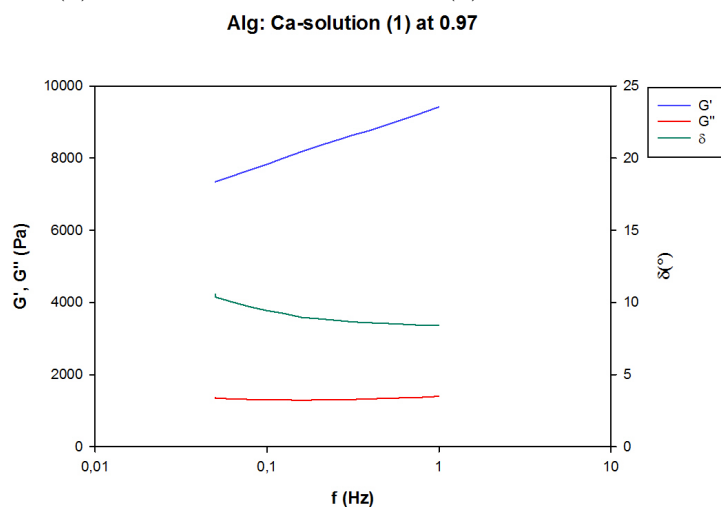


hold time was included to the protocol to allow the gel to relax. Relaxation of the gel is observed as the decline in normal force.

To determine if the initial increase in normal force is likely due to a contact point being established, the frequency sweep performed at 0.98 mm and 0.97 mm height reduction was further investigated. The obtained value for elastic modulus ( $G'$ ), viscous modulus ( $G''$ ) and change in phase angle ( $\delta$ ) at each gap height was plotted against the frequency range. The resulting data is presented in Figure 4.2.2.



(a) Frequency sweep of Alg-Ca(1) gel at 0.98 mm



(b) Frequency sweep of Alg-Ca(1) gel at 0.97 mm

Figure 4.2.2: (a) Frequency sweeps of Alg-Ca(1) gel at 0.98 mm. (b) Frequency sweep of Alg-Ca(1) at 0.97 mm. Elastic modulus (blue), viscous modulus (red) and phase angle (green) is plotted on y-axis against the frequency on the x-axis. For 1.8 % (w/v) alginate gel gelled with 50 (mM)  $\text{CaCl}_2$  solution. Frequency sweeps (1-0.05 Hz) was performed at 20°C with a constant at shear strain at 0.1 % and 10 measurements per decade.

A study on characterizing the elastic modulus of 2 % (w/v) alginate hydrogel with  $\text{CaCl}_2$  after 1 hour postfabrication, presented that the average elastic moduli of 2% alginate gels ranged from  $\sim 5$  to 20 kPa [53]. These range of values were observed in a different study, when dynamic measurements was performed to characterize alginate

gels [54]. The aforementioned study also provide the values for viscous component and the phase angle as a function of frequency. The viscous component is measured ranging between  $\sim 100$ - $700$  Pa for alginate concentration between 1.0-1.75% (w/v). The values for the phase angle obtained in the same study is measured to be from  $\sim 7^\circ$  at low frequency and  $\sim 12^\circ$  at higher frequency [54]. The values obtained from these studies is also supported by additional papers, where the obtained values for  $G'$ ,  $G''$  and  $\delta$  range in the same magnitude of values, despite different methodology [55][56] [57] [54]. In light of the prior research, specific criteria have been established for the current study to evaluate the quality of the obtained data for  $G'$ ,  $G''$ , and  $\delta$ .

The frequency sweep graph visualizes the gel's response to oscillatory forces at different frequencies. When the height was 0.98 mm the elastic modulus is measured to be 5828 Pa at 0.05 Hz and 8222 Pa at 1 Hz 0.05 Hz, as presented in Figure 4.2.2a. At 0.97 mm the elastic modulus is 7344 Pa at 0.05 Pa and 9415 Pa at 1 Hz. In a biopolymeric gel the storage modulus is greater than the loss modulus, indicating predominance of elastic behavior [40], which is observed for the frequency sweeps at 0.98 mm and 0.97 mm.

Moreover, the phase angle is measured to be  $13.8^\circ$  at 0.05 Hz and  $8.8^\circ$  at 1 Hz. The obtain value at 0.05 Hz for the phase angle is higher than the expected initial value based on previous frequency sweeps performed on alginate gels [57] [58]. Based on these observation, it can be hypothesized that the initial increase in normal force was due to the instrument being in contact with a part of the gel. When  $\text{Ca}^{2+}$ -ions are introduced to the alginate structure the rapid ion-binding and formation of network produce an inwardly moving gelling zone [20]. Syneresis can be influences by by excess, insufficient, or non-uniformly distributed cations in the alginate gels [59]. This differential gelation can result in uneven shrinkage or expansion, leading to a curved surface. This would also result in a a weaker gel network on the surface of the gel, which could results in a higher value for phase angle. Based on the established research for the expected values, frequency sweep for Alg-Ca(1) at 0.98 mm do not meet the criteria of values for  $G'$  and  $\delta$  for a pure alginate gel. When the gap height was reduced to 0.97 mm, the phase angle at 0.05 Hz is  $10.6^\circ$  at 0.05 Hz and  $8.4^\circ$  at 1 Hz. The frequency sweep obtained at 0.97 mm is within the criteria set for an alginate gel. This appears to be a contact point between the instrument and the entire gel surface where a valid and reliable value for the rheological data can be obtained.

The results suggests that the alginate gel is syneretic within the expected boundaries. By compensating for syneresis through reducing the height, the rheological data for the alginate gel is obtainable. The resulting values for  $G'$ ,  $G''$  and  $\delta$  at 0.97 mm is in accordance with expected value based on criteria established by previous research for alginate gels. However, gels are unlikely to retain a perfect cylindrical shape during syneresis. Therefore it is necessary to make a value judgment about the quality and examine the reproducibility of the data obtained.

#### 4.2.2 Reproducibility of rheological data obtained for alginate gels in $\text{CaCl}_2$ -solution

In order to obtain reliable measurements, accurate and consistent data must be produced with repeated measurements of the same material under similar conditions yielding consistent results. Hence, additional measurement with 1.8 % (w/v) alginate (60  $\mu\text{L}$ ) solution

and (50mM)  $\text{CaCl}_2$ - solution (2 mL) as gelling solution was performed. The measured normal force acted on the probe applied by the gels were plotted against the reducing gap height, resulting in Figures 4.2.3. Here the gap was reduced to 0.92 mm before an increase in normal force was observed.

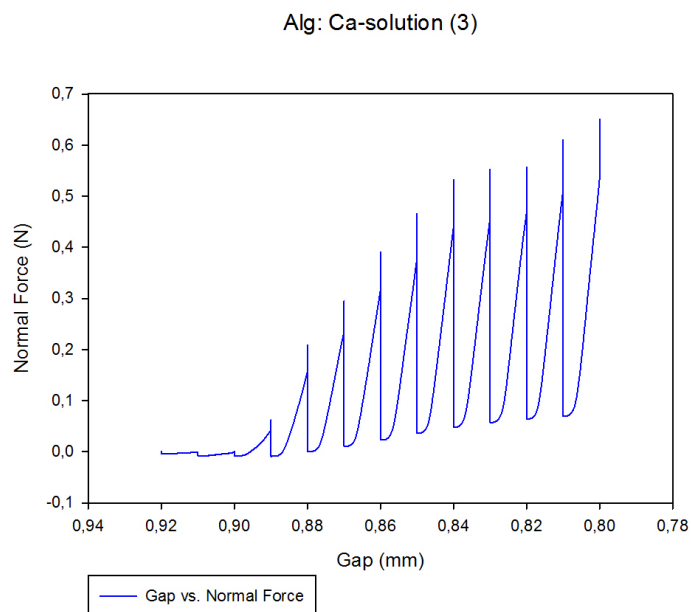
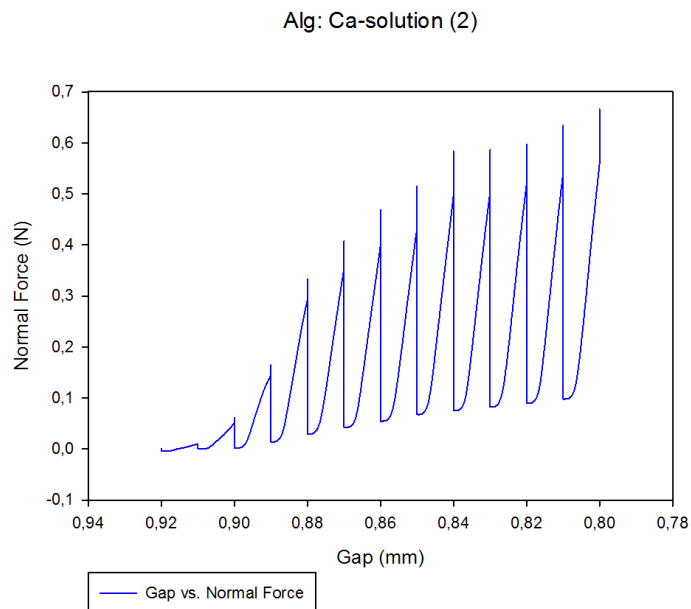
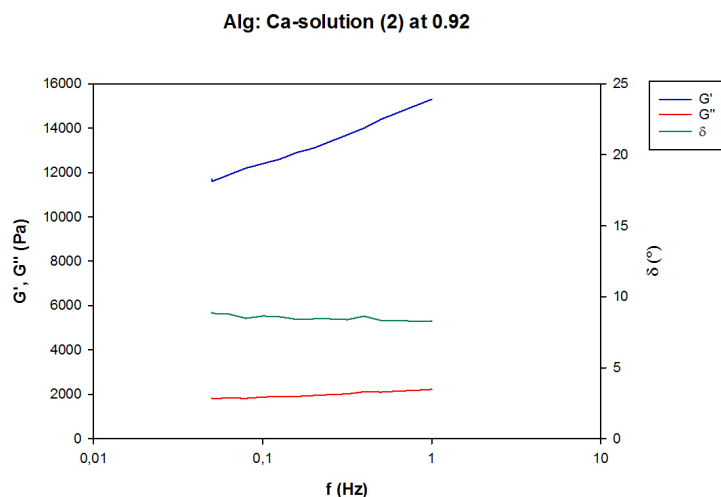


Figure 4.2.3: (a) Normal force as a function of measuring height for Alg-Ca(2) gel. (b) Normal force as a function of measuring height for Alg-Ca(3) gel. Both measurements was performed by loading 1.8 % (w/v) alginate solution ( $60 \mu\text{L}$ ) to the lower geometry and the distance between the plates was set to 1 mm. 50 mM  $\text{CaCl}_2$  (2mL) was added to the lower geometry for gelling. One hour of gelation occurred before the gap was reduced by 0.01 mm stepwise to a total reduction to 0.80 mm.

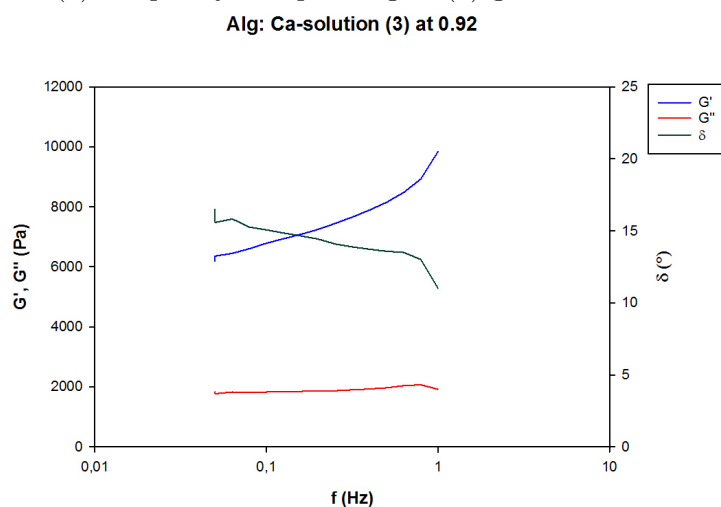
Alg-Ca (2) and Alg-Ca (3) shows an increase in normal force at 0.92 mm, as pre-

sented in Figure 4.2.3a and Figure 4.2.3b, respectively. The corresponding y-value ( $x=0.92$  mm) was set to zero and the remaining value for normal force measured at each height was adjusted to match the respective y-value. The initial increase in measured normal force indicate a resistance to compression is applied on the probe, which is most likely by the gel. This indicate that at 0.92 mm the probe has likely reached the gel. Further, after establishing a contact point the gel undergoes compression, which leads to a rapid increase in normal force with reducing height. The relaxation of the gel during the hold time is denoted with the dissipation of measured normal force.

To determine if the initial increase in normal force measured was due to reaching a contact point between the instrument and the gel, the frequency sweep obtained at 0.92 mm is looked into for both gels. The obtained values for  $G'$ ,  $G''$  and  $\delta$  is plotted against the frequency range. The resulting plot for Alg-Ca(2) gel and Alg-Ca(3) gel is given in Figure 4.2.4.



(a) Frequency sweep of Alg-Ca(2) gel at 0.92 mm



(b) Frequency sweep of Alg-Ca(3) gel at 0.92 mm

Figure 4.2.4: (a) Frequency sweeps of Alg-Ca (2) gel at 0.92 mm (b) Alg-Ca(3) gel at 0.92 mm. Elastic modulus (blue), viscous modulus (red) and phase angle (green) is plotted on y-axis against the frequency on the x-axis. For 1.8 % (w/v) alginate gel gelled with 50 (mM)  $\text{CaCl}_2$  solution. Frequency sweeps (1-0.05 Hz) are performed at 20°C with a constant shear strain at 0.1 % and 10 measurements per decade.

Figure 4.2.4a present the frequency sweep performed at 0.92 mm for Alg-Ca(2) gel. The elastic modulus is measured to be 21800 Pa at 0.05 Hz and 17510 Pa at 1 Hz. The phase angle is measured to be 8.1° at 0.05 Hz and 7.5° at 1 Hz, within the expected values. The frequency sweep at 0.92 for Alg-Ca(2) align with the established criteria from prior research. Which implies that reliable data for the rheological properties can be obtained from this point.

Figure 4.2.4b present results from the frequency sweep performed at 0.92 for Alg-Ca(3). The elastic modulus is measured to be 6197 Pa at 0.05 Hz and 9844 Pa at 1 Hz, indicating a dominant elastic behavior in the gel. Further, the phase angle was measured to be 11.0° at 0.05 Hz and 16.7° at 1 Hz. A change in phase angle over the frequency range could be related to degree of slip. To investigate if this is the observed phenomenon, the  $G'$ ,  $G''$  and  $\delta$  at 0.91 was plotted against the frequency range, resulting in Figure 4.2.5.

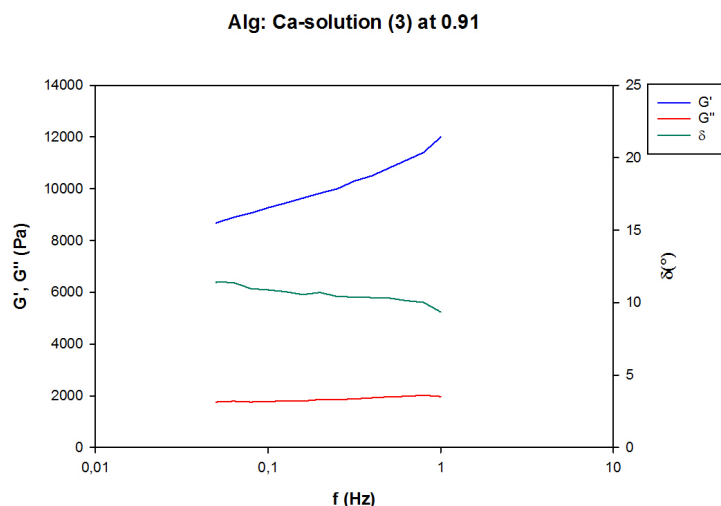


Figure 4.2.5: Frequency sweeps of Alg-Ca(3) gel at 0.91 mm. Elastic modulus (blue), viscous modulus (red) and phase angle (green) is plotted on y-axis against the frequency range on the x-axis for 1.8 % (w/v) alginate gel gelled with (50 mM)  $\text{CaCl}_2$ -solution. All values are obtained from frequency sweeps (1-0.05 Hz) performed at 20°C, a constant shear strain at 0.1 % and 10 measurements per decade.

Figure 4.2.5 present the mechanical spectra obtained at 0.91 mm for Alg-Na(3) gel. The elastic modulus is the dominant factor for the rheological behavior.  $G'$  is measured to be 8681 Pa at 0.05 Hz and 11990 Pa at 1 Hz, which is in accordance with the expectations. Further, the phase angle was measured to be 11.4° at 0.05 Hz and 9.4° at 1 Hz, which is within in the expected range of values for an alginate gel. The values for  $G'$ ,  $G''$  and  $\delta$  meets the established criteria for the rheological properties in an alginate gel. At 0.91 mm the contact point between the gel and the instrument is sufficient enough to determine reasonable rheology for the pure alginate gel.

Overall, Alg-Ca(1) gel, Alg-Ca(2) gel and Alg-Ca(3) gel were all synergetic. However, the degree of syneresis appear to differ, which could be due to practical challenges. Alginate is a highly viscous solution and accurate pipetting is difficult to achieve. Additionally, initial volume in these experiments were determined to be 60  $\mu\text{L}$ , a variation in initial volume loaded to the lower geometry could have resulted in different degree of syneresis. When experiments are performed with smaller volumes there is also a probability to have an increased higher percentage effect on the outcome, which could give variation between each measurement. Considering the aforementioned challenges, the data obtained from the measurements may make comparison more difficult.

### 4.2.3 Dependence of elastic modulus in alginate gel stored in $\text{CaCl}_2$ on measuring height

All three alginate gels exhibited dominant elastic behavior at all times. To get a comprehensive understanding on how the elastic modulus develops with reducing gap,  $G'$  at 1 Hz was plotted against gap height. The Figure 4.2.6 is the resulting plot.

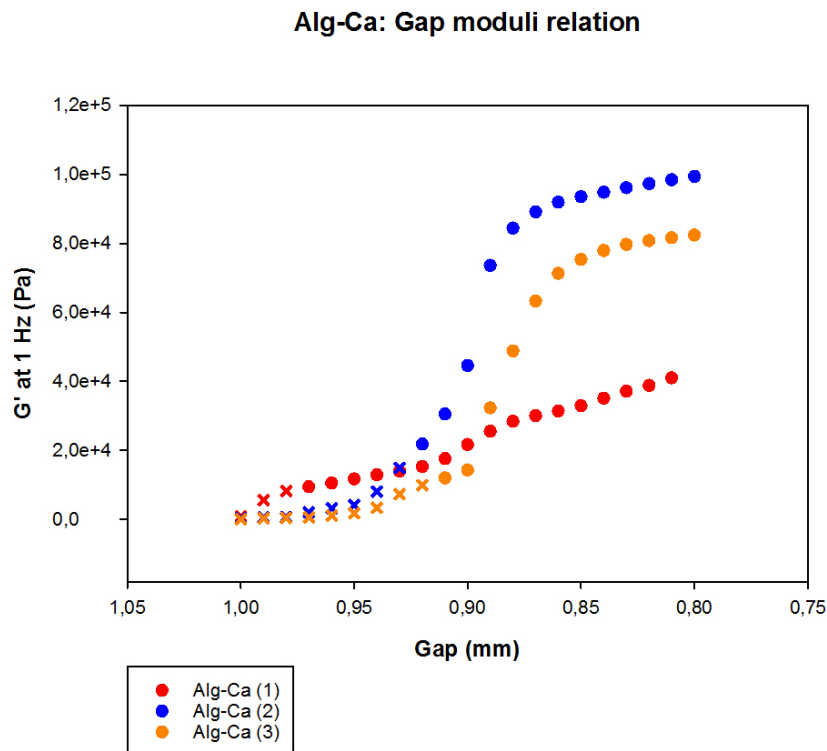


Figure 4.2.6:  $G'$  at 1 Hz (Pa) plotted against the gap height for Alg-Ca (1) gel (red), Alg-Ca(2) gel (blue) and Alg-Ca (3) gel (orange). Values for  $G'$  before establishing contact point is noted with is noted with a cross.

Figure 4.2.6 illustrate that the elastic modulus is increasing with reducing gap height for all three gels. Theoretically, when deformation is acted upon the gel chains are forced closer together and in presence of excess  $\text{Ca}^{2+}$ -ions new junction zones can be formed [4], contributing to an increased elastic modulus. Additionally, compression results in volume change in the gel through expulsion of water, that leads to a higher concentration of alginate [59]. A part of the increased elastic modulus upon compression could then be due increase concentration within the gel [57]. Increased alginate concentration can enhance its gelation and strengthen the gel network. In this study,  $G'$  has been increasing with compression for Alg-Ca (1) gel, Alg-Ca (2) gel and Alg-Ca (3) gel, in accordance with the theoretical expectation when excess  $\text{Ca}^{2+}$ -ions have been present. For Alg-Ca(1) gel the elastic modulus is increasing more gradually relative to the other gels, this could be due to practical differences in e.g starting volume.

It is evident from Figure 4.2.6 that increased compression of the gel after establishing contact with the probe alters the elastic modulus significantly, when excess  $\text{Ca}^{2+}$ -ions are present. This implies that a correct establishment of gel gap for a synretic alginate is important to measure accurate rheological values.

### 4.3 Rheological analysis of alginate/fucoidan gel in $\text{CaCl}_2$ -solution

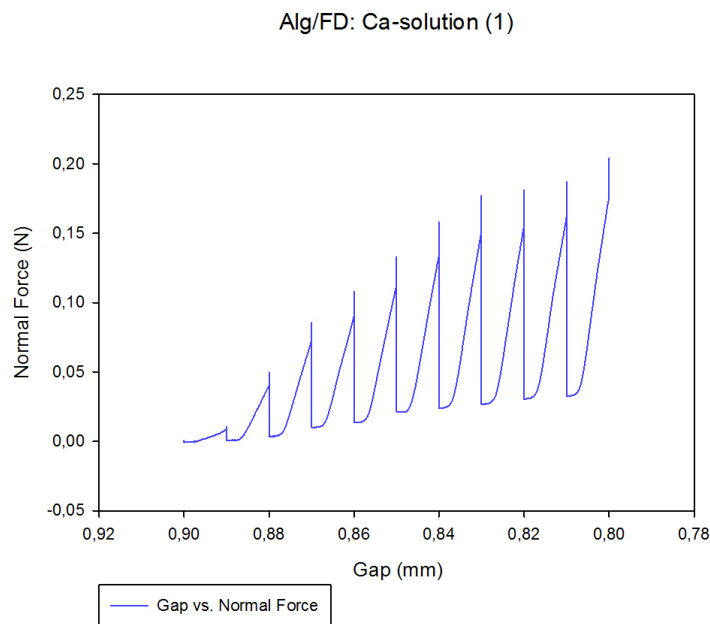
Alginate hydrogels mixed with fucoidan have been proposed as an alternative material for tissue engineering purposes. In this section, effect on the mechanical properties when

replacing a fraction of alginate gel with fucoidan was looked into. For all measurements 1.8 % (w/v) 80/20 alginate/fucoidan solution (60  $\mu\text{L}$ ) was loaded to the lower geometry. Gap between the measuring plates were adjusted to 1 mm distance between the plates, to ensure proper loading. (50 mM)  $\text{CaCl}_2$  solution (2mL). The stepwise reduction in gap height took place after one hour of gelation.

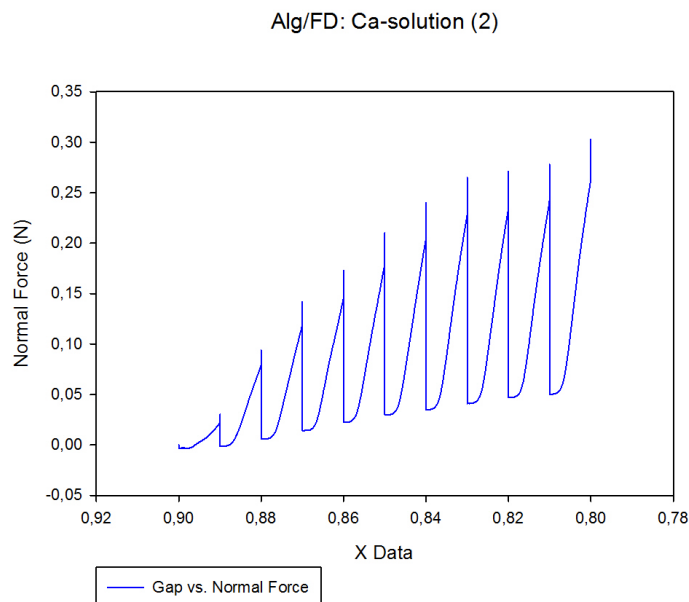
### 4.3.1 Evaluating syneresis in alginate/fucoidan gel

To establish a contact point between the alginate/fucoidan solution and the instrument the gap was reduced and normal force was monitored. The normal force acting on the probe by the gel was measured and then plotted against the gap height. The result is given in Figure 4.3.1.





(a) Alg/FD- Ca (1) gel



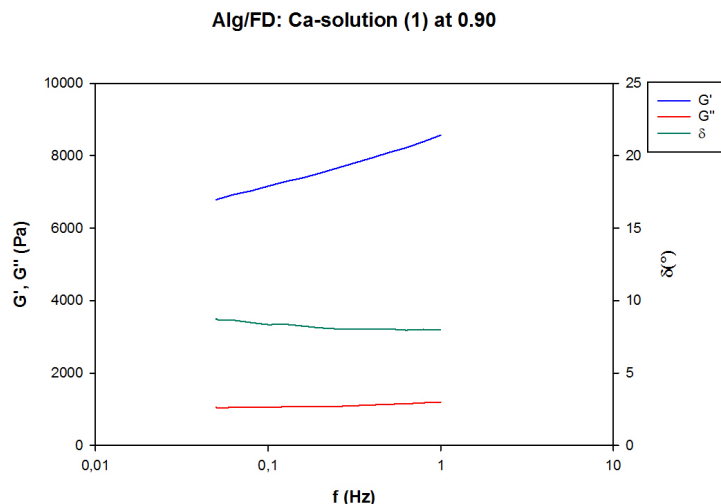
(b) Alg/FD-Ca (2) gel

Figure 4.3.1: (a) Normal force as a function of measuring height for Alg/FD-Ca(1) gel. (b) Normal force as a function of measuring height for Alg/FD-Ca(2) gel. Both measurements was performed by loading 1.8 % (w/v) 80/20 alginate/fucoidan solution ( $60 \mu\text{L}$ ) to the lower geometry. Gap between the plates were adjusted to 1 mm. 50 mM  $\text{CaCl}_2$  (2 mL) was added as gelling solution to the lower geometry. One hour of gelation took place, before the gap reduction of 0.01 mm stepwise to a total height reduction to 0.80 mm for both gels.

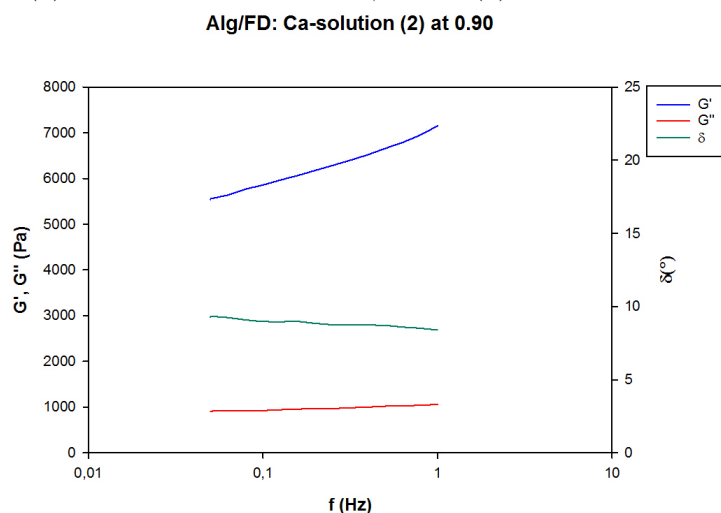
The first increase in normal force is observed at 0.90 mm in Figure 4.3.1a for Alg/FD-Ca(1) gel and in Figure 4.3.1b for Alg/FD-Ca(2) gel. This indicates that a contact between the instrument and gel has reached. The corresponding y-value ( $x=0.90$  mm) was set to zero. Subsequent values for normal force was adjusted to the respective y-value. The normal force is measured to be increasing rapidly with reducing gap. After

contact had been established the gel undergo compression, which is indicated by the rapid increase in normal force. The relaxation after compression in the gel is observed as the decrease in the value for the normal force. Further, the fraction of alginate do not appear to be interrupting the gel network, in terms of how the normal force develops. As the curve is developing in a similar pattern as observed in alginate gels (Figure 4.2.3). However, the absolute values for normal force is significantly lower for alginate/fucoidan gels, implying that the alginate/fucoidan gels are less resistant towards compression compared to the alginate gels.

In order to characterize the rheological properties for Alg/FD gels, a frequency sweep after each gap reduction was performed. To determine if the initial increase in normal force is likely to be a contact point between the instrument and the whole gel, the mechanical spectra obtained at 0.90 mm in further examined for both gel. Figure 4.3.2 present the obtained  $G'$ ,  $G''$  and  $\delta$  at 0.90 mm for Alg/FD-Ca(1) gel and Alg/FD-Ca(2) gel.



(a) Frequency sweep of Alg/FD-Ca(1) gel at 0.90 mm



(b) Frequency sweep of Alg/FD-Ca(2) gel at 0.90 mm

Figure 4.3.2: (a) Frequency sweeps of Alg/FD-Ca (1) gel at 0.90 mm. (b) Frequency sweeps of Alg/FD-Ca (2) gel at 90 mm. Elastic modulus (blue), viscous modulus (red) and phase angle (green) is plotted on y-axis against the frequency on the x-axis. For 1.8 % (w/v) alginate gel gelled with 50 (mM)  $\text{CaCl}_2$  solution. Frequency sweeps (1-0.05 Hz) was performed at 20°C with a constant shear strain at 0.1 %, with 10 measurements per decade.

For Alg/FD-Ca(1) gel the elastic modulus is measured to be 6789 Pa at 0.05 Hz and 8570 Pa at 1 Hz. The phase angle is measured to be 8.8 ° at 0.05 Hz and 8.0° at 1 Hz, as presented in Figure 4.3.2a. For Alg/FD-Ca(2) gel, Figure 4.3.2b present the elastic modulus to be 5538 Pa and 7149 Pa at 0.05 Hz and 1 Hz, respectively. The phase angle is 9.3° and 8.4° at 0.05 Hz and 1 Hz, respectively. The mechanical spectra for both gels illustrates that the elastic modulus is dominant in both gels. Moreover, there are limited research on rheological properties on alginate incorporated with fucoidan which makes it challenging to determine the anticipated values for  $G'$ ,  $G''$  and  $\delta$ . However, both mechanical spectra are within the criteria values for alginate gels, indicating that the fucoidan present in the solution do not effect the obtained values for  $G'$ ,  $G''$  and  $\delta$ . When the gap between the plates is 0.90 mm, it is appears to be a contact point established

between the instrument and gel, it is possible to make a reasonable assessment of the rheological properties of the gel after this point.

### 4.3.2 Dependence of elastic modulus in alginate/fucoidan gel on measuring height

In order to get a complete understanding of the effect of substituting a fraction of alginate with fucoidan, the development of elastic modulus with gap height should be studied further.  $G'$  obtained at 1 Hz plotted against measuring height is presented in Figure 4.3.3.

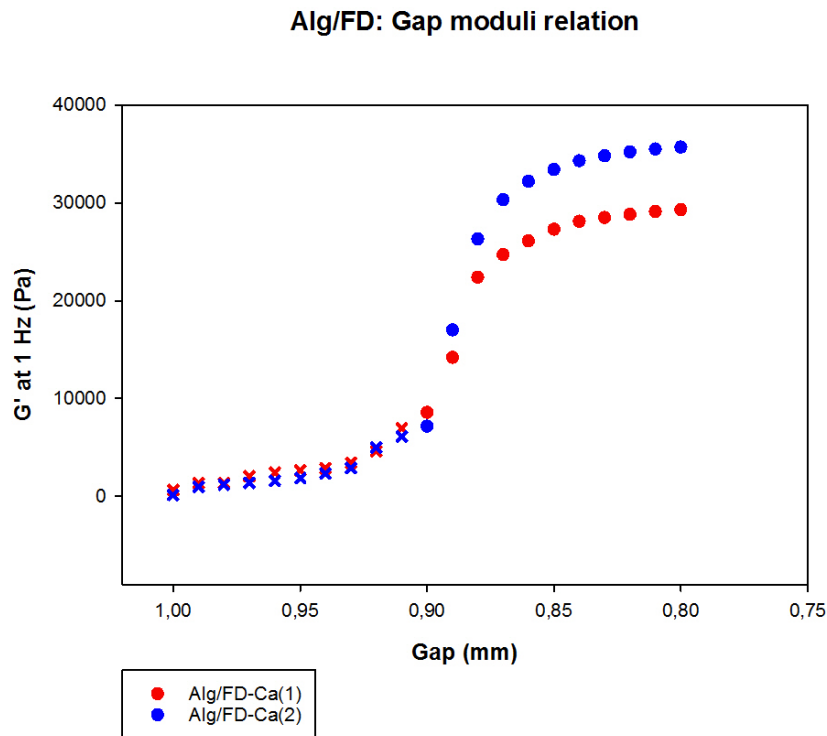


Figure 4.3.3:  $G'$  at 1 Hz (Pa) plotted against the gap height for Alg-Ca (1) gel (red), Alg-Ca(2) gel (blue) and Alg-Ca (3) gel (orange). Values for  $G'$  before establishing contact point is noted with a cross.

Figure 4.3.3 show increasing values for elastic modulus with with continued reduction in gap after establishing contact for Alg/FD-Ca(1) gel and Alg/FD-Ca(2) gel. Fucoidan do not contribute to gelation with divalent ions like  $\text{Ca}^{2+}$  due to the lack of gelling properties [38]. This implies that alginate is most likely the only structure that contributes to increased gel stiffness. As mentioned, increased compression results in a volume change in the gel through expulsion of water and an effective increase in alginate concentration [57]. The change in alginate concentration could be the reason for an increased elastic modulus observed in Figure 4.3.3. Additionally, from my earlier work on specialization project, I examined the leaked material from alginate/fucoidan microbeads. The results from that study suggests that fucoidan is the leaking material from the gel network [14]. This indicates that fucoidan is most likely mobile in the gel matrix, which would prevent the rapid increase in elastic modulus during the initial compression. With consecutive compression fucoidan is most likely squeezed out of the the gel network, in addition to

water, resulting in a even higher concentration of alginate. When excess  $\text{Ca}^{2+}$ -ions are present throughout the measurements, alginate could form additional cross links, that leads to a increase in elastic modulus, as observed after 0.90 mm.

Moreover, when the data obtained for alginate/fucoidan gels appear to vary less between each measurement, compared to pure alginate gels. Implying that when fucoidan is present in the sample there is less resistance towards deformation, causing less alteration between the elastic moduli with increasing height reduction.

Based on the data obtained, the presence of additional  $\text{Ca}^{2+}$ -ions appear to alter  $G'$  significantly for alginate gels. Which makes it difficult to establish a gap height to compensating for syneresis, without inducing substantial modification in the elastic modulus. This presents a greater challenge to compare the data obtained for the different samples.

#### 4.4 Inhibiting additional $\text{Ca}^{2+}$ -crosslinks during reduction in measuring height: altering the storage solution

In order to minimize the variation between the different measurements and produce consistent data, new measurements with different storing solutions was performed. The ionic nature of alginate hydrogels causes several complications during evaluation of these materials, including swelling, syneresis, and ion exchange. These issues can be influenced by excess, insufficient, or non-uniformly distributed cations in the alginate gels, making the surrounding environment of the hydrogels during storage and testing is an important consideration [59]. For alternative options to store the gel, NaCl solution (150mM, 2mM  $\text{CaCl}_2$ ) and no-storing solutions were looked into.

Removing excess  $\text{Ca}^{2+}$ -ions could cause a reduction in number and/or length of junction zones [22], expecting a reduction in variation of  $G'$ -values. When a gel undergoes compression, it will eventually lead to syneresis [29]. Hypothesizing that the expulsion of water from the gel will be sufficient enough to prevent the gel from drying out, measurement with no storing solution was also performed. Again, the normal force acting on the probe by the gels were measured and plotted against the change in gap. Figure 4.4.1 shows the results.

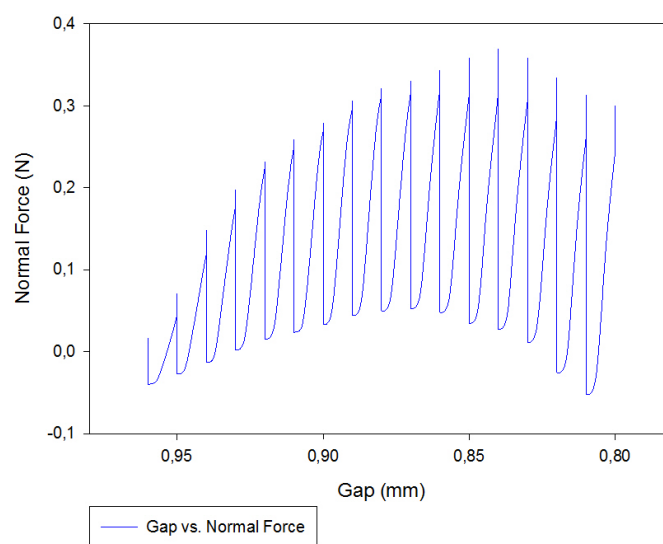
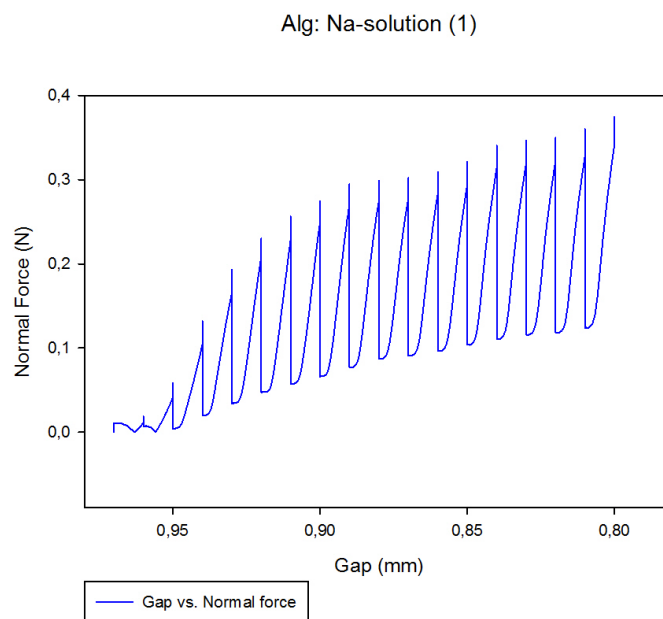


Figure 4.4.1: (a) Normal force as a function of measuring height for alginate gel stored with NaCl solution. (b) Normal force as a function of measuring height for alginate gel stored in no storing solution. Both measurements were performed by loading 1.8 % (w/v) Alginate solution ( $60 \mu\text{L}$ ) to the lower geometry. Gap between the plates were adjusted to 1 mm.  $50\text{mM CaCl}_2$  (2 mL) as gelling solution. One hour of gelation took place before the gap was by 0.01 mm stepwise until a total reduction to 0.80mm.

Alginate gels stored with NaCl-solution shows an increase in normal force after at 0.95 mm, as observed in Figure 4.4.1a. The corresponding y-value ( $x=0.95$  mm) was set to zero. Subsequent values for normal force were adjusted to the respective y-value. The normal force is measured to be increasing rapidly after establishing contact point as the gap is reduced, indicating that deformation is applied on the gel. Additionally, a increasing incline in baseline for the starting value for normal force after each height

reduction is observed for alginate gel stored in NaCl-solution.

This trend is also observed for the gel with no storing solution until 0.85 mm. After this point, the normal force is measured to be lower than the initial starting value, as observed in Figure 4.4.1b. The shrinkage of the gel under the probe could be the reason for intense reduction in measured the normal force. The moisture from the liquid separated from the gel matrix, was not sufficient enough to prevent the gel from drying.

#### 4.4.1 Dependence of elastic modulus in alginate gels in alternative storing solution on measuring height

Further, to examine the effect of changing the storing solution on the rheological properties, frequency sweep were performed on both gels at each height. The elastic modulus measured at 1 Hz plotted against the change in height is given in Figure 4.4.2.

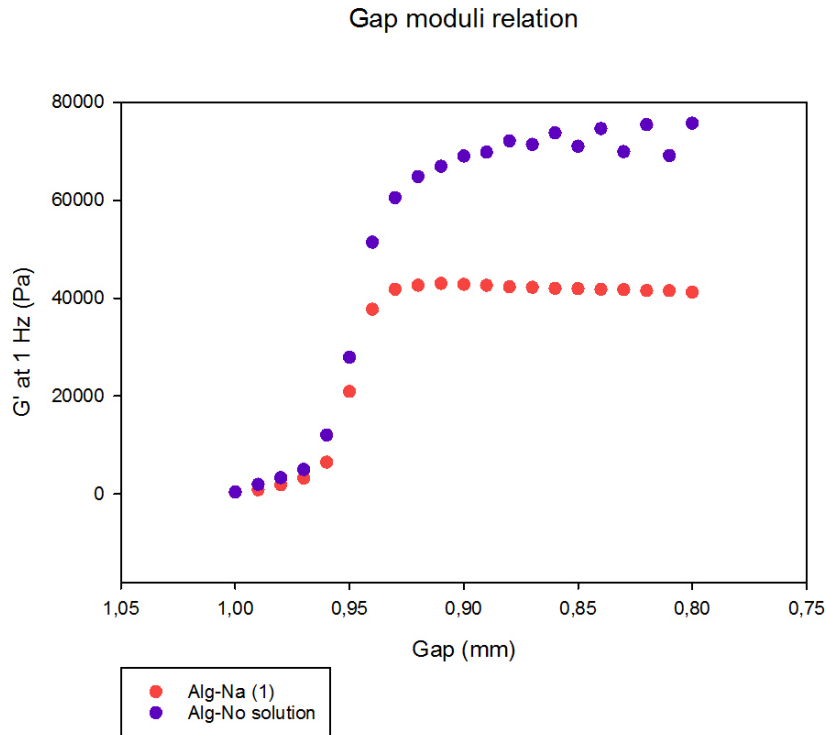


Figure 4.4.2:  $G'$  at 1 Hz (Pa) plotted against the gap height for Alg-Na (1) gel (red) and Alg-no solution gel (purple).

For both measurements, the elastic modulus is increasing with reducing height as observed in Figure 4.4.2. Storage solutions are designed to preserve the properties of the material being studied and ensure its stability over time. Based on initial results from the measurements in NaCl-solution and with no storing solution appear to inhibit additional  $\text{Ca}^{2+}$ -crosslinks during reduction in measuring height, resulting in less alteration in elastic modulus with reducing gap.

The elastic modulus has fluctuating values with increasing compression, this could be an indication of the gel drying out. The values obtained from this measurements will not give a realistic value for  $G'$ . However, the gel stored in NaCl solution have promising results as  $G'$  appear to be less altered with reducing height.

## 4.5 Rheological analysis of alginate gels in NaCl solution

Initial analysis of alginate gels stored with NaCl-solution demonstrate promising data, in terms of inhibiting the addition  $\text{Ca}^{2+}$ -ions cross-links during compression. To further assess the reliability of the obtained values, it is necessary to evaluate the gel with regard to syneresis.

### 4.5.1 Evaluating syneresis in alginate gels stored with NaCl solution

Figure 4.4.1a demonstrated an initial increase in normal force when the gap was reduced to 0.95 mm. In investigate if the initial increase in normal force is due a contact point establishing between the instrument and gel, the mechanical spectra at 0.95 mm for Alg-Na(1) was further examined. Figure 4.5.1 present the mechanical spectra for Alg-Na(1) at 0.95 mm.

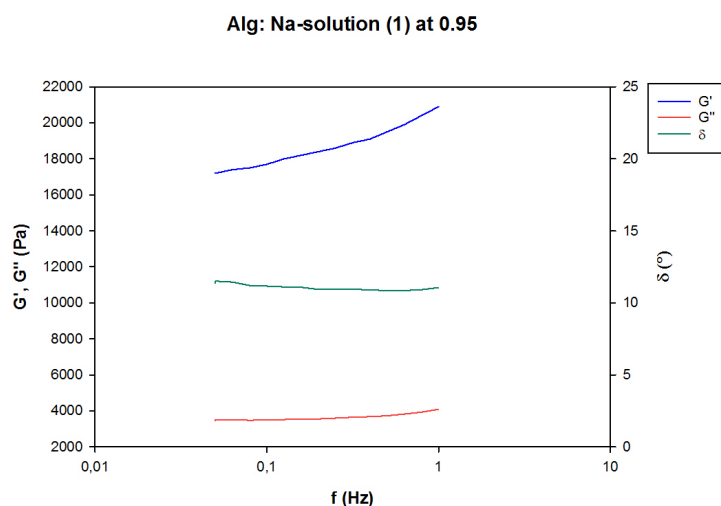


Figure 4.5.1: Frequency sweeps of Alg-Na (1) at 0.95 mm. Elastic modulus (blue), viscous modulus (red) and phase angle (green) is plotted on y-axis against the frequency on the x-axis for 1.8 % (w/v) alginate gel gelled with (50 mM)  $\text{CaCl}_2$  solution and stored in NaCl solution. All values are obtained from frequency sweeps (1-0.05 Hz) performed at 20°C with 0.1 % constant shear strain and 10 measurements per decade

At 0.95 mm gap reduction the frequency sweeps show a elastic dominant behavior for all alginate gels, as the  $G' > G''$ , observed in Figure 4.5.1 for Alg-Na(1) gel. The phase angle is measured to be 11.4° at 0.05 Hz and 11.1° at 1 Hz, which aligns with the expected values. Figure 4.5.1 present the mechanical spectra within the criteria, which confirms that a contact point between the gel and the instrument has been established. This implies that reasonable rheological data could be obtained from this point.

Initial analysis of alginate gel stored with NaCl solution appear to be showing promising results, when evaluated in terms of syneresis. Contact point is established between the gel and instrument in order to reasonably determine the rheology for the gel. In order



to have reliable data for alginate gel stored with NaCl solution, these measurements must be repeated.

#### **4.5.2 Reproducibility of rheological data obtained for alginate gels in NaCl solution**

The initial analysis of alginate gels stored with NaCl-solution appear to produce promising data. The experiments were repeated to ensure reproducibility of the values. Additional measurements was performed by loading 1.8% (w/v) alginate solution to the lower geometry. Gap between the plate was adjusted to 1 mm, to ensure proper loading. (50 mM)  $\text{CaCl}_2$  solution (2 mL) was added to the lower geometry. Gelation occurred for one hour before  $\text{CaCl}_2$  solution was removed and NaCl (2 mL) solution was added. The gap was then reduced by 0.01 mm stepwise.

To determine the contact point between the instrument and the gel, the gap was reduced and normal force was monitored to locate the contact point. The measured normal force was then further plotted against the gap height resulting in Figure 4.5.2 for alginate gels.

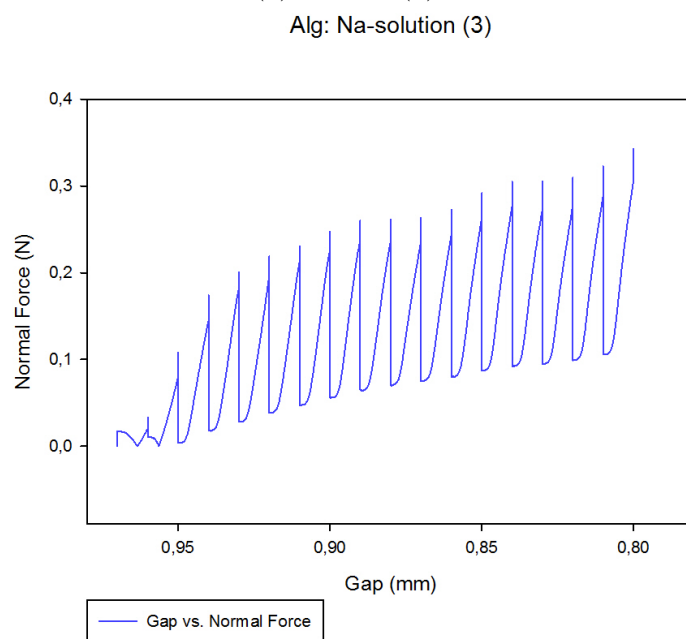
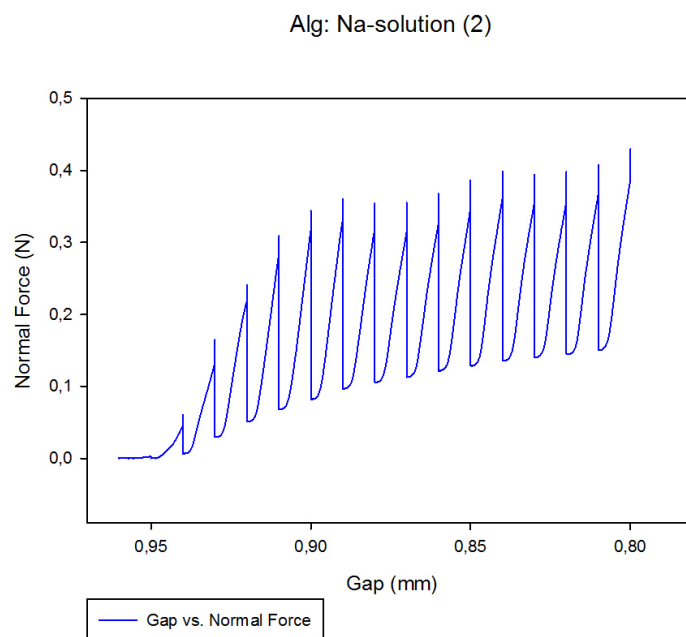
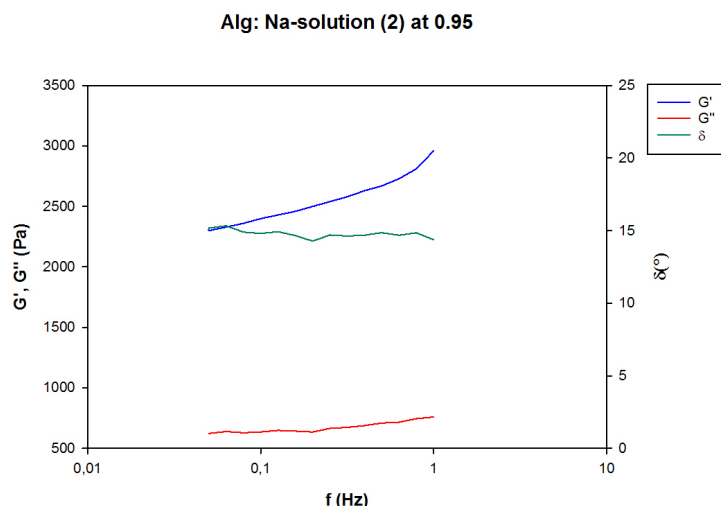


Figure 4.5.2: (a) Normal force as a function of measuring height for Alg-Na(2) gel. (b) Normal force as a function of measuring height for Alg-Na(3) gel. Both measurements were performed on 1.8 % (w/v) 80/20 alginate/sulfated alginate solution ( $60 \mu\text{L}$ ) which was loaded to the lower geometry and the distance between the plates was set to 1 mm. 50 mM  $\text{CaCl}_2$  (2mL) was added to the lower geometry for gelling. One hour of gelation occurred before removing the  $\text{CaCl}_2$  solution and adding NaCl solution was added. The gap was reduced by 0.01 mm stepwise to a total reduction to 0.80 mm.

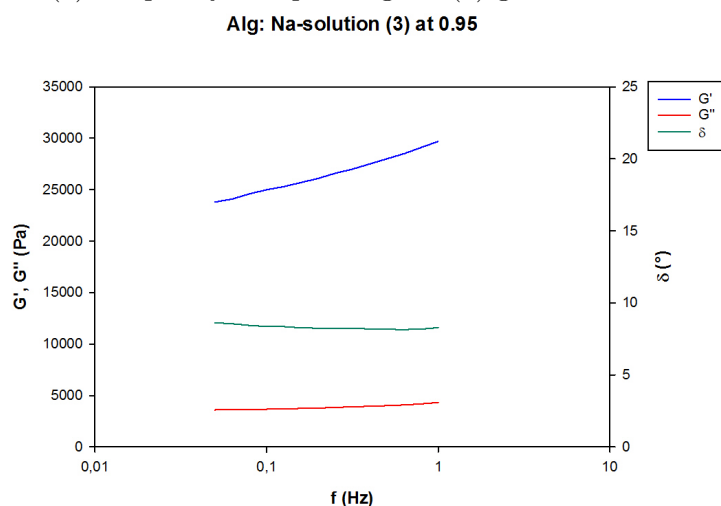
Initial increase in normal force occurred when the gap was reduced at 0.95 mm for Alg-Na(2) gel and Alg-Na(3) gel, implying that some contact point had been established between the gel and the instrument. The curve was adjusted by setting the corresponding

y-value ( $x = 0.95$  mm) to zero and adjusting the subsequent the values for normal force according to the y-value. As presented in Figure 4.5.2a and 4.5.2b, for Alg-Na(2) gel and Alg-Na(3) gel respectively. After establishing contact, the gap was further reduced to understand the consequences of compression on the gel. With reducing gap, the normal force is measured to be increasing rapidly with each compression. The values for normal force do not return to its initial starting value during the hold time, before the gap is reduced further. This is observed as an incline in the starting value for normal force. This trend is observed for both gels.

Further, frequency sweep of the gels was performed to characterized the mechanical properties for both gels. To ensure that the contact point for each gel occurred at 0.95 mm the mechanical spectra at 0.95 mm was further looked into for the pure alginate gels and presented in Figure 4.5.3.



(a) Frequency sweep of Alg-Na (2) gel at 0.95 mm



(b) Frequency sweep of Alg-Na (3) gel at 0.95 mm

Figure 4.5.3: (a) Frequency sweeps of Alg-Na(2) gel at 0.95 mm. (b) Frequency sweeps of Alg-Na(3) gel at 0.95 mm. Elastic modulus (blue), viscous modulus (red) and phase angle (green) is plotted on y-axis against the frequency on the x-axis for both gels. For 1.8 % (w/v) alginate gel gelled with 50 (mM)  $\text{CaCl}_2$  solution and stored in NaCl solution. All values were obtained from frequency sweeps (1-0.05 Hz) performed at 20°C with constant shear strain at 0.1% and 10 measurements per decade.

At 0.95 mm gap reduction the frequency sweeps show an elastic dominant behavior for both alginate gels, as the  $G' > G''$ , observed in Figure 4.5.3a for Alg-Na(2) gel and Figure 4.5.3b for Alg-Na (3) gel. Moreover, for Alg-Na(2) the phase angle is measured to be 15.0° at 0.05 Hz and 14.4° at 1 Hz. The initial high value for phase angle could be an indication of the instrument being in contact with a part of the gel. Syneresis causes shrinkage which could lead to uneven surface on the gel. The initial increase in normal force could be caused by being in contact with the uneven surface. The mechanical spectra obtained at 0.95 mm for Alg-Na(2) gel do not meet the criteria established by previous work on characterizing the rheological properties of alginate, due to the elevated values obtained for the phase angle. For Alg-Na(3) gel the phase angle was measured to be 8.6° at 0.05 Hz and 8.3° at 1 Hz and, which is in accordance with the expected values

for the phase angle.

To see if gap reduction could compensate for syneresis in Alg-Na(2) the gap was reduced further. The mechanical spectra at 0.94 mm was therefore further looked into, presented in Figure 4.5.4

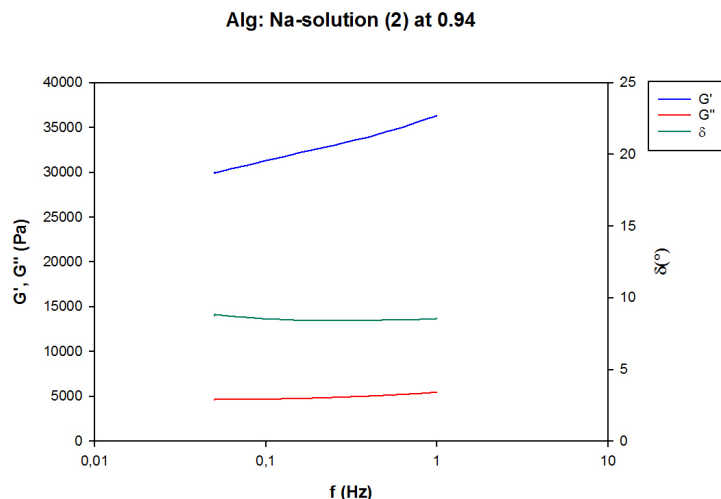


Figure 4.5.4: Frequency sweeps of Alg-Na(2) at 0.94 mm. Elastic modulus (blue), viscous modulus (red) and phase angle (green) is plotted on y-axis against the frequency on the x-axis. For 1.8 % (w/v) alginate gel gelled with (50 mM)  $\text{CaCl}_2$  solution. All values are obtained from frequency sweeps (1-0.05 Hz) performed at 20°C with 0.1 % constant shear strain, with 10 measurements per decade.

When the gap was reduced further by 0.01 mm it is with certainty that the frequency sweep was performed on the entire gel surface, as the mechanical spectra illustrates an elastic dominant behavior with a phase angle in the expected range of values. This demonstrate that syneresis could be compensated by reducing the gap between plates, to obtain sufficient contact to provide reasonable rheological data for Alg-Na(2) gel.

### 4.5.3 Dependence of elastic modulus in alginate gel stored in NaCl solution on measuring height.

The elastic behavior of a material under compression can be studied further by exploring the development of  $G'$  at 1 Hz against the reducing gap height. Figure 4.5.5 presents the resulting plot.

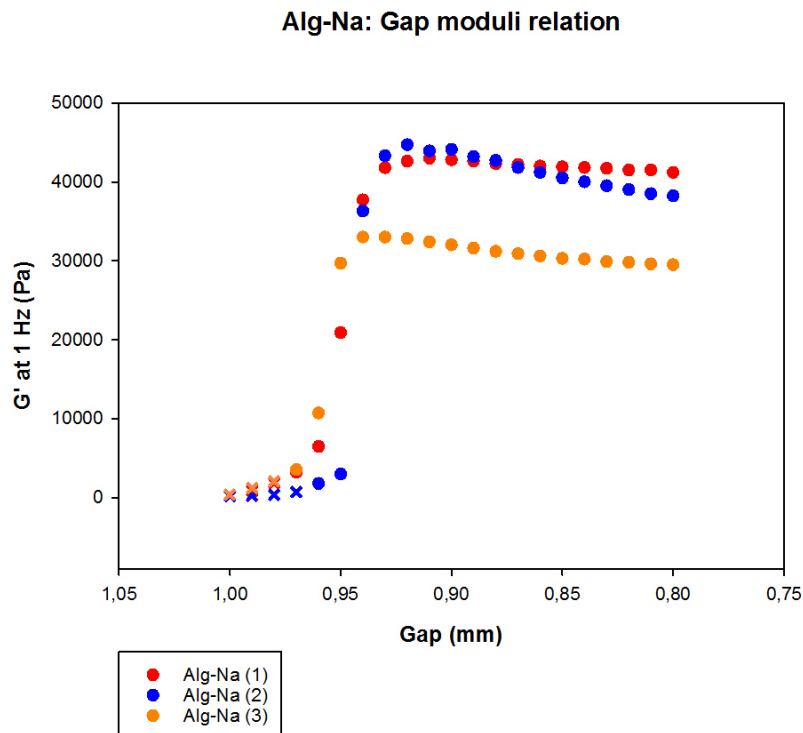


Figure 4.5.5:  $G'$  at 1 Hz (Pa) plotted against the gap height for Alg-Na (1) gel (red), Alg-Na(2) gel (blue) and Alg-Na (3) gel (orange). The values are from the first contact point with the gel and the measured  $G'$ -value, any value measured before that is noted with a cross.

Elastic modulus is observed to be increasing with reducing gap height as seen in Figure 4.5.5. The initial increase in moduli could be due to additional cross-links formed with  $\text{Ca}^{2+}$ -ions, if removal of  $\text{CaCl}_2$  is not sufficient.

Overall, all three measurements have a similar trend, where the elastic modulus reaches a plateau rapidly with reducing gap height. The plateau region in the  $G'$  curve signifies that the material has attained a maximum level of structural rigidity, implying that the gel is highly cross-linked or microdamages occurring in the gel. Microdamage could be a result of a weaker gel network as a consequence of storing the gels in NaCl solution. The removal of cross-linking ions (e.g  $\text{Ca}^{2+}$ ) causes a reduction in the number and/or length of junction zones, which destabilizes the network and weakens the resistance against the external osmotic pressure [60]. Making the gel more prone towards microdamage. This was further looked into in Appendix D, however the results were not sufficient enough to make a conclusion on whether microdamage had occurred or not.

Initial analysis of alginate gels stored with NaCl solution suggested that removing the additional  $\text{Ca}^{2+}$ -cross-links will result in less alteration in elastic modulus. To some extent this appear to be true, as the elastic modulus does not exhibit the rapid growth in values with increasing compression. However the rapid reach of plateau for alginate gels in NaCl solution, makes it challenging to determine the accuracy of the measured values for  $G'$ ,  $G''$  and  $\delta$ . Moreover, to investigate if this is the case for alginate/sulfated alginate gel and alginate/fucoidan gel, further measurements with NaCl solution as storage solutions was conducted.

## 4.6 Rheological analysis of alginate/sulfated alginate gels in NaCl solution

Chemical modification of alginate is widely used to transform physicochemical properties of alginate [7]. Introduction of sulfate groups to the alginate structure leads to changes in gelling properties, that would effect the viscoelastic properties of the gel. To investigate this further, a fraction of alginate solution was replaced with sulfated alginate and the viscoelastic properties of this gel was characterized.

For all measurements 1.8 % (w/v) 80/20 alginate/sulfated alginate solution was loaded to the lower geometry. Gap between the measuring plates were adjusted to 1 mm between the plates, ensure proper loading of sample. (50 mM)  $\text{CaCl}_2$  solution (2mL) was added for gelation. One hour of gelation took place, before  $\text{CaCl}_2$  solution was removed and (150 mM) NaCl solution was added. The gap was then reduced stepwise by 0.01 mm.

### 4.6.1 Evaluating syneresis in alginate/sulfated alginate gels

The normal force acting on the probe by the gels were measured after each compression and plotted against the gap height. Gap height plotted against normal force for Alg/SA-Na(1) gel given in Figure 4.6.1.

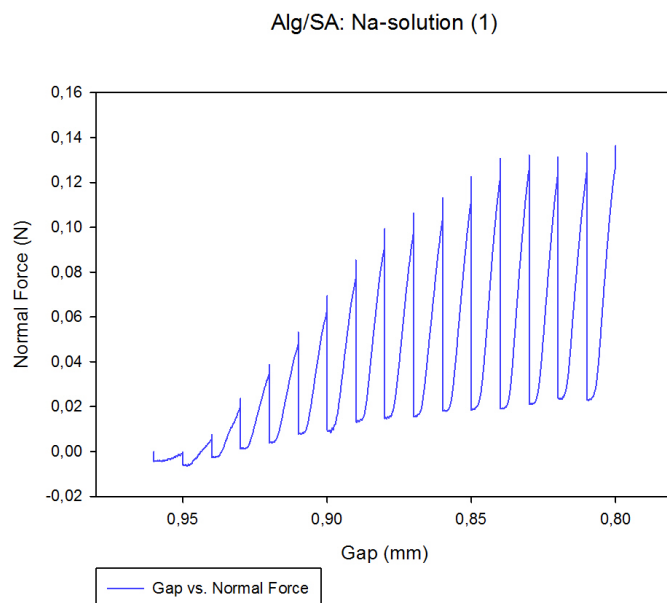


Figure 4.6.1: Normal force as a function of measuring height for Alg/SA-Na(1) gel. Measurement was performed on 1.8 % (w/v) 80/20 alginate/sulfated alginate solution (60  $\mu\text{L}$ ) was loaded to the lower geometry and the distance between the plates was set to 1 mm. 50 mM  $\text{CaCl}_2$  (2mL) was added to the lower geometry for gelling. One hour of gelation occurred before removing  $\text{CaCl}_2$  solution and adding NaCl solution (2 mL) was added. The gap was reduced by 0.01 mm stepwise to a total reduction to 0.80 mm.

The first initial measurement of normal force was recorded at 0.96 mm as observed in Figure 4.6.1. The rapid increase in measured normal force is due to increasing compression applied on the gel after establishing contact. Further, the gel is appearing to

be relaxing during the hold time which is noted by the reduced values for normal force. Overall, the plot is behaving similarly as pure alginate gels, apart for the absolute values for normal force is measured to be lower for alginate/sulfated alginate gels.

To determine if the initial increase in normal force is likely due to a contact point establishing between the instrument and the gel, the mechanical spectra at 0.96 mm is looked into. The values for  $G'$ ,  $G''$  and  $\delta$  obtained from performing a frequency sweep at 0.96 mm is plotted against the frequency range, resulting in Figure 4.6.2

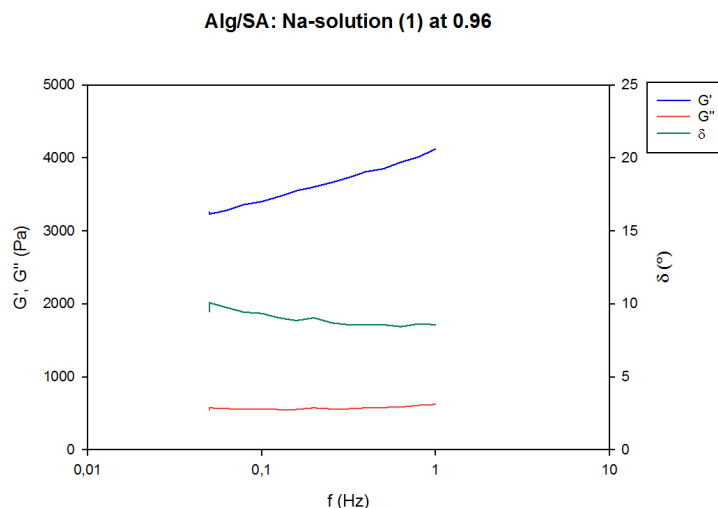


Figure 4.6.2: Frequency sweeps of Alg/SA-Na(1) gel at 0.96 mm. Elastic modulus (blue), viscous modulus (red) and phase angle (green) is plotted on y-axis against the frequency on the x-axis. Values are obtained for 1.8 % (w/v) 80/20 alginate/sulfated gelled with 50 (mM)  $\text{CaCl}_2$  solution and stored in NaCl solution. Frequency sweep (1-0.05 Hz) was performed at 20°C with a constant shear strain at 0.1 %, with 10 measurements per decade.

Figure 4.6.2 shows that at 0.96 height the elastic behavior is the dominant behavior. The phase angle 9.6° at 0.05 Hz and 8.6° at 1 Hz. Initial value for phase angle for is slightly elevated than the expected average value for alginate gels. This could be due the a fraction of alginate being replaced with sulfated alginate. Since there is limited research based on dynamic measurements of sulfated alginate, increasing the difficulty to determine the expected value. However, phase angle did not have a considerable increase and the values can be considered acceptable.

#### 4.6.2 Reproducibility of the rheological data obtained for alginate/sulfated alginate gels stored with NaCl solution

The initial measurement of alginate/sulfated alginate present data that could provide reasonable results. To further verify the results, the measurements must be repeated. Additional measurements with alginate/sulfated alginate was performed. The measured normal force applied on the probe by the gels was monitored and plotted against the change in gap given in Figure 4.6.3 for both measurements.



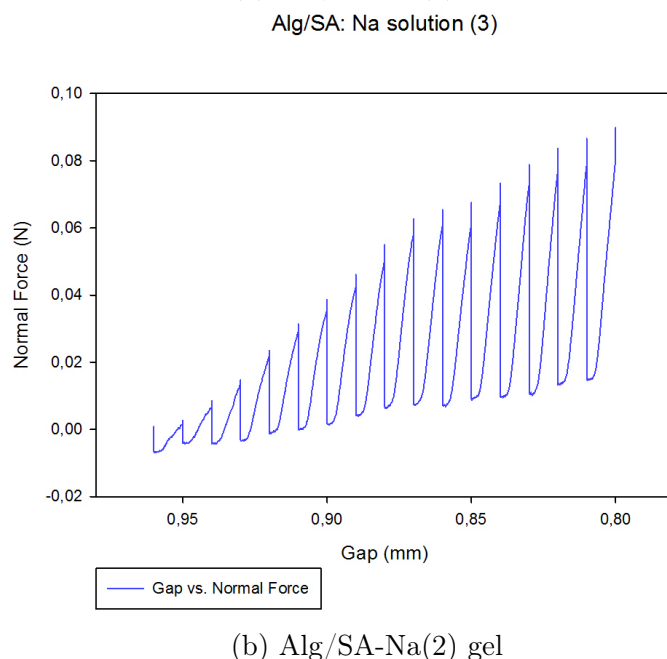
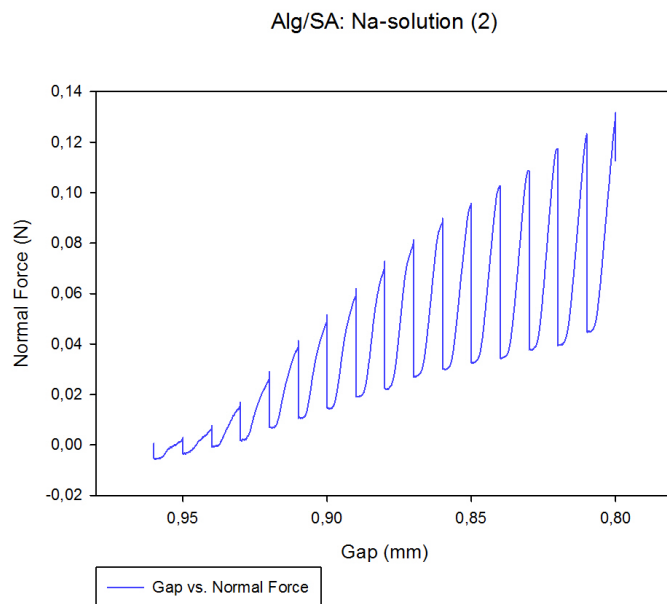
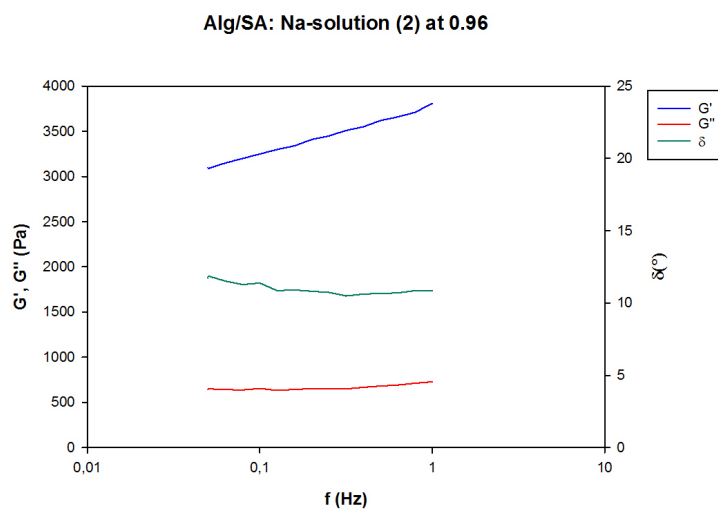


Figure 4.6.3: (a) Normal force as a function of measuring height for Alg/SA-Na(2) gel. (b) Normal force as a function of measuring height for Alg/SA-Na(3) gel. Measurements were performed by loading 1.8 % (w/v) 80/20 alginate/sulfated alginate solution ( $60 \mu\text{L}$ ) the lower geometry and the distance between the plates was set to 1 mm. 50 mM  $\text{CaCl}_2$  (2mL) was added to the lower geometry for gelling. One hour of gelation occurred before  $\text{CaCl}_2$  solution was removed and NaCl solution was added. The gap was reduced by 0.01 mm stepwise to a total reduction to 0.80 mm for both gels.

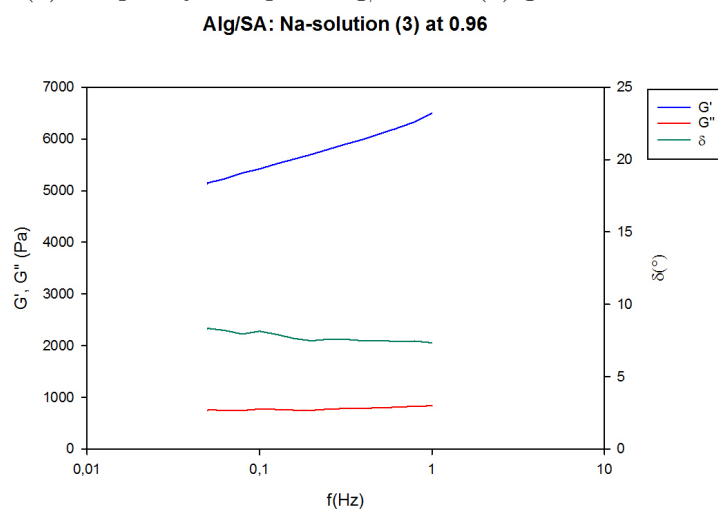
The first initial measurement of normal force was observed at 0.96 mm for both gels. The corresponding y-value ( $x = 0.96 \text{ mm}$ ) was set to zero. Subsequent values for normal force was adjusted to the y-value, resulting in Figure 4.6.3a for Alg/SA-Na(2) gel and Figure 4.6.3b for Alg/SA-Na(3) gel. Normal force acted on the probe applied by the gel was monitored through the gap reduction and is appearing to be increasing with gap

reduction, in the same pattern as observed for Alg/SA-Na(1) gel.

Further, to determine whether the initial increase in normal force was due to reaching the contact point between the instrument and the gel, the mechanical spectra at 0.96 mm for all three gels were further looked into. Figure 4.6.4 present the mechanical spectra for Alg/SA-Na(2) gel and Alg-SA-Na(3) gel.



(a) Frequency sweep of Alg/SA-Na (2) gel at 0.96 mm



(b) Frequency sweep of Alg/SA-Na (3) gel at 0.96 mm

Figure 4.6.4: (a) Frequency sweep of Alg/SA-Na(2) gel at 0.96 mm. (b) Frequency sweep of Alg/SA-Na (3) gel at 0.96 mm. Elastic modulus (blue), viscous modulus (red) and phase angle (green) is plotted on y-axis against the frequency on the x-axis for both gels. For 1.8 % (w/v) 80/20 alginate/sulfated gelled with 50 (mM)  $\text{CaCl}_2$  solution and stored in NaCl solution. Frequency sweeps (1-0.05 Hz) were performed at 20°C with a constant shear strain at 0.1 % and 10 measurement per decade.

Figure 4.6.4 shows that at 0.96 mm the elastic behavior in the gel is dominant. The phase angle has a slightly elevated value for compared to pure alginate for both gels, in accordance with the results obtained for Alg/SA-Na(1).

All three gels with alginate/sulfated alginate suggests that reasonable data for the rheological properties are obtainable at 0.96 mm.

### 4.6.3 Dependence of elastic modulus in alginate/sulfated alginate gels stored in NaCl-solution on measuring height

Further, frequency sweep was performed on the gel at each set gap. The resulting  $G'$ ,  $G''$  and  $\delta$  values were plotted against the frequency for each gel to understand how the gels responds to the deformation applied. To get an overview of how the elastic behavior of the gel with change in height.  $G'$  at 1 Hz was plotted against the gap height, and the results are given in Figure 4.6.5.

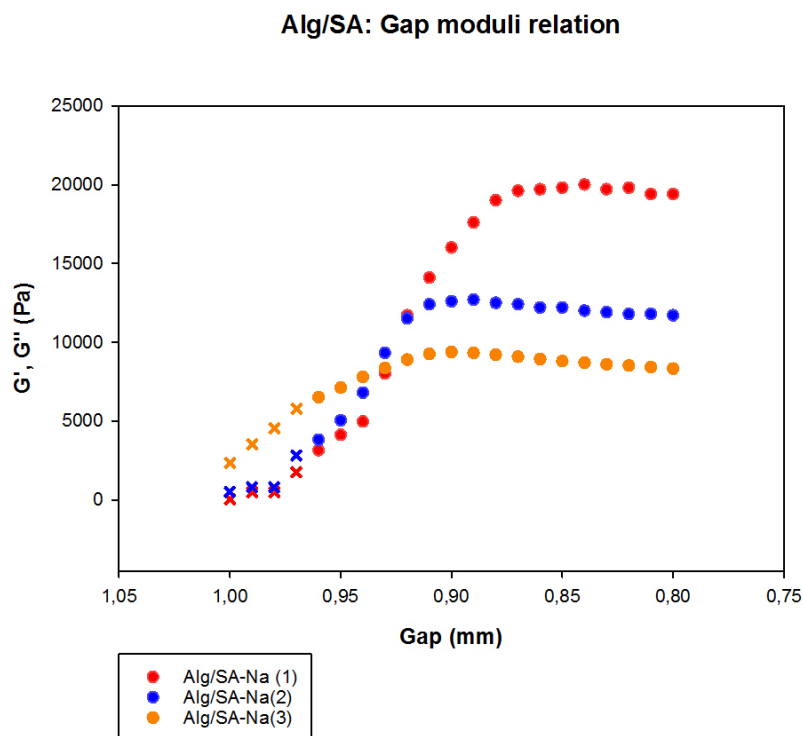


Figure 4.6.5:  $G'$  at 1 Hz (Pa) plotted against the gap height for Alg/SA-Na (1) gel (red), Alg/SA-Na(2) gel (blue) and Alg/SA-Na (3) gel (orange). The values are from the first contact point with the gel and the measured  $G'$ -value, any value measured before that is noted with a cross.

The elastic moduli in alginate/sulfated alginate develops gradually before a plateau is reached with reducing gap height. The initial increase at lower degree of compression could be due to alginate forming cross-links with  $\text{Ca}^{2+}$ -ions, if removal of  $\text{CaCl}_2$  solution was not sufficient enough. In addition, sulfated alginate are binding polymers [7], depending on the substitution degree, the structure still consist of G-blocks that contribute to the gelation with divalent ions like  $\text{Ca}^{2+}$ -ions, that will contribute to the increased elastic modulus. Moreover, the elastic modulus is observed to reach a plateau, which is most likely due to storing the gel in NaCl solution, that does not contribute to increasing the gel's elastic moduli.

Moreover, contrary to alginate gels the elastic modulus appear to increase more gradually before reaching a plateau. This could indicate that substitution of a fraction of

alginate with sulfated alginate appear to interfere with the gel matrix. The presence of sulfated alginate might make the gel less resistant towards deformation, leading to a gradual increase in elastic modulus with reducing gap. This trend is observed for all three measurements with 80/20 alginate/sulfated alginate mixture.

## 4.7 Rheological analysis of alginate/fucoidan gels stored in NaCl-solution

Initial data obtained from alginate/fucoidan in  $\text{CaCl}_2$  solution provided promising for elastic modulus. The presence of excess  $\text{Ca}^{2+}$ -ions altered the  $G'$ -values during compression for alginate/fucoidan, although not to the same extent as pure alginate. Based on the current findings, it can be inferred that storing the gel in NaCl-solution would result in a lower degree of alteration under increased compression. This could result in a more reasonable data for 80/20 alginate/fucoidan gels.

For all measurements 1.8 % (w/v) 80/20 alginate/fucoidan solution was loaded to the lower geometry. Gap between the measuring plates were adjusted to 1 mm between the plates, ensure proper loading of sample. (50 mM)  $\text{CaCl}_2$  solution (2mL) was added for gelation. One hour of gelation took place, before  $\text{CaCl}_2$  solution was removed and (150 mM) NaCl solution was added. The gap was then reduced stepwise.

### 4.7.1 Evaluating syneresis in alginate/fucoidan gel stored with NaCl-solution

To evaluate effect of syneresis in alginate/fucoidan gel stored with NaCl solution, the gap height was reduced and normal force was monitored through the reduction. The measured values for normal force was then plotted against the change in gap height. Resulting plot for Alg/FD-Na(1) is presented in Figure 4.7.1.

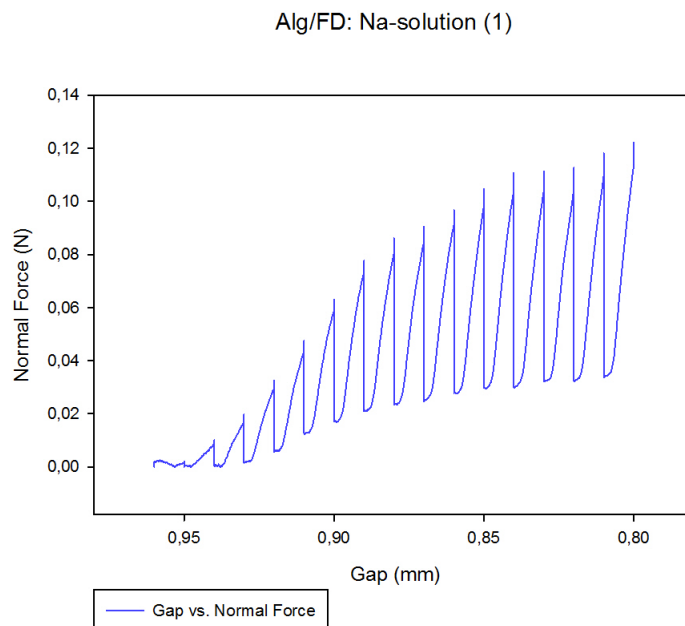
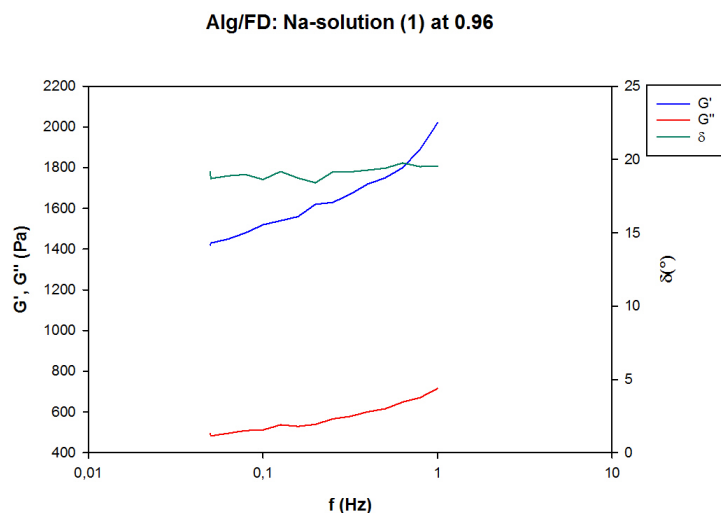


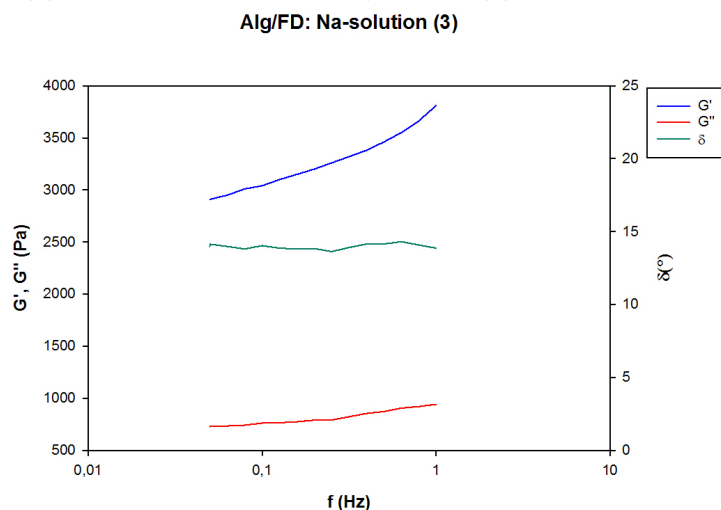
Figure 4.7.1: Normal force as a function of measuring height for Alg/FD-Na(1) gel. Measurement was performed by loading 1.8 % (w/v) 80/20 alginate/sulfated alginate solution ( $60 \mu\text{L}$ ) the lower geometry and the distance between the plates was set to 1 mm. 50 mM  $\text{CaCl}_2$  (2mL) was added to the lower geometry for gelling. One hour of gelation occurred before  $\text{CaCl}_2$  solution was removed and NaCl solution (2 mL) was added. The gap was reduced by 0.01 mm stepwise to a total reduction to 0.80 mm.

The normal force is developing in the same manner as previously obtained data for alginate/fucoidan in  $\text{CaCl}_2$  solution. The initial increase in normal force is measured to be after the gap is reduced by 0.96 mm. After the initial increase, the normal force is measured to be increasing rapidly with reducing height. This indicates that compression is applied on the gel. Relaxation occurring in the gel during the hold time, is observed as the dissipation of measured normal force.

To determine whether the initial increase in normal force was due to reaching the contact point between the instrument and the entire gel surface, the mechanical spectra at 0.96 mm and 0.95 mm presented in Figure 4.7.2 for Alg/FD-Na(1) gel was looked into.



(a) Frequency sweep of Alg/FD-Na (1) gel at 0.96 mm



(b) Frequency sweep of Alg/FD-Na (1) gel at 0.95 mm

Figure 4.7.2: (a) Frequency sweeps of Alg/FD-Na(1) gel at 0.96 mm. (b) Frequency sweeps of Alg/FD-Na(1) at 0.95 mm. Elastic modulus (blue), viscous modulus (red) and phase angle (green) is plotted on y-axis against the frequency on the x-axis for both gels. For 1.8 % (w/v) 80/20 alginate/sulfated gelled with 50 (mM)  $\text{CaCl}_2$  solution and stored in NaCl solution (2 mL). Frequency sweeps (1-0.05 Hz) were performed at 20°C with a constant shear strain at 0.1 % and 10 measurement per decade.

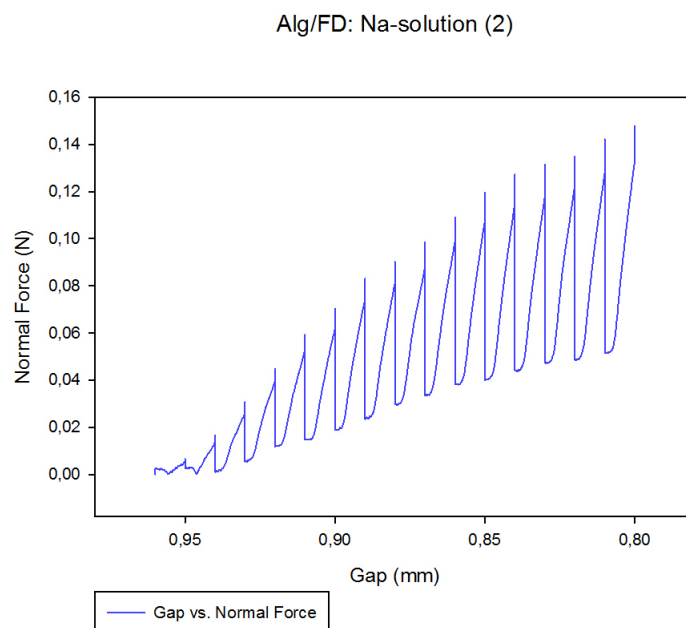
The mechanical spectra at 0.96 presented in Figure 4.7.2a illustrate a elastic dominant behavior in the gel. The elastic modulus is also measured to be 1423 Pa at 0.05 Hz and 2016 Pa at 1 Hz. The phase angle is measured to be 19.2 ° at 0.05 Hz and 19.6° at 1 Hz. The initial high value for phase angle is contrary to the obtained value for alginate/fucoidan gel in  $\text{CaCl}_2$  solution. This could be due to not establishing sufficient enough contact between the gel and the instrument, to provide reasonable data for the rheological properties. The obtained values for  $G'$ ,  $G''$  and  $\delta$  at 0.96 mm for alginate/fucoidan in NaCl solution do not align with criteria established by previous for alginate gel.

Further when gap height was reduced to 0.96 mm the mechanical spectra present in Figure 4.7.2b values for  $G'$ ,  $G''$  and  $\delta$  in accordance with the expected values. The values are

also consistent with the values obtained for alginate/fucoidan gels in  $\text{CaCl}_2$  solution. This indicate that a contact point have been established between the gel and the instrument, that provides reasonable data for the rheological properties.

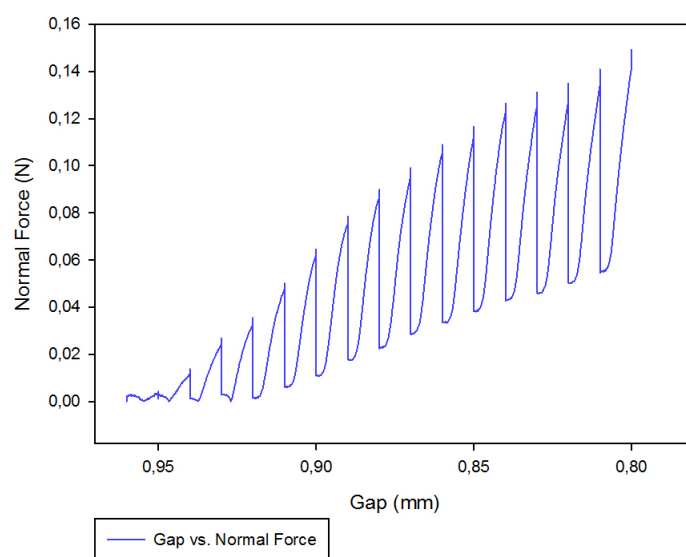
#### **4.7.2 Reproducibility of the rheological data obtained for alginate/fucoidan gels**

In order to obtain reliable measurements, accurate and consistent data must be produced with repeated measurements of the same material under similar conditions yielding consistent results. Hence, additional measurement with alginate/fucoidan solution was conducted. The measured normal force applied on the probe by the gels were plotted against the reducing gap height resulting in Figure 4.7.3.



(a) Alg/FD-Na (2) gel

Alg/FD: Na-solution (3)



(b) Alg/FD-Na (3) gel

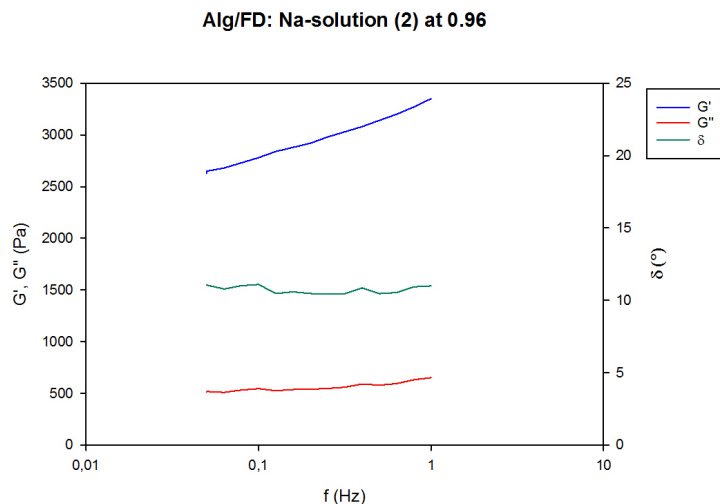
Figure 4.7.3: (a) Normal force as a function of measuring height for Alg/FD-Na(2). (b) Normal force as a function of measuring height for Alg/FD-Na(3). Measurement was performed by loading 1.8 % (w/v) 80/20 alginate/fucoidan solution ( $60 \mu\text{L}$ ) the lower geometry and the distance between the plates was set to 1 mm. 50 mM  $\text{CaCl}_2$  (2mL) was added to the lower geometry for gelling. One hour of gelation occurred before  $\text{CaCl}_2$  solution was removed and NaCl solution was added. The gap was reduced by 0.01 mm stepwise to a total reduction to 0.80 mm.

The development of normal force as a function of measuring height is observed for Alg/FD-Na(1) gel is applicable for Alg/FD-Na(2) gel and Alg/FD-Na(3) gel. When Figure 4.7.3a and 4.7.3b is studied, the contact point is appearing to be around 0.96 as there is a initial increase in normal force. Corresponding y-value ( $x=0.96$  mm) was set to zero,

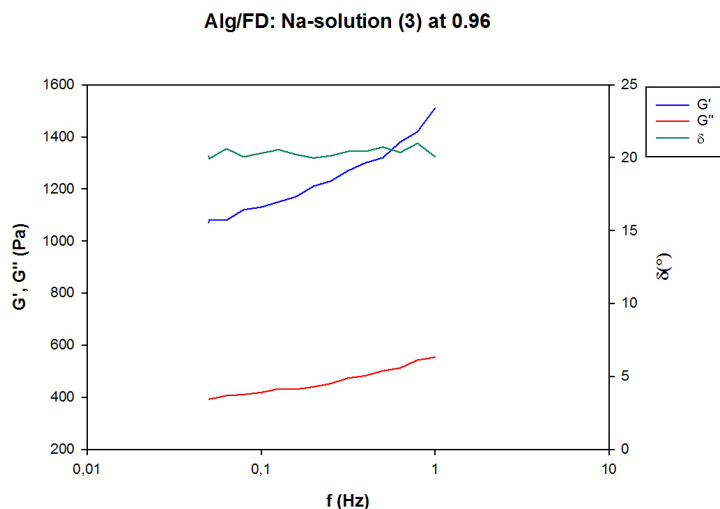


and the subsequent values for normal force was adjusted to the zero value.

To determine whether the initial increase in normal force was due to reaching the contact point between the instrument and the gel, the mechanical spectra at 0.96 mm for both gels were further looked into given in Figure 4.7.4.



(a) Frequency sweep of Alg/FD-Na (2) gel at 0.96 mm



(b) Frequency sweep of Alg/FD-Na (3) gel at 0.96 mm

Figure 4.7.4: (a) Frequency sweeps of Alg/FD-Na(2) at 0.96 mm. (b) Frequency sweeps of Alg/FD-Na(2) at 0.96 mm. Elastic modulus (blue), viscous modulus (red) and phase angle (green) is plotted on y-axis against the frequency on the x-axis, for 1.8 % (w/v) 80/20 alginate/sulfated gelled with 50 (mM)  $\text{CaCl}_2$  solution and stored in NaCl solution. Frequency sweeps (1-0.05 Hz) were performed at 20°C with a constant shear strain at 0.1 % and 10 measurements per decade.

At 0.96 mm the elastic behavior is dominant for both gels. For Alg/FD-Na(2) the phase angle is measured to be in accordance with the previous results obtained for alginate/fucoidan in  $\text{CaCl}_2$  solution, as observed in Figure 4.7.4a. For Alg/FD-Na(1) and Alg/FD-Na(3) the phase angle is measured to 20.2° at 0.05 Hz and 20.1° at 1 Hz, as seen in Figure 4.7.4b. This indicates that contact between the probe and gel has not been

established properly yet or the contact has been established with a part of surface gel, that results in higher initial phase angle-value. When the gap is reduced further with 0.01 mm, the resulting mechanical spectra illustrates adequate contact point between the gel and the instrument to obtain reasonable rheological data, as presented in Figure 4.7.5.

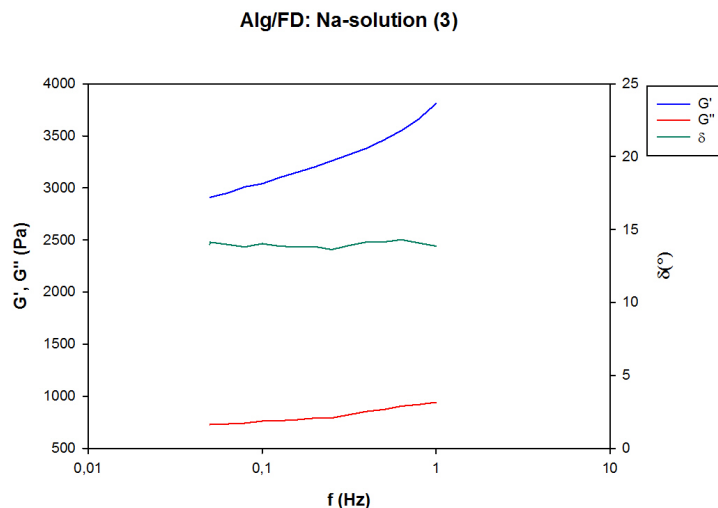


Figure 4.7.5: Frequency sweeps of Alg/FD-Na(3) gel at 0.95 mm. Elastic modulus (blue), viscous modulus (red) and phase angle (green) is plotted on y-axis against the frequency on the x-axis, for 1.8 % (w/v) 80/20 alginate/sulfated gelled with 50 (mM)  $\text{CaCl}_2$  solution and stored in NaCl solution (2 mL). Frequency sweeps (1-0.05 Hz) were performed at 20°C with a constant shear strain at 0.1 % and 10 measurements per decade.

The values obtained at 0.95 mm align with the criteria established for alginate gels as observed in Figure 4.7.5. This implies that reasonable rheological data is obtainable at this point.

### 4.7.3 Dependence of elastic modulus in alginate/fucoidan on measuring height

Properties of the gels, frequency sweep was performed at each set gap. The resulting  $G'$ ,  $G''$  and  $\delta$  was plotted against the frequency at each height. To study the influence of sulfate group on the elastic behavior,  $G'$  at 1 Hz was plotted against gap height, presented in Figure 4.7.6.

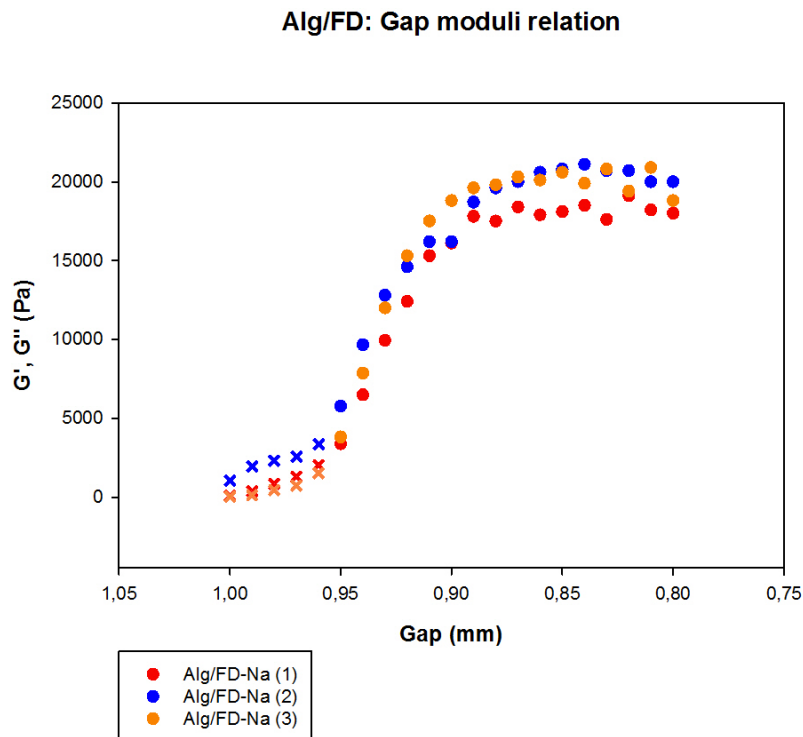


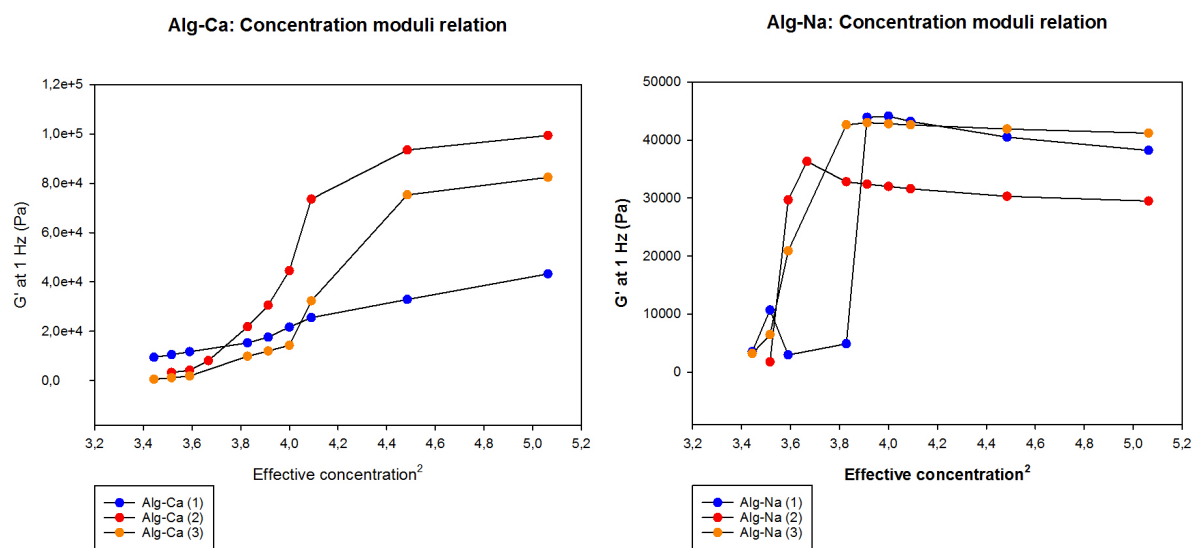
Figure 4.7.6:  $G'$  at 1 Hz (Pa) plotted against the gap height for Alg/FD-Na (1) gel (red), Alg/FD-Na(2) gel (blue) and Alg/FD-Na (3) gel (orange). The values are from the first contact point with the gel and the measured  $G'$ -value, any value measured before that is noted with a cross.

The elastic moduli in alginate/fucoidan gels is gradually increases when the gap is reducing, before reaching plateau. Fucoidan is known to have a softer and less rigid structure [34] compared to alginate, as well as non-gelling properties. The increased modulus as a consequence of increased compression observed in alginate/fucoidan gels in  $\text{CaCl}_2$  solution also applies to alginate/fucoidan gels in  $\text{NaCl}$  solution. The increase in elastic modulus is mostly contributed by the cross-links between junction zones found in alginate and  $\text{Ca}^{2+}$ -ions. However, the enhanced compression of the gel does not significantly modify  $G'$  for alginate/fucoidan gels in  $\text{NaCl}$  solution to the same extent as observed for alginate/fucoidan gel in  $\text{CaCl}_2$  solution. Indicating that storing the gel in  $\text{NaCl}$  solution did have an inhibiting effect on  $\text{Ca}^{2+}$ -cross-links that altered the elastic modulus significantly with increasing compression.

Overall, the elastic moduli in alginate, alginate/sulfated alginate and alginate/fucoidan appear to develop differently. The rapid reach in plateau for  $G'$ -values observed for alginate gels ( Figure 4.5.5) is not observed for alginate/fucoidan, even though alginate is most likely the only structure contributing to increased elastic behavior. The presence of sulfated polymer in the gel appear to prevent the rapid reach of plateau, as observed for alginate/fucoidan and alginate/sulfated alginate gels. This could indicate that when sulfated alginate or fucoidan is present in the gel it functions as driving factor against the rapid growth in  $G'$ -values. In alginate gels there is no additional factors present that prevents the rapid reach of plateau for elastic modulus.

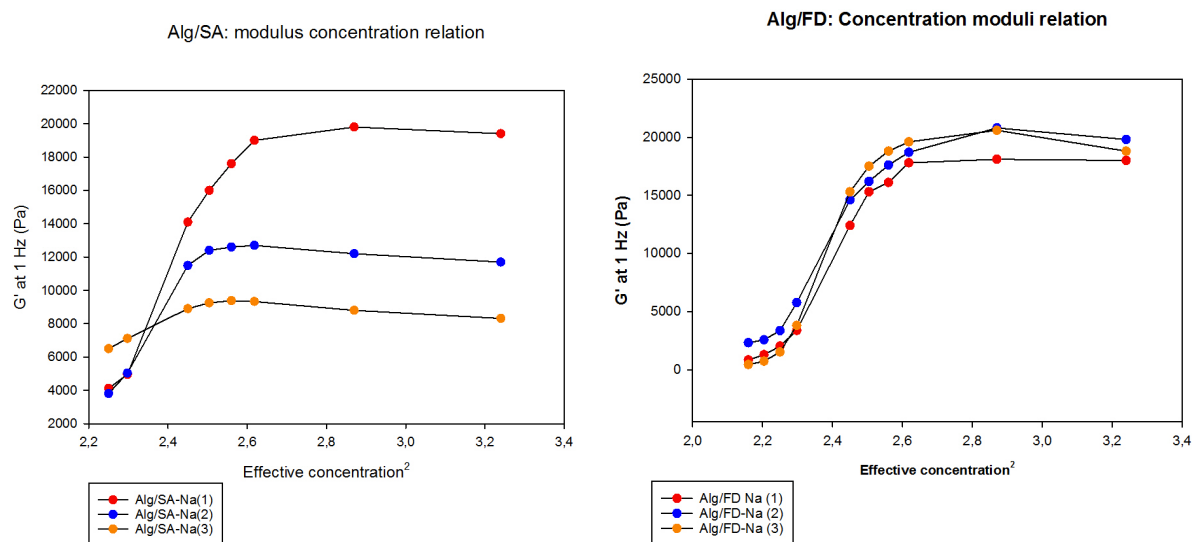
## 4.8 Effective concentration

Dependence of elastic modulus in alginate-based gels on measuring heights, indicate that with compression a volume change occurs in the gels through expulsion of water and an effective increase in alginate concentration within the gel. Under compression a thin disc has limited capacity to accommodate height changes whilst maintaining a constant volume [57]. Theoretically the moduli is proportional to the concentration squared, given that the concentration is the dominant drive of rheological behavior [57]. To examine if a change in concentration leads to increased moduli,  $G'$  at 1 Hz was plotted against effective concentration<sup>2</sup>. Figure 4.8.1 present the resulting plots for alginate gel stored with  $\text{CaCl}_2$  solution and NaCl solution. Figure 4.8.2 illustrates the resulting plots for alginate/ sulfated alginate gels and alginate/fucoidan gels in NaCl solution.



(a) Concentration moduli relation for Alg-Ca gels  
(b) Concentration moduli relation for Alg-Na gels

Figure 4.8.1:  $G'$  at 1 Hz plotted against effective concentration<sup>2</sup> for (a) Alg-Ca gels gelled and stored with  $\text{CaCl}_2$  solution and (b) Alg-Na gels gelled with  $\text{CaCl}_2$  solution and stored in NaCl solution.



(a) Concentration moduli relation for Alg/SA-Na gels (b) Concentration moduli relation for Alg/FD-Na gels

Figure 4.8.2:  $G'$  at 1 Hz plotted against effective concentration<sup>2</sup> for (a) Alg/SA-Na gels gelled with  $\text{CaCl}_2$  solution and stored in NaCl and (b) Alg/FD-Na gels gelled with  $\text{CaCl}_2$  solution and stored in NaCl solution.

For Alg-Ca gels increase linearly with effective concentration at lower degree of compression as observed in Figure 4.8.1a. The proportionality observed at lower degree of compression (up to gap 0.89) for these gels indicate that the alginate concentration was the dominant driving factor for the rheological behavior. The proportionality observed for Alg-Ca gels indicate that at lower degree of compression the modulus is largely a function of effective concentration. This observation provides valuable insights, since compression may be necessary to obtain good contact with both upper and lower geometries to obtain reliable rheological data. At higher degree of compression the elastic modulus increase to most likely due to production of new junction zones. Theoretically, forced rearrangement of polymer chains would force the chains closer together and when excess  $\text{Ca}^{2+}$ -ions are present, new junction zones could be formed [57][4]. This would explain the increase in moduli with increasing compression for pure alginate gels stored with excess calcium with increasing compression applied on the Alg-Ca gels.

Inhibiting the additional  $\text{Ca}^{2+}$  cross-links by changing storing solution, leads to a significant change in elastic modulus. Alg-Na gels have an interesting behavior when  $G'$  is plotted against effective concentration, that is contrary to the other gels. There is no proportionality between moduli and the concentration squared, as Figure 4.8.1b presents. This suggests that the modulus is not a function of the effective concentration. There is another factor is the dominant driver of the rheological behavior, that leads to a increase in modulus for the pure alginate gels stored in  $\text{Na}^+$ -solution.

For Alg/SA-Na gels and Alg/FD-Na gels proportionality between the effective concentration squared and moduli is observed at lower degree of compression, presented in Figure 4.8.2a and Figure 4.8.2b, respectively. The linearity observed for the initial concentrations indicate that with a increasing concentration of alginate could form additional

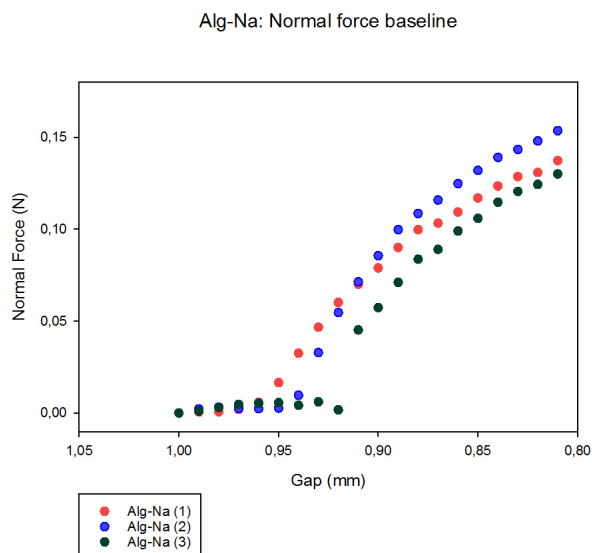
cross-links that would lead to increased modulus. However, after the gap is reduced by 11% the elastic modulus reaches a plateau, this is due to no excess  $\text{Ca}^{2+}$ -ions present in the storing solution, which prevents the increase value for elastic modulus. Sulfated alginate and fucoidan are both sulfated polymers and contain bulky sulfate groups in the structure that would contribute poorly to the gelling network [7] [34]. When a part of alginate is substituted with these structures, it could lead to a reduction cross-links, which would effect the elastic modulus with increasing compression.

For Alg-Ca, Alg/SA and Alg/FD gels the concentration change is a driving factor for the rheological behavior at lower degree of compression. For Alg-Na gels linearity was not observed between the concentration and moduli at any degree of compression. A plateau is observed in all gels, which could indicate anisotropic behavior within the gel at higher degree of compression. Compression can cause the alginate gel to deform and change its native structure leading to a more anisotropic network. The polymer chains may align in the direction of compression, leading to a more ordered network structure [41]. During compression, shear forces are exerted on the gel network. These forces can cause the polymer chains to align and rearrange, potentially disrupting the original homogeneity of the gel [25]. The resulting data obtained from plateau region may not accurately reflect the true nature of the system, due to the anisotropic and inhomogeneous structure within the gel.

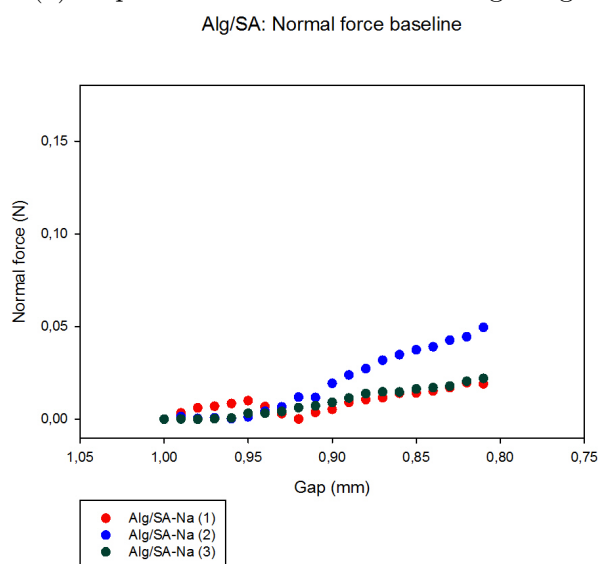
## 4.9 Measuring height normal force relation

In order to have comparable data for the different gels, the dominant driving factor for the rheological behavior in the gels should be constant across the samples. The results obtained until now, suggest that the dominant driving factor in the pure alginate gels stored in NaCl-solution differ from the dominant driving factor in alginate/sulfated alginate and alginate/fucoidan gels.

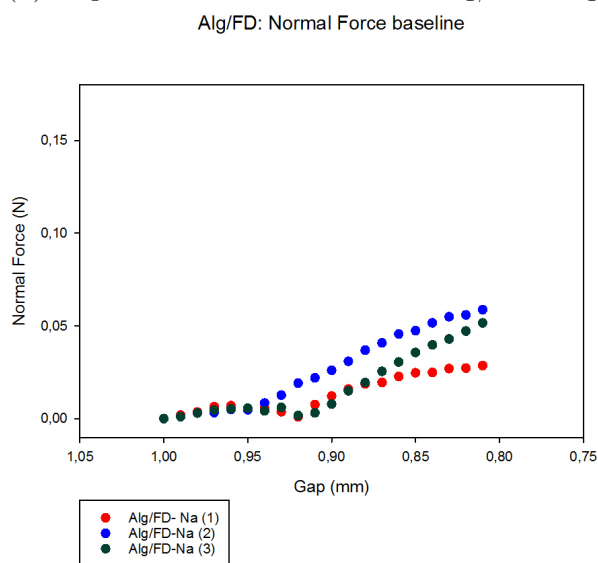
Additional factors that could potentially be the dominant driver of rheological behavior of the gel were therefore further investigated. Experiments performed to this point suggests that there is a variation between the gels, in terms of the absolute values obtained for normal force through gap reduction. In order to study the gap normal force relation, the normal force measured at the starting point at each measuring height was plotted against the gap height. Figure 4.9.1 present the baseline for the measured normal force in each gel stored in NaCl solution.



(a) Gap normal force relation for Alg-Na gels



(b) Gap normal force relation for Alg/SA-Na gels



(c) Gap normal force relation for Alg/FD-Na gels

Figure 4.9.1: Normal force value at the start of each measuring height starting point plotted against the gap height (mm) for Alg-Na gels, Alg/SA-Na gels and Alg/FD-Na gels.

Figure 4.9.2 present the baseline for normal force values for each gel relative to each other.

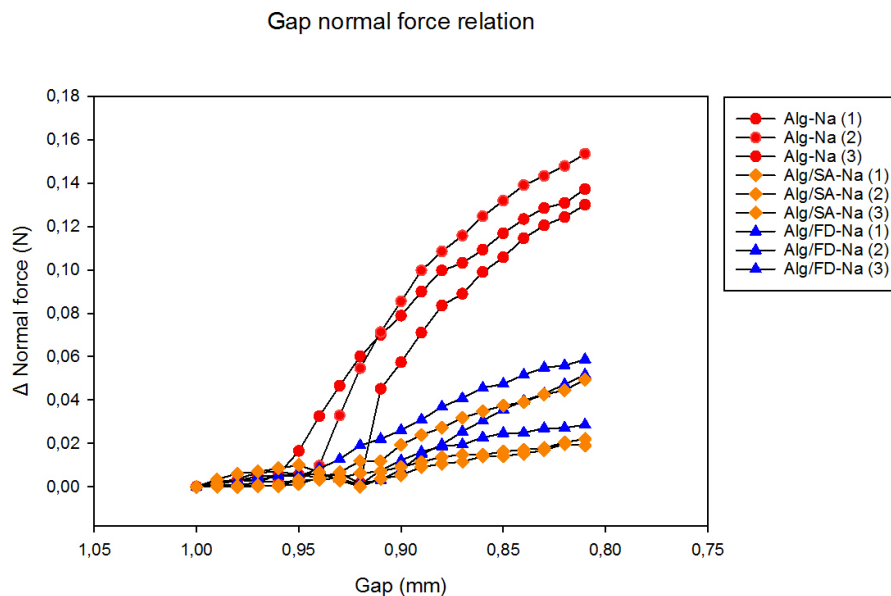


Figure 4.9.2: A overview of normal force values at the start point of each measuring height plotted against the gap height (mm) for Alg-Na gels, Alg/SA-Na gels and Alg/FD-Na gels relative to each other.

Figure 4.9.1a evidently illustrate the inclined baseline for pure alginate gels. Pure alginate gels stored in NaCl-solution have steepest increase, while Alg/SA gels seem to have a more gradually increase with increasing compression as seen in Figure 4.9.1b. Alg/FD gels seem to have a gradual increase up to gap 0.92 before increasing rapidly, as observed in Figure 4.9.1c.

Most biopolymer gels are energetic rather than entropic networks. This implies that the major contribution to the elasticity of the network per elastically active chain, is because the response to deformation involves the adoption of conformationally higher energy states. Once the deformation is removed polymer rearranges to its native state, this is observed as the dissipation of normal force [41] [42]. At each set gap a frequency sweeps was performed on the gel to understand the reaction upon on applying deformation. Hold time was incorporated into the protocol to allow the gel to relax before the gap was reduced further. However, Figure 4.9.2 shows that the gels do not return to it's native state before the gap was reduced further, implying that there is still some stress remaining in the gel, causing an increased value for normal force at each gap height. Based on these measurements, it is evident that the induced stress acts as a artifact causing the  $G'$  to increase steeply, making it challenging to obtain a realistic value for  $G'$ .

The time needed to reach relaxation state is varying for the different for the gels. The results clearly indicate that the pure alginate gel has the most stress remaining in the gel network between each frequency sweep. The induced stress in the gel most likely contribute to rapid increase in elastic modulus as previously observed (Figure 4.5.5). Since the gel is not able to reach its native state before a new deformation is applied, it is necessary to make a value judgment about the quality of the data obtained for alginate



gels in NaCl-solution. Moreover, the incline in starting value for normal force at each measuring height, is also observed for Alg/SA gels and Alg/FD gels at much lower degree. This indicate that these gels are less resistant towards deformation. With these structure present in the solution, the gels are able to return to its native state during the hold time, before additional compression is applied.

## 4.10 Rheological analysis of alginate gels with increased hold time

The effects of induced stress within the gel could be minimized by increasing the relaxation time for the gel. By increasing the hold time between each frequency sweep will allow the gel to return to its native state, before a new gap reduction.

### 4.10.1 Evaluating syneresis in alginate gel with increased hold time

New experiment with increased hold time were performed on alginate gels. 1.8 % (w/v) alginate solution ( $\mu\text{L}$ ) was loaded to the lower geometry and (50mM)  $\text{CaCl}_2$  solution (2mL) added for gelation. Gap between the measuring plates were adjusted to 1mm between the plates, to ensure proper loading of the sample. Gelation occurred for one hour, before  $\text{CaCl}_2$  solution was removed and NaCl solution was added. Probe height was then reduced and a frequency sweep was performed, hold time was increased to one hour before the gap was reduced stepwise further. The normal force was monitored through the gap reduction and plotted against the height, resulting in Figure 4.10.1.

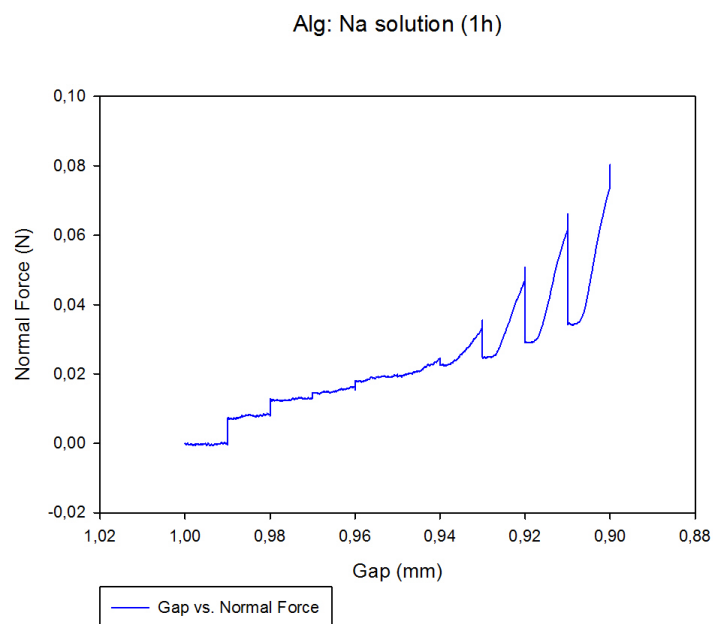
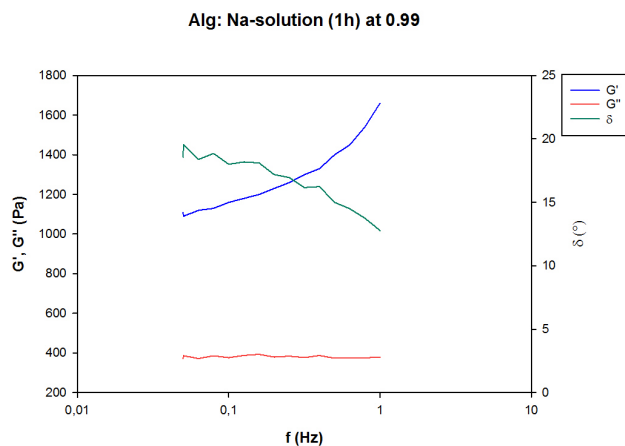


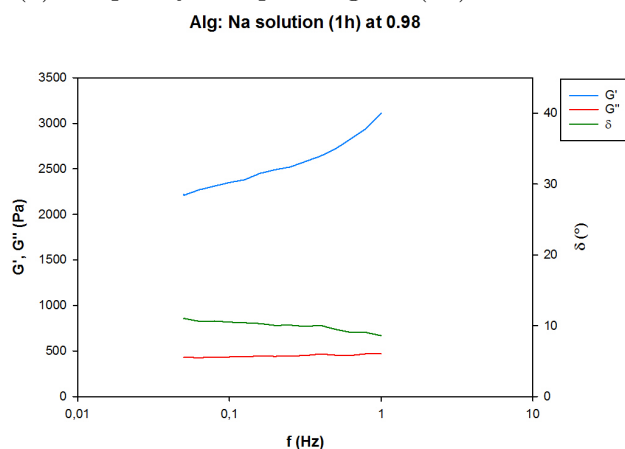
Figure 4.10.1: Normal force as a function of measuring height for Alg/-Na(1 h). Measurements were performed on 1.8 % (w/v) alginate solution (60  $\mu\text{L}$ ) loaded to the lower geometry and the distance between the plates was set to 1 mm. 50 mM  $\text{CaCl}_2$  (2mL) was added to the lower geometry for gelling. One hour of gelation occurred before  $\text{CaCl}_2$  (2 mL) solution was removed and NaCl solution was added (2 mL). The gap was reduced by 0.01 mm stepwise, where one hour was waited before a new height reduction to a total reduction to 0.90 mm.

During these measurements the hold time was increased from 120s to 1 h. There is a slight increase in normal force at 0.99 mm. This could indicate that the contact has been established between the gel and the instrument.

To further ensure that the increase in normal force is due to reaching the contact point, the mechanical spectra at 0.99 mm was investigated. The mechanical spectra at 0.99 mm and 0.98 mm is given in Figure 4.10.2.



(a) Frequency sweep of Alg-Na (1h) at 0.99 mm



(b) Frequency sweep of Alg-Na (1h) at 0.98 mm

Figure 4.10.2: (a) Frequency sweeps of Alg-Na (1h) at 0.99 mm. (b) Frequency sweeps of Alg-Na (1h) at 0.98 mm. Elastic modulus (blue), viscous modulus (red) and phase angle (green) is plotted on y-axis against the frequency on the x-axis for both gels. For 1.8 % (w/v) alginate gel gelled with 50 (mM)  $\text{CaCl}_2$  solution and stored in NaCl solution. Frequency sweeps (1-0.05 Hz) were performed at 20°C with a constant shear strain at 0.1 % and 10 measurement per decade.

The mechanical spectra at 0.99 mm show a dominant elastic behavior, as presented in Figure 4.10.2a. Initial phase angle was measured to be 12.8° at 0.05 Hz and 18.5° at 1 Hz, which may be related to a degree of slip. The mechanical spectra obtained at 0.99 mm do not meet the criteria established for an alginate gel. The gap was then reduced further to 0.98 mm, the resulting mechanical spectra is presented in Figure 4.10.2b demonstrate a dominance of elastic behavior in the gel. Further, the mechanical spectra obtained at 0.98 is presented in Figure 4.10.2b is within the expected range of values and meets the criteria for an alginate gel. The obtained values for  $G'$ ,  $G''$  and  $\delta$  at 0.98 mm is also consistent with previously measured values for alginate gels stored in NaCl solution.

### 4.10.2 Dependence of elastic modulus in alginate gel with increasing hold time On measuring height

Furthermore, it is interesting to investigate the effect of increase hold time on elastic modulus with consecutive compression. The  $G'$ ,  $G''$  and  $\delta$  obtained at each height plotted against the frequency and  $G'$  at 1 Hz plotted against gap height is given in Figure 4.10.3

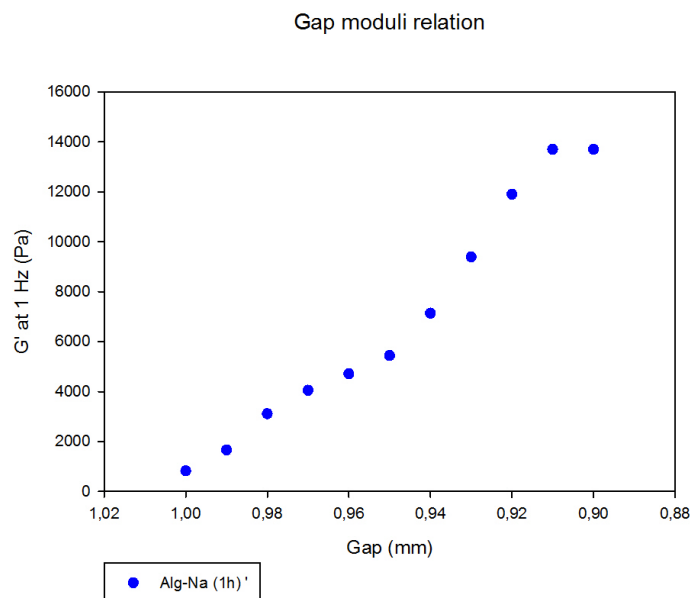
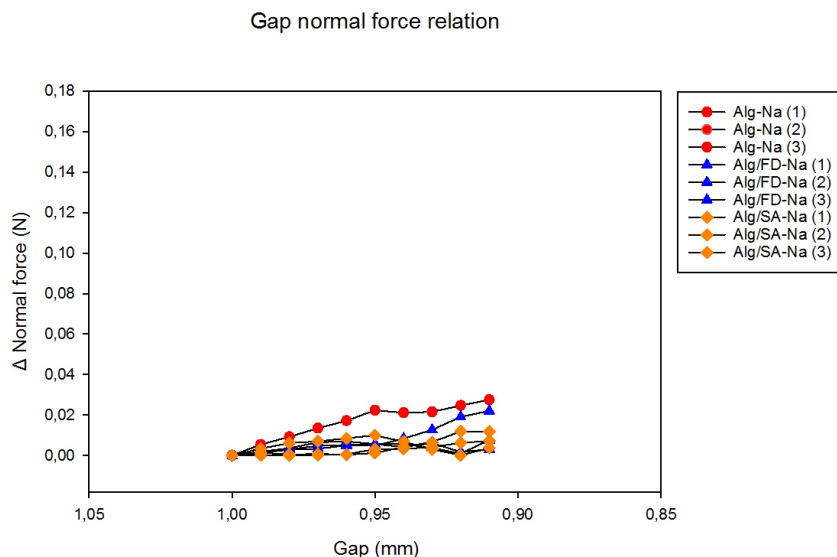


Figure 4.10.3:  $G'$  obtained at 1 Hz at each height was plotted against the reducing gap for alginate gel with increased hold time.

Figure 4.10.3 present a gradual increase with change in height. When the hold time was increased to one hour between each frequency sweep, resulted a gradual increase in elastic modulus, compared to previous results (Figure 4.5.5).

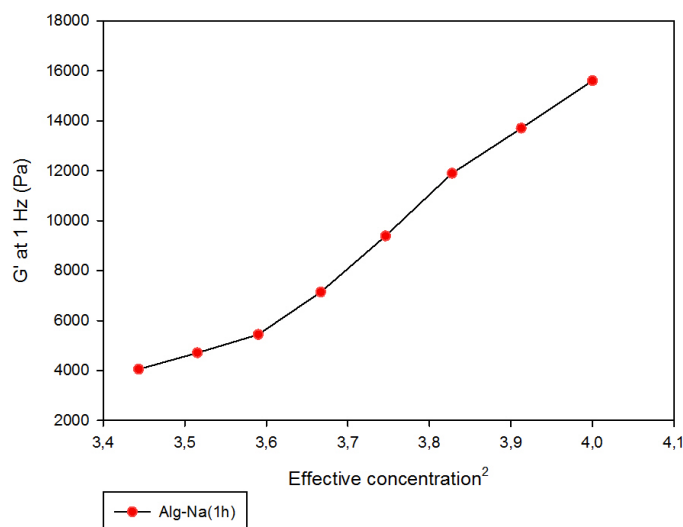
### 4.10.3 Driving factors for the rheological behavior in alginate gels

To further look into the driving factor for the rheological behavior for pure alginate gel,  $G'$  at 1 Hz was plotted against the effective concentration squared. Additionally, the baseline for the normal force plotted against the gap height relative to alginate/sulfated alginate gels and alginate/fucoidan gels. Figure 4.10.1 shows resulting plots.



(a) Normal force baseline for Alg-Na (1h) relative to previous results

Alg-Na(1h): Concentration moduli relation



(b) Effective concentration for Alg-Na (1h)

Figure 4.10.4: (a) Normal force values measured at each gap reduction plotted against the gap height for Alg-Na(1h) gel relative to the previously obtained results with alginate/sulfated alginate and fucoidan gels. (b)  $G'$  at 1 Hz plotted against the effective concentration squared after establishing contact point for Alg-Na(1h) gel.

The measuring height normal force relation is reduced significantly for the alginate with increasing hold time, as illustrated in Figure 4.10.4a. This indicates that with increasing hold time the gel is able to relax and return to its native state after the deformation is removed and before the gap is reduced further. The obtained values for  $G'$ ,  $G''$  and  $\delta$  during each set gap is therefore more reliable, as the frequency sweeps are performed on the gel in its true nature rather than in an induced stressed/compressed state. Moreover,  $G'$  at 1 Hz plotted against the effective concentration squared revealed proportionality as observed in Figure 4.10.4, indicating that the effective alginate concentration is the dominant driver of rheological behavior during this frequency range, in accordance with the theoretical expectations.

## **4.11 Rheological analysis of alginate/sulfated alginate and alginate/fucoidan gels, with increased hold time**

Altered sequence where the hold time was increased from 120s to 1 hour between each frequency sweep was performed on alginate/sulfated alginate and alginate/fucoidan gels as well. The normal force was measured through each gap reduction and plotted against the gap height, resulting in plots are presented in Figure 4.11.1.

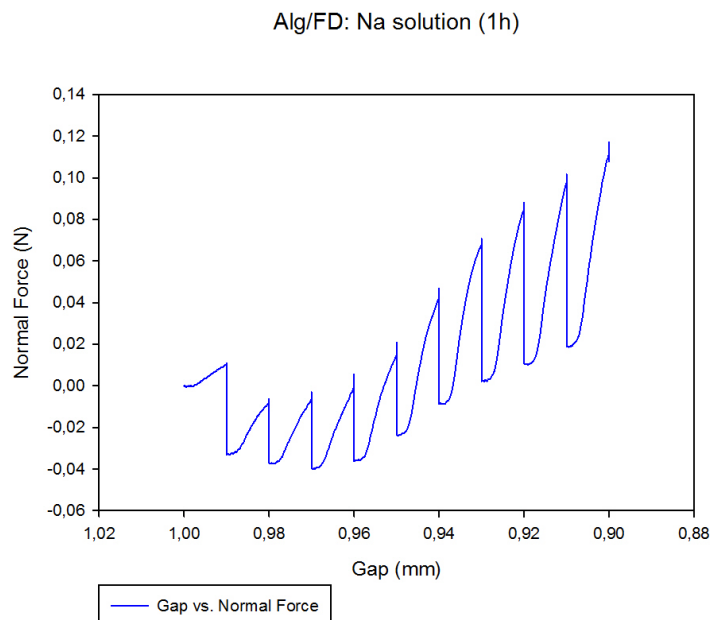
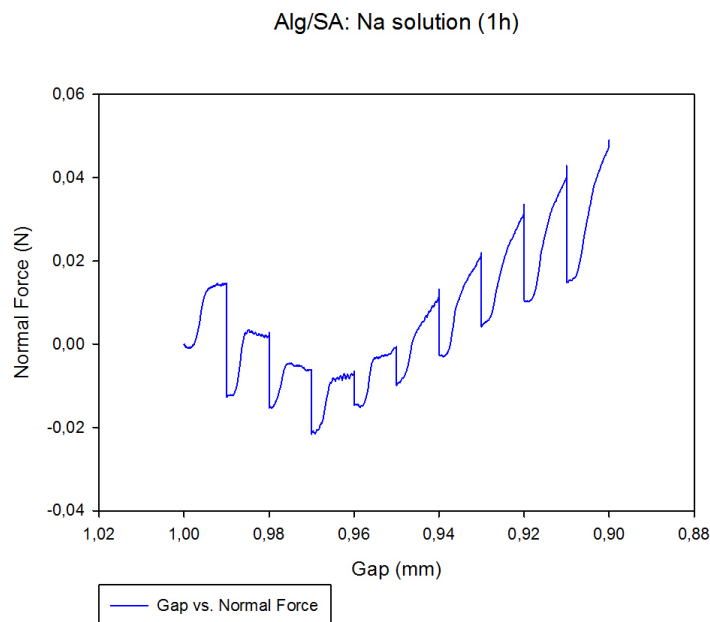


Figure 4.11.1: (a) Normal force as a function of measuring height for Alg/SA-Na(1 h). (b) Normal force as a function of measuring height for Alg/FD-Na(1 h). Measurements was performed on 1.8 % (w/v) 80/20 alginate/sulfated alginate solution or 80/20 alginate/fucoidan solution ( $60 \mu\text{L}$ ) was loaded to the lower geometry and the distance between the plates was set to 1 mm. 50 mM  $\text{CaCl}_2$  (2mL) was added to the lower geometry for gelling. One hour of gelation occurred before  $\text{CaCl}_2$  (2 mL) solution was removed and NaCl solution was added (2 mL). The gap was reduced by 0.01 mm stepwise, where one hour was waited before a new height reduction to a total reduction to 0.90 mm.

Alg/SA gel have an interesting development of normal force values through the measurement. The gel appear to be relaxing during compression at all set gaps, as the normal force is measured to be dissipating while the gap is reducing simultaneously, as seen in

Figure 4.11.1a. This observation is contrary to the previous results. A similar trend is observed for alginate/fucoidan gels as well. The gel is appear to be relaxation noted by the decrease in normal force value during the gap reduction, Figure 4.11.1b is studied further, which is not observed previously.

Further, the influence of increased hold time on the gels were analyzed by performing frequency sweep on both gels. The resulting value of  $G'$ ,  $G''$  and  $\delta$  were plotted against frequency. The results are presented in Figure 4.11.2.

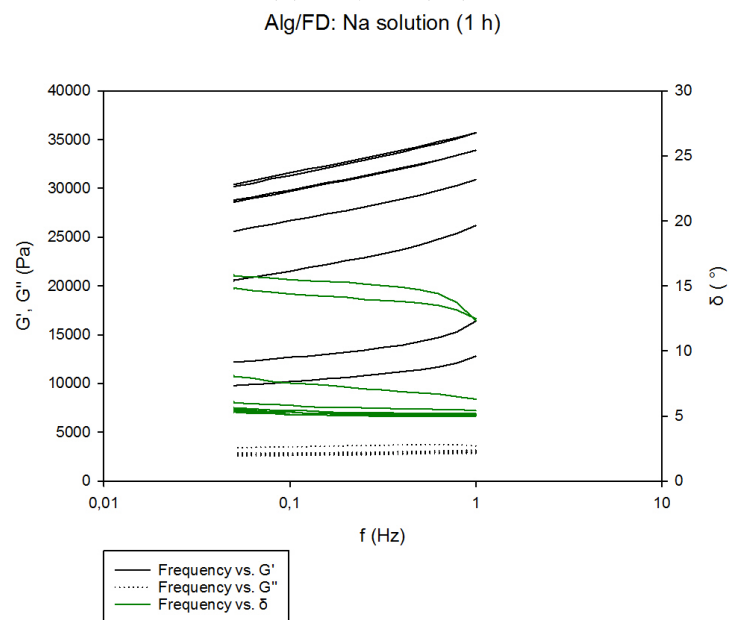
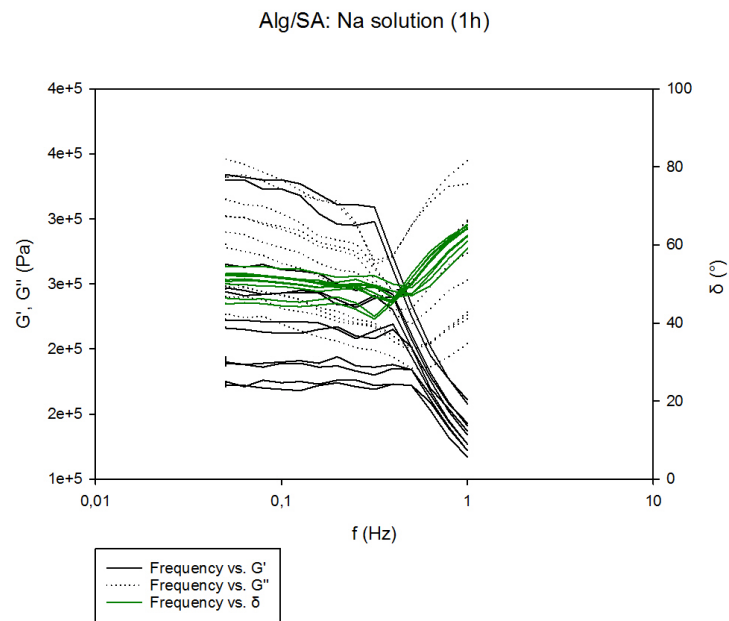


Figure 4.11.2: (a)  $G'$ ,  $G''$  and  $\delta$  at each height measurements plotted against the frequency range for Alg/SA (1h). (b)  $G'$ ,  $G''$  and  $\delta$  at each height measurements plotted against the frequency range for Alg/FD (1h). Valus for  $G'$ ,  $G''$  and  $\delta$  was obtained at 20°C were obtained by performing frequency sweeps from 1-0.05 Hz, at constant 0.1 % shear strain.



When a part of the alginate is replaced with sulfated alginate the elastic moduli have rapid increase from 237800 Pa at 0.05 Hz and 363300 Pa at 1 Hz . The elastic moduli is also observed to have decrease with increasing frequency as shown in Figure 4.11.2a. Moreover, for Alg/FD gels elastic moduli was measured to be increasing from 35740 Pa at 0.05 Hz and 2057 Pa at 1 Hz, as seen in Figure 4.11.2b.

When hold time increased for the Alg/SA the results were quite contrary from the results seen before. The elastic modulus at each measuring height had a initial high value and continued to increase with increasing compression. The mechanical spectra for alginate/sulfate gel is showing the gel alternate between elastic and viscous behavior with reducing gap. The phase angle is also measured to have an initial value of  $59.2^\circ$  at 0.05 and  $64.2^\circ$  at 1 Hz, which is above  $45^\circ$ , indicating a viscous solution. However, the sample was observed to be a gel before it was discarded which is contradictory to the obtained mechanical spectra.

At first glance, the mechanical spectra obtained (Figure 4.11.2b) for alginate/fucoidan gel appear to be similar to the previously obtained result (Figure C.6). However, the obtained values for  $G'$  is measured to be greater than the results obtained earlier. Based on prior findings, it has been established that the elastic modulus should not exceed that of alginate, since fucoidan do not contribute to the gel network. There is no theoretically or practical explanation to why these results differ from the previous results obtained in this study. Due to time limitations, further measurements with increased hold time for pure alginate, alginate/sulfated alginate and alginate/fucoidan was not performed.

Overall, the purpose with increasing hold time between each frequency sweep was to minimize the induced stiffness observed in pure alginate gels. This was obtained in the pure alginate gels as the baseline for the normal force was reduced, resulting in rheological behavior similar to the Alg/SA and Alg/FD without increased hold time, as presented in Figure 4.10.1.

## 4.12 Mechanical characterization of alginate-based gels

The mechanical characterization of pure alginate gel, alginate/sulfated alginate gels and alginate/fucoidan gels were evaluated in terms of measuring the elastic modulus and determining the Young's modulus at 0.95 mm.

### 4.12.1 Rheological characterization of alginate-based gels and calculation of Young's modulus

The data collected from the three different samples can be compared effectively if the underlying driving forces remain consistent across all observation. Mechanical spectra obtained at 0.95 mm for alginate gel, alginate/sulfated alginate gels and alginate/fucoidan gels suggest that sufficient contact has been established between the gel and instrument, to provide reasonable rheological data for all three gels. Further, at this point the elastic modulus is also proportional to the effective concentration squared in all three gels and gels appear to be in their native state rather than a compressed state. Based on these observation, reliable and comparable value for elastic modulus for alginate gel, 80/20

alginate/sulfated alginate gel and 80/20 alginate/fucoidan gel could be obtained. Table 4.12.1 present the elastic modulus at 1 Hz at 0.95 mm.

Table 4.12.1: The individual  $G'$  values at 1 Hz for each measurement and the calculated mean and standard deviation for alginate gel, 80/20 alginate/sulfated alginate gels and 80/20 alginate/fucoidan gels. The values are obtained from frequency sweep (1-0.05 Hz) at 0.95 mm.

Gel	$G'$ at 1 Hz [Pa]	$\overline{G'}$ at 1 Hz $\pm \sigma$ [Pa]
Alg-Na (1h)	5441	NA
Alg/SA-Na (1)	4964	5703 $\pm$ 1218
Alg/SA-Na (2)	5036	
Alg/SA-Na (3)	7109	
Alg/FD-Na (1)	3371	4314 $\pm$ 1274
Alg/FD-Na (2)	5764	
Alg/FD-Na (3)	3807	

A overview of elastic modulus at 1 Hz for each sample relative to each other obtained at 0.95 mm is presented in Figure 4.12.1. The values are obtained by performing a frequency sweep at 0.95 mm.

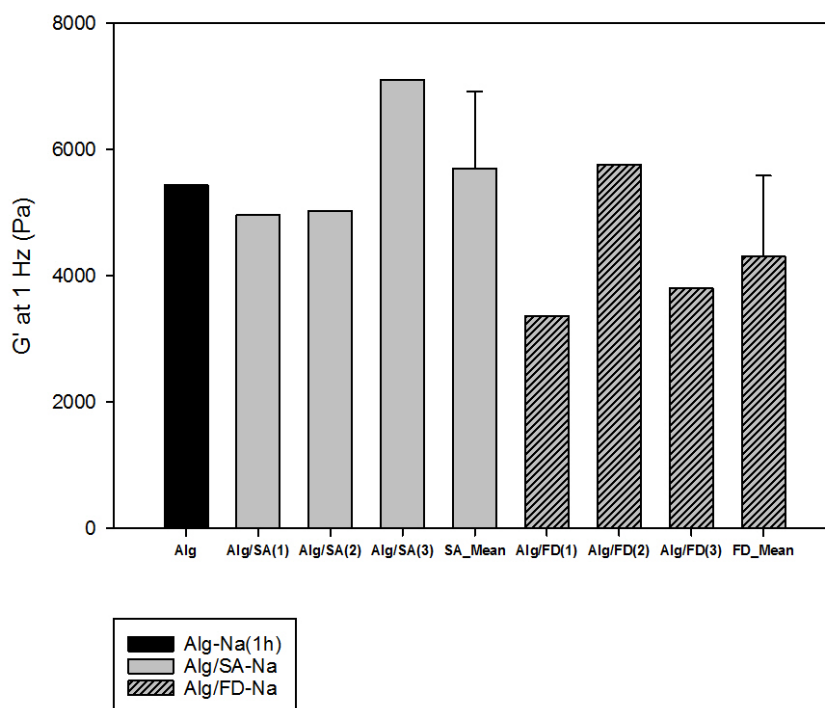


Figure 4.12.1: The individual  $G'$  values at 1 Hz for each measurements and the calculated mean and standard deviation for alginate gel, 80/20 alginate/sulfated alginate gels and 80/20 alginate/fucoidan gels, relative to each other. The values are obtained from frequency sweep (1-0.05 Hz) at 0.95 mm.

In this study, elastic modulus value for pure alginate gel was found to be 5441 Pa at 1 Hz. When a fraction of alginate gel was replaced with sulfated alginate the resulting elastic modulus was found to be 4964 Pa Alg/SA-Na(1) gel, 5036 Pa for Alg/SA-Na(2) gel and 7109 Pa Alg/SA-Na(3) gel as presented in Figure 4.12.1. Elastic modulus at 1 Hz was measured to be 3371 Pa for Alg/FD-Na(1) gel, 5764 Pa for Alg/FD-Na(2) gel and 3807 for Alg/FD-Na(3) gel.

The obtained results were then further validated by calculating the Young's modulus at 0.95 mm. Calculations for Young's modulus is given in Appendix E. Table 4.12.2 present the calculated values Young's modulus for alginate gel, 80/20 alginate/sulfated alginate gel and 80/20 alginate/fucoidan gel.

Table 4.12.2: The individual calculated Young's modulus for each measurements and the calculated mean and standard deviation for alginate gel, 80/20 alginate/sulfated alginate gels and 80/20 alginate/fucoidan gels. The values are obtained by performing a linear regression on the initial slope of the stress-strain curve at 0.95 mm.

Gel	E [Pa]	$\bar{E} \pm \sigma$ [Pa]
Alg-Na (1h)	11791	NA
Alg/SA-Na (1)	28468	$26572 \pm 3421$
Alg/SA-Na (2)	22612	
Alg/SA-Na (3)	28636	
Alg/FD-Na (1)	20849	$28389 \pm 6934$
Alg/FD-Na (2)	34492	
Alg/FD-Na (3)	29826	

An overview of the calculated Young's modulus values for each sample relative to each other is presented in Figure 4.12.2.

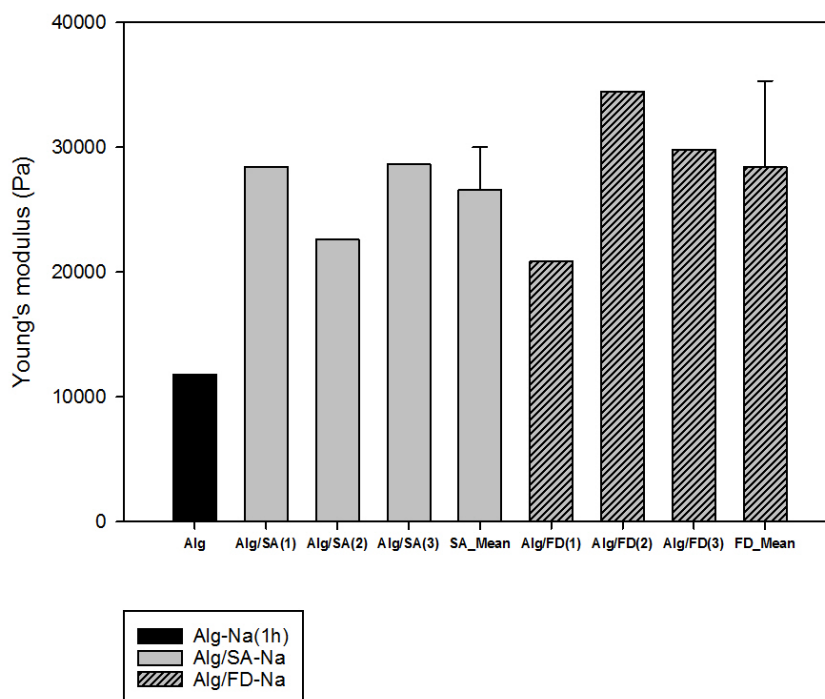


Figure 4.12.2: The individual calculated Young's modulus values for each measurements and the calculated mean and standard deviation for alginate gel, 80/20 alginate/sulfated alginate gels and 80/20 alginate/fucoidan gels, relative to each other. The values are obtained by performing a linear regression on the initial slope of the stress-strain curve at 0.95 mm..

The elastic modulus at 0.95 mm appear to be a outlier, when Figure 4.10.3 is studied

further. A linear regression analysis on  $G'$  at 1 Hz for Alg-Na(1h) gel, would have yielded a  $G'$  value closer to 6000 Pa. Despite of this, the elastic modulus is still in the acceptable range of values ( $\sim 5$ -20 kPa) for alginate gels established by previous studies.

The Young's modulus measured for alginate was calculated to be 11791 Pa. Previous work done by Tore K. Wæhre on alginate/fucoidan hydrogels suggests that expected value should lie within 30.5 kPa - 54.05 kPa for pure alginate gel [61]. This range of values are also supported by previous work done by Ragnhild Aaen [62] on measuring the mechanical properties of alginate/sulfated alginate. In both studied, the Young's modulus was determined by the use of a longitudinal compression test, with alginate gel cylinders (5 kg) prepared from 2 % (w/v) alginate solution utilizing internal gelling method. The compression was also performed on  $\text{CaCl}_2$  saturated gels. While, in this study the Young's modulus was calculated after few % compression on 1.8 % (w/v) alginate solution gelled through the diffusion method. Additionally, the values in this study, are obtained from measurements most likely performed on the surface of the gel stored in NaCl solution over a longer period of time, leading to lower content of  $\text{Ca}^{2+}$ -ions on the surface. This could result in a lower Young's modulus. The difference in measured values are most likely connected to the difference in methodology utilized to form an alginate hydrogel and different degree of compression.

The replacement of a fraction of alginate may affect the strength and stability of the hydrogel formed. When alginate is replaced with a different substance, the composition and structure of the polysaccharide could change. If the substitute substance does not contain guluronic acid residues or has a lower proportion of guluronic acid compared to alginate, it can lead to a reduction in G-blocks that would effect the gelling properties[63] [4]. The alteration in gelling characteristics will result in a change in the gel's elastic modulus and Young's modulus.

Relative to unmodified alginate, sulfated alginates have been found to contribute poorly in junction zone formation [7], due to the bulky sulfate groups being present in the structure, that prevents optimal gel network organization. With this property being present in the gel network, the gel stiffness is expected to decrease compared to alginate gel. Study on the characterizing the mechanical properties of sulfated alginate [7] found that introduction of highly sulfated alginate in the mixed gels resulted in a prominent decrease in gel stiffness [64]. However, contrary to the expectation the alginate/sulfated alginate gels have a storage modulus in the same magnitude as alginate as observed in Figure 4.12.1. A study on determining the elastic modulus for sulfated alginate demonstrated that sulfated alginate are capable of forming gels itself when the degree of sulfation is less than 0.50 [64]. The sulfated alginate used for the current study had a DS value of 0.55, which could have have contributed to gel network rather than interfere, that resulted in a elastic modulus in the same range as alginate gel. SEC-MALLS analysis indicated that the sulfation of UP-MVG led to some depolymerization. Correlation between chemical and physical properties of alginate beads revealed that gel strength increases with increasing molecular weight for  $M_w$  less  $2.4 \cdot 10^5$ . The gel strength in sulfated alginate utilized in the current study is could most likely be a function of  $M_w$  [65], influencing the mechanical properties of the hydrogel.

Alg/SA-Na(3) gel had a substantially elevated value for the elastic modulus compared

to alginate gel. The chemical modification of alginate by sulfation leads to higher negative charge on the polymer than alginate itself. For alginate/ sulfated alginate gels, the calcium content in a gel microbead was quantified. The studied revealed that the presence of a higher negatively charged polymer, could theoretically elevate the calcium binding potential by increasing the amount of possible electrostatic points for cations as previously indicated by Arlow et. al [64] [8]. Considering the small volume small volume utilized for measurements in the current study, the increased electrostatic points in the sample could have led to a higher value  $G'$  for Alg/SA-Na(3) gel at 0.95 mm.

The elastic modulus values show some inconsistency up to a certain extent, as Alg/SA-Na(3) measurement indicates a slightly higher value. Considering the small sample volume, one would expect some inconsistency. In order to ensure the reliability of the data, it is necessary to repeat the measurements.

In order to understand the effect of substituting a fraction of alginate with sulfated alginate on the gel stiffness, values obtained in this study is compared to values for alginate in the study done by Tore K. Wæhre, since they are in the expected range of values. For alginate gels the Young's modulus is measured to be ranging from  $\sim 30.5$  kPa - 54.05 kPa [61]. In this study, the Young's modulus was calculated 28468 Pa, 22612 Pa and 28635 Pa for Alg/SA-Na (1) gel, Alg/SA-Na (2) gel and Alg/SA-Na (3) gel, respectively, showing a decrease in Young's modulus when sulfated alginate is replaced a fraction of alginate. This is in accordance with the expectations, since similar results were obtained from previous work, where it was reported a significant reduction in Young's modulus for alginate/sulfated alginate gels, with increasing concentrations and degrees of substitution of sulfated alginate [18][8] [62].

There has been a limited research conducted on the incorporation of fucoidans into hydrogels in general, and even fewer studies have examined the mechanical characteristics of these gels. Fucoidan is a partially branched polysaccharide, largely containing fucose where sulfated groups are attached to the fucose unit [33][34]. Based on the structural similarities, the closest point of reference for Alg/FD gels in literature would be based on literature established on Alg/SA gels. Elastic modulus at 1 Hz was measured to be 3371 Pa for Alg/FD-Na(1), 5764 for Alg/FD-Na(2) and 3807 for Alg/FD-Na(3). From Figure 4.12.1 it is evident that when a fraction of alginate was replaced with fucoidan the elastic modulus decreased, except for Alg/FD-Na(3) that remained in the same range of values as for alginate. The reduction in elastic modulus is in accordance with the expectations, as fucoidan do not have any gelling properties and could possibly interfere with the gelling network [38] [34]. The elastic modulus have shown to decrease with increasing degree of sulfation and increasing concentration of sulfated alginate [7]. Fucoidan used in this study had a DS value of 1.7 which could have prevented a optimal gel network organization, due the bulky sulfate groups being present. Contrary to sulfated alginate, fucoidan do not exhibit any gelling properties which could be the reason for the lower values for  $G'$ . Additionally, there are inconsistencies in the values obtained from alginate/fucoidan gels. To accurately determine the elastic modulus of these gels, it is necessary to repeat the measurements using this protocol.

The Young's modulus was calculated to be 20849 Pa for Alg/FD-Na(1), 34492 Pa for Alg/FD-Na(3) and 29826 Pa for Alg/FD-Na (3), in accordance with previous obtained values for 80/20 alginate/fucoidan [61]. The gel stiffness appear to be reduced, as a consequence of disruption in gel formation that is most likely due to sulfated nature of sulfated

alginate and fucoidan. The presence of negatively charged components in fucoidan and sulfated alginate can hinder the formation of cross-links with  $\text{Ca}^{2+}$  ions, leading to a decrease in Young's modulus.

Overall, when a fraction of alginate gel is substituted with sulfated alginate and fucoidan, the latter appear to the highest impact on the mechanical properties, in terms of elastic modulus and Young's modulus. The obtained  $G'$ - and  $E$  values suggests that fucoidan do interfere with the gelling network, resulting in fewer cross-links resulting in a decrease in elastic modulus values. Further, for alginate/sulfated alginate gels the elastic modulus was measured to be in the same magnitude of values. This could be due to sulfated alginate had a lower DS-value, relative to fucoidan. The obtained values for  $G'$  and  $E$  is consistent with previous measurements on alginate/sulfated gels and alginate/fucoidan hydrogels, indicating that reliable results are produced with this new protocol [54] [61] [62].

Table 4.12.2 show that measured Young's modulus values is inconsistent with the values obtained when storage modulus was measured. For instance Alg/SA-Na (1) gel has a higher Young's modulus value than Alg/SA-Na(2), when the storage modulus at 1 Hz had the opposite values. Young's modulus describes a material's stiffness under static loading conditions, while storage modulus characterizes its ability to store elastic energy under dynamic conditions [45] [42]. The variation in values for the mechanical properties indicates the anisotropy within the gels [66]. The mechanical properties appear to vary in the different direction, which is most likely a result of consecutive compression applied on the gel.

Equation 2 present the relation between the Young's modulus and elastic modulus, that makes the Young's modulus measurements proportional to the elastic modulus, the results are presented in Table E.2. Hydrogels do not conform to the equation as they are not ideal elastic materials. On the other hand the values for Young's modulus presented in 4.12.1 were calculated after few compression applied on the gel, which could also indicate a realistic value for  $E$  was not obtained through this method. There is uncertainty connected to both calculation, however the values obtained presented in Table 4.12.1 align with previously obtained values for 80/20 alginate/sulfated alginate gels and 80/20 alginate/fucoidan gels.

Hydrogel materials are capable of mimicking certain elastic and viscoelastic properties that are characteristic of soft biological tissue [67]. Previous studies on the viscoelastic characterization of biological tissue have reported that the elastic modulus of epithelial cells, for instance, falls within the range of  $\sim 5$ -7 kPa [68]. The viscoelastic analysis conducted additional soft adipose tissue resulted in a elastic modulus of 2.5 (kPa) [69] in another study. The obtained values  $G'$  at 1 Hz and calculated values Young's modulus for alginate-based hydrogels in this study, appear to cover the range of many soft biological tissues[70], making them applicable materials in tissue engineering.

### 4.13 Future work

Through characterizing the rheological properties of these alternative gelling system, we can predict their behavior and maximize their performance capabilities in tissue engi-

neering.

The initial rheological experiments with  $\text{CaCl}_2$  solution as gelling solution and  $\text{NaCl}$  as storing solution presented a promising results for 80/20 alginate/sulfated alginate gel and 80/20 alginate/fucoidan alginate gel. For alginate gels the same protocol with increased hold time resulted in a realistic value for elastic modulus. For future work the reproducibility of these data needs to be verified. Due to time limitation data obtained with increased hold time between each frequency sweep for pure alginate were not repeated. Additionally, in order to have comparable data, the samples that are subjected to comparison must be treated identically. This was not done in this study, as the data obtained from alginate/sulfated alginate and alginate/fucoidan gels with increased hold time were incoherent with the results obtained with shorter hold time. This should be explored further, to ensure accurate characterization on the rheological properties when a fraction of alginate is substituted with a sulfated polymer.

Furthermore, alginate have a higher affinity towards  $\text{Ba}^{2+}$ -ions [15]. Addition of  $\text{Ba}^{2+}$ -ions to the gelling solution would form a more stable gel. Therefore, characterizing the difference between gels gelled with only  $\text{Ca}^{2+}$  ions versus gels gelled with  $\text{Ca}^{2+}/\text{Ba}^{2+}$ -ions will provide valuable insight in the stability of these gels. The stability of these gels in physiological conditions is highly relevant for their future potential as an immunisulatory material [15].

When employing alginate hydrogels mixed with sulfated alginate or fucoidan in tissue engineering, it is necessary to conduct further analysis on supplementary parameters beyond viscoelastic properties. For instance, stress relaxation is a key characteristic of cell-ECM interactions and as an important design parameter of biomaterials for cell culture [9]. The stress relaxation in these hydrogels should be examined and characterized, in order to optimize the potential for alginate-based hydrogels for tissue engineering.





## CONCLUSIONS

In this study alginate was successfully sulfated using chlorosulfonic acid and formamide. The resulting degree of sulfation was determined to be 0.55 and 0.71 for LF200S alginate and UP-MVG alginate, respectively.

Further, the rheological behavior for alginate-based gels were examined. The initial experiments suggested that storing the gels in  $\text{CaCl}_2$  solution resulted in significant alteration for elastic modulus with increasing compression. This made it challenging to obtain a realistic value for  $G'$ , when the height was corrected regards to syneresis for alginate gels. Further, utilizing NaCl as storing solution inhibited the additional  $\text{Ca}^{2+}$  cross-links that lead to alteration of  $G'$ . However, the elastic modulus reached a plateau in values rapidly due to induced stress within the gel and the quality of the data was not sufficient enough obtain a realistic value for  $G'$ . Increasing the hold time between each frequency sweep obtained a realistic value for the elastic modulus for pure alginate gels.

The elastic modulus for alginate gel was then compared to the data obtained when a fraction of alginate gel was replaced with sulfated alginate and fucoidan stored in NaCl solution without increased hold time. When a fraction of alginate gel was replaced with sulfated alginate the elastic modulus was measured to be in the same range of values. Further, when a fraction of alginate was replaced with fucoidan the elastic modulus appeared to decrease. The decrease in elastic modulus could be due to fucoidan not exhibiting gelling properties.

Further, to relate the results found in this study to previous research, Young's modulus for each gels at 0.95 mm. Young's modulus calculated for alginate were contradicting to previous obtained results, which is likely due to storing the gel in NaCl-solution that could destabilize the gelling network. However, the Young's modulus value for alginate/sulfated alginate and fucoidan appear to be in the expected range. Comparing these values for the expected value for alginate gel from previous studies, suggests that when a fraction is substituted with a sulfated polymer the gel stiffness decreases. This is most likely due to charged sulfate groups being present in the gel, interfering with the gelling network.

In conclusion, the results from this study demonstrate that reliable data on alginate-based hydrogel is achievable also with minimal sample volumes.



## REFERENCES

- [1] M. Leach and J. P. Langer R. & Vacanti. *Principles of Tissue Engineering*. Academic press, 2011.
- [2] Steven R Caliani & Jason A Burdick. *A practical guide to hydrogels for cell culture*. *Nature Methods*, Vol. 13, Iss. 5, 405-414. 2016. URL: <https://doi.org/10.1002/bit.260390210>.
- [3] Joachim S. Kjesbu et al. *Alginate and tunicate nanocellulose composite microbeads – Preparation, characterization and cell encapsulation*. *Carbohydrate Polymers*, Volume 286. 2022. URL: <https://doi.org/10.1016/j.carbpol.2022.119284>.
- [4] Kuen YongLee & David J.Mooney. *Alginate: Properties and biomedical applications*. *Progress in Polymer Science*, 37(1), 106-126. 2012. URL: <https://doi.org/10.1016/j.progpolymsci.2011.06.003>.
- [5] A. Martinsen 1, I. Storrø, and G. Skjærk-Braek. *Alginate as immobilization material: III. Diffusional properties*. *Biotechnology and Bioengineering*,, 39, 186-194. 2016. URL: DOI:10.1002/bit.260390210.
- [6] Alexander D. Augst and Hyun Joon Kong & David J. Mooney. *Alginate Hydrogels as Biomaterials*. *Macromolecular bioscience*, 6(8), 623–633. 2006. URL: <https://doi.org/10.1002/mabi.200600069>.
- [7] Øystein Arlov & Gudmund Skjåk-Bræk. *Sulfated Alginates as Heparin Analogues: A Review of Chemical and Functional Properties*. 2018. URL: doi:%2010.3390/molecules22050778.
- [8] Øystein Arolv et al. *Biomimetic sulfated hydrogels suppress IL-β-induced inflammatory in human chondrocytes*. s. 1-25. Norwegian university of Science and Technology, 2016.
- [9] Ovijit Chaudhuri et al. *Hydrogels with tunable stress relaxation regulate stem cell fate and activity*. *Nature Mater*, Vol. 15, 326–334. 2016. URL: %7Bhttps://doi.org/10.1038/nmat4489%7D.
- [10] Esmail Jabbari. *Hydrogels In Tissue Engineering*. MDPI, 2018.
- [11] Narine Sarvazyan. *Tissue Engineering*. Springer, 2020.
- [12] M. L. Oyen. *Mechanical characterisation of hydrogel materials*. *International Materials Reviews* , 59(1), 44-59. 2014. URL: <https://doi.org/10.1179/1743280413Y.0000000022>.
- [13] Sougata Jana & Subrata Jana. *Alginate Biomaterial*. Springer, 2023.

- [14] Abishana Saravani. *Preparation of alginate/fucoidan microbeads and characterization of leaked material*. 1-38. 2022.
- [15] Berit L. Strand and Abba E. Coron & Gudmund Skjåk-Bræk. *Current and Future Perspectives on Alginate Encapsulated Pancreatic Islet*. *Stem Cells Translational Medicine*, 6(4), 1053-1058. 2017. URL: <https://doi.org/10.1002/sctm.16-0116>.
- [16] Ainhoa Murua et al. *Cell encapsulation technology: Towards clinical application*. *Controlled Release*, 132(2), 76-83. 2008. URL: <https://doi.org/10.1016/j.jconrel.2008.08.010>.
- [17] Jun Li and Yoshihito Osada & Justin Cooper-White. *Functional Hydrogels as Biomaterials*. 1-95. Springer, 2008. ISBN: 978-3-662-57509-3.
- [18] Abba E. Coron et al. *Pericapsular fibrotic overgrowth mitigated in immunocompetent mice through microbead formulations based on sulfated or intermediate G alginates*. *Acta Biomaterialia*, Volume 137, 2022, Pages 172-185. 2022. URL: <https://doi.org/10.1016/j.actbio.2021.10.004>.
- [19] Olav Andreas Aarstad. *Alginate sequencing*. s. 1-57. Norwegian University of Science and Technology, 2014.
- [20] Kurt Ingar Draget et al. *Alginates*. s. 1-46. Taylor & Francis Group, 2006.
- [21] Olav Andreas Aarstad. *Alginate sequencing: Block distribution in alginates and its impact on macroscopic properties*. s. 4-21. Norwegian University of Science and Technology, 20.
- [22] Olav Andreas Aarstad, Anne Tøndervikr, and Håvard Sletta & Gudmund Skjæk-Bræk. *Alginate Sequencing: An Analysis of Block Distribution in Alginates Using Specific Alginate Degrading Enzymes*. *Biomacromolecules* 2012, 13, 1, 106–116. 2012. URL: <https://doi.org/10.1021/bm2013026>.
- [23] Chuhuan Hu et al. *Ions-induced gelation of alginate: Mechanisms and applications*. *International Journal of Biological Macromolecules*, Volume 177, 578-588. 2021. URL: <https://doi.org/10.1016/j.ijbiomac.2021.02.086>.
- [24] Thiago Silva et al. *Alginate and Sericin: Environmental and Pharmaceutical Applications*. *Environmental and Pharmaceutical Applications*. 2017. URL: DOI: 10.5772/65257.
- [25] Kurt I. Draget & Catherine Taylor. *Chemical, Physical and biological properties of alginates and their biomedical implications*. *Food Hydrocolloids*, 25 (2), 251-256. 2011. URL: <https://doi.org/10.1016/j.foodhyd.2009.10.007>.
- [26] Kurt Ingar Draget and Kjetill Østgaard & Olav Smidsrød. *Homogeneous alginate gels: A technical approach*. *Carbohydrate Polymers*, 14(2), 159-178. 1990. URL: [https://doi.org/10.1016/0144-8617\(90\)90028-Q](https://doi.org/10.1016/0144-8617(90)90028-Q).
- [27] Kurt Ingar Draget and Gudmund Skjåk-Bræk & Olav Smidsrød. *Alginate based new materials*. *International Journal of Biological Macromolecules*, 32(2-1), 47-55. 1997. URL: [https://doi.org/10.1016/S0141-8130\(97\)00040-8](https://doi.org/10.1016/S0141-8130(97)00040-8).
- [28] Draget K. I., Simensen M. K., and Onsøyen E. & O. Smidsrød. *Gel strength of Ca-limited alginate gels made in situ*. *Hydrobiologia volume*, 260, 563–565. 1993. URL: <https://doi.org/10.1007/BF00049071>.

- [29] Kurt Ingar Draget et al. *Effects of molecular weight and elastic segment flexibility on syneresis in Ca-alginate gels*. *Food Hydrocolloids*, 15(4-6), 485-490. 2001. URL: DOI:%20https://doi.org/10.1016/S0268-005X(01)00046-7.
- [30] Tezar Ramdhana and Sangeeta Prakasha & Bhesh Bhandaria Su Hung Chingb. *Time dependent gelling properties of cuboid alginate gels made by external gelation method: Effects of alginate-CaCl<sub>2</sub> solution ratios and pH*. *Food Hydrocolloids*, Volume 90, 232-240. 2019. URL: <https://doi.org/10.1016/j.foodhyd.2018.12.022>.
- [31] Øystein Arlov. *Sulfated alginate: Characterizing and applications as biomaterials*. s. 8-26. Norwegian university of Science and Technology, 2016.
- [32] Andreas Sichert et al. *Ion-exchange purification and structural characterization of five sulfated fucoidans from brown algae*. *Glycobiology*, 31(4), 352-357. 2021. URL: DOI:10.1093/glycob/cwaa064.
- [33] Georg Kopplin et al. *Structural Characterization of Fucoidan from Laminaria hyperborea: Assessment of Coagulation and Inflammatory Properties and Their Structure-Function Relationship*. *CS Applications of Bio Material*, 1(6), 1880-1892. 2018. URL: DOI:%2010.1021/acsabm.8b00436.
- [34] Guðmundur Óli Hreggviðsson et al. *Biocatalytic refining of polysaccharides from brown seaweeds*. *Sustainable Seaweed Technologies*, 447-504. 2020. URL: <https://doi.org/10.1016/B978-0-12-817943-7.00016-0>.
- [35] Maria I. Bilan ans Alexander S. Shashkov & Anatolii I. Usov. *Structure of a sulfated xylofucan from the brown alga Punctaria plantaginea*. *Carbohydrate Research*, Vol.393, 1-8. 2014. URL: <https://doi.org/10.1016/j.carres.2014.04.022>..
- [36] Dörschmann P, Kopplin G, and Roider J & Klettner A. *Effects of Sulfated Fucans from Laminaria hyperborea Regarding VEGF Secretion, Cell Viability, and Oxidative Stress and Correlation with Molecular Weight*. *Marine Drugs*, 17(10), 548. 2019. URL: <https://doi.org/10.3390/md17100548>.
- [37] Andriy Synytsya et al. *Structure and antitumour activity of fucoidan isolated from sporophyll of Korean brown seaweed Undaria pinnatifida*. *Carbohydrate Polymers*, 8 (1), 41-48. 2010. URL: <https://doi.org/10.1016/j.carbpol.2010.01.052>..
- [38] Bo Li, Fei Lu, and Xinjun Wei & Ruixiang Zhao. *Fucoidan: Structure and Bioactivity*. *Molecules*, 13(8), 1671-1695. 2008. URL: <https://doi.org/10.3390/molecules13081671>.
- [39] Tatiana N. Zvyagintseva et al. *Structural diversity of fucoidans and their radioprotective effect*. *Carbohydrate Polymers*, Volume 273. 2021. URL: <https://doi.org/10.1016/j.carbpol.2021.118551>.
- [40] Yu-Li Wang & HDennis E. Discher. *Methods in Cell Biology*. 4-26. Elsevier Inc, 2007. ISBN: 978-0-12-370500-6.
- [41] S.B Ross Murphy. *Biophysical Methods in Food Research. Critical Reports on Applied Chemistry*, Vol 5, 138-200. 2022.
- [42] Faith A. Morrison. *Understanding Rheology*. s. 105-169. Oxford University Press, 2001.

- [43] Jeff Gotro. *Rheology of Thermosets Part 2: Rheometers*. *Polymer Innovation Blog*. 2014. URL: <https://polymerinnovationblog.com/rheology-thermosets-part-2-rheometers/>.
- [44] Vincent A. Hackley & Chiara F. Ferraris. *The Use of Nomenclature in Dispersion Science and Technology*. National Institute of Standards and Technology, 2001.
- [45] J.R. Keaton. *Young's Modulus*. *Encyclopedia of Engineering Geology*. 2018. URL: [https://doi.org/10.1007/978-3-319-73568-9\\_298](https://doi.org/10.1007/978-3-319-73568-9_298).
- [46] D. Beauchemin et al. *Discrete sample introduction techniques for inductively coupled plasma mass spectrometry*. s. 3-15. Wilson & Wilson's, 2000.
- [47] Thomas R. *Practical guide to ICP-MS; a tutorial for beginners, 3d ed.* CRC Press, 2013.
- [48] S. Mori & H.G. Barth. *Size Exclusion Chromatography*. Springer, 1999.
- [49] Stepan Podzimek. *Light Scattering, Size Exclusion Chromatography and Asymmetric Flow Field Flow Fractionation: Powerful Tools for the Characterization of Polymers, Proteins and Nanoparticles*. s. 37-98. John Wiley & Sons, 2011. ISBN: 9780470386170.
- [50] Adam M. Syanda et al. *Sulfated Alginate Reduces Pericapsular Fibrotic Overgrowth on Encapsulated cGMP-Compliant hPSC-Hepatocytes in Mice*. *Front. Bioeng. Biotechnol*, Volume 9, Article: 816542. 2022. URL: DOI:10.3389/fbioe.2021.816542.
- [51] Inbar Freeman and Alon Kedem & Smadar Cohen. *The effect of sulfation of alginate hydrogels on the specific binding and controlled release of heparin-binding proteins*. *Biomaterials*, 29(22), 3260-3268. 2008. URL: <https://doi.org/10.1016/j.biomaterials.2008.04.025>.
- [52] Ciro Siviello and Francesco Grecoc & Domenico Larobina. *Analysis of linear viscoelastic behaviour of alginate gels: effects of inner relaxation, water diffusion, and syneresis*. *Soft Matter*, 11(3), 645-654. 2015. URL: DOI:10.1039/c5sm01244a.
- [53] Cassandra L. Roberge et al. *Viscoelastic Properties of Bioprinted Alginate Microbeads Compared to Their Bulk Hydrogel Analogs*. *Journal of biomechanical engineering*, 145(3). 2023. URL: <https://doi.org/10.1115/1.4055757>.
- [54] Mauro Moresi and Maria Mancini % Roberto Rancini. *Viscoelastic properties of alginate gels by oscillatory dynamic tests*. *Journal of texture studies*, 32(5-6),375-396. 2001. URL: <https://doi.org/10.1111/j.1745-4603.2001.tb01243.x>.
- [55] Benjamin E. Larsen et al. *Rheological characterization of an injectable alginate gel system*. *BMC Biotechnology*, 15(1). 2023. URL: <http://dx.doi.org/10.1186/s12896-015-0147-7>.
- [56] Takayaoshi Matsumoto & Kim Mashiko. *Viscoelastic Properties of Alginate Aqueous Solutions in the Presence of Salts*. *Biopolymers*, 29(14), 375-396. 1990. URL: <https://doi.org/10.1111/j.1745-4603.2001.tb01243.x>.
- [57] Catherine Taylor Nordgaard. *CTN Preliminary report: Diffusion set cast alginate gels*. *Unpublished*. 2020.

- [58] D.C. Sioutopoulos et al. *Rheological and permeability characteristics of alginate fouling layers developing on reverse osmosis membranes during desalination. Journal of membrane science*, 434, 74-84. 2013. URL: <https://doi.org/10.1016/j.memsci.2013.01.018>.
- [59] Kenneth R. Webber Rebecca E & Shull. *Strain Dependence of the Viscoelastic Properties of Alginate Hydrogels. Macromolecules*, 37(16), 6153-6160. 2004. URL: <https://doi.org/10.1021/ma049274n>.
- [60] Beate Thu et al. *Alginate polycation microcapsules. Biomaterials*, 17(11), 1069-1079. 1994. URL: [https://doi.org/10.1016/0142-9612\(96\)85907-2](https://doi.org/10.1016/0142-9612(96)85907-2).
- [61] Tore K. Wæhre. *Characterization of the mechanical properties, stability and biological potential of alginate/fucoidan hydrogels*. s. 1-105. Norwegian university of Science and Technology, 2022.
- [62] Ragnhild Aaen. *Characterization of Sulfated Alginate Hybrid Gels for Tissue Engineering*. s. 1-165. Norwegian University of Science and Technology, 2015.
- [63] Bjørn T. Stokke, Olav Smidsroed, and Per Bruheim & Gudmund Skjåk-Bræk. *Distribution of uronate residues in alginate chains in relation to alginate gelling properties. Macromolecules*, 24(16), 4637-4645. 1991. URL: <https://doi.org/10.1021/ma00016a026>.
- [64] Ø. Arlov et al. *Biomimetic sulphated alginate hydrogels suppress IL-1 $\beta$ -induced inflammatory responses in human chondrocytes. European Cells and Materials*, Volume 33. 2017. URL: DOI:%2010.22203/eCM.v033a06.
- [65] A. Martinsen, G. Skjåk-Bræk, and O. Smidsrød. *Alginate as immobilization material: I. Correlation between chemical and physical properties of alginate gel beads. Biotechnology and bioengineering*, 33(1), 79-89. 1989. URL: <https://doi.org/10.1002/bit.260330111>.
- [66] Susumu Mori. *Principles, Methods, and Applications of Diffusion Tensor Imaging. Brain Mapping: The Methods*, 379-397. 2002. URL: <https://doi.org/10.1016/B978-012693019-1/50017-4>.
- [67] Martha M. Fitzgerald, Katherine Bootsma, and Jason A. Berberich & Jessica L. Sparks. *Tunable Stress Relaxation Behavior of an Alginate-Polyacrylamide Hydrogel: Comparison with Muscle Tissue. Biomacromolecules*, 16(5), 1497-1505. 2015. URL: <https://doi.org/10.1021/bm501845j>.
- [68] Anshu B. Mathur et al. *Endothelial, cardiac muscle and skeletal muscle exhibit different viscous and elastic properties as determined by atomic force microscopy. Journal of biomechanics*, 34(12), 1545-1553. 2001. URL: doi : 10 . 1016 / S0021 - 9290(01)00149 - X.
- [69] J. T. Iivarinen and R. K. Korhonen<sup>1</sup> & J. S. Jurvelin<sup>1</sup>. *Experimental and numerical analysis of soft tissue stiffness measurement using manual indentation device – significance of indentation geometry and soft tissue thickness. Skin research and technology*, 20(3), 347-354. 2013. URL: <https://doi.org/10.1111/srt.12125>.
- [70] Clayton T. McKee, Julie A. Last, and Christopher J. Russell Paul & Murphy. *Indentation Versus Tensile Measurements of Young's Modulus for Soft Biological Tissues. Tissue engineering. Part B, Reviews*, 17(3), 155-164. 2011. URL: <https://doi.org/10.1089/ten.teb.2010.0520>.



- [71] Chris Schaller. *Polymer Chemistry*. 1-140. Elsevier Inc, 2023. ISBN: LibreTexts.

# APPENDICES

## A Calculation of the degree of sulfation from elemental analysis data

The data from the ICP-MS analysis are given as  $\frac{\mu\text{gsulfur}}{\text{gsample}}$  which can easily be converted to the weight fraction of sulfur (% S) in the sample. To calculate the degree of sulfation (DS) a standard curve was constructed to give the relationship between % S and DS. The standard curve was constructed by calculating % S for a range of theoretical values for DS. When % S is plotted as a function of DS, a second degree polynomial curve was obtained. The second degree polynomial allows for the calculation of an approximate DS when % S is known.

The second degree polynomial curve for each for LF200S alginate is given as an example in Figure A.1:

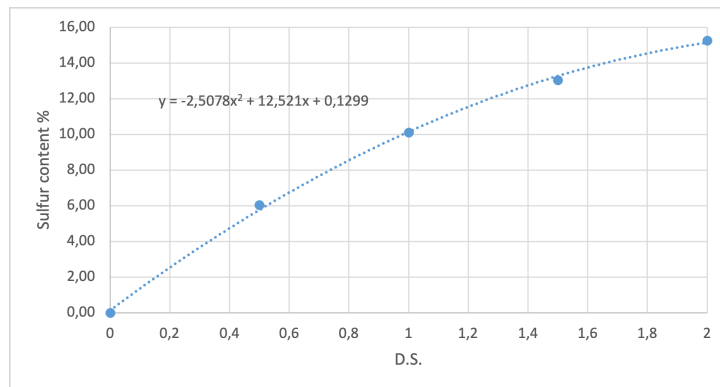


Figure A.1: Second degree polynomial curve for LF200S alginate. % S plotted against theoretical obtained DS values to estimate DS for the sample.

The DS value can then be calculated from % S values from the elemental analysis by using the formula given in Equation

$$DS = \frac{-12.824 + \sqrt{12.824^2 - 4 \cdot 2.667 \cdot \%S}}{-2 \cdot 2.6627} \quad (1)$$

## B SEC-MALLS analysis of sulfated alginate

Molecular weight averages and dispersity were determined with size exclusion chromatography with multi-angle laser light scattering (SEC-MALLS).

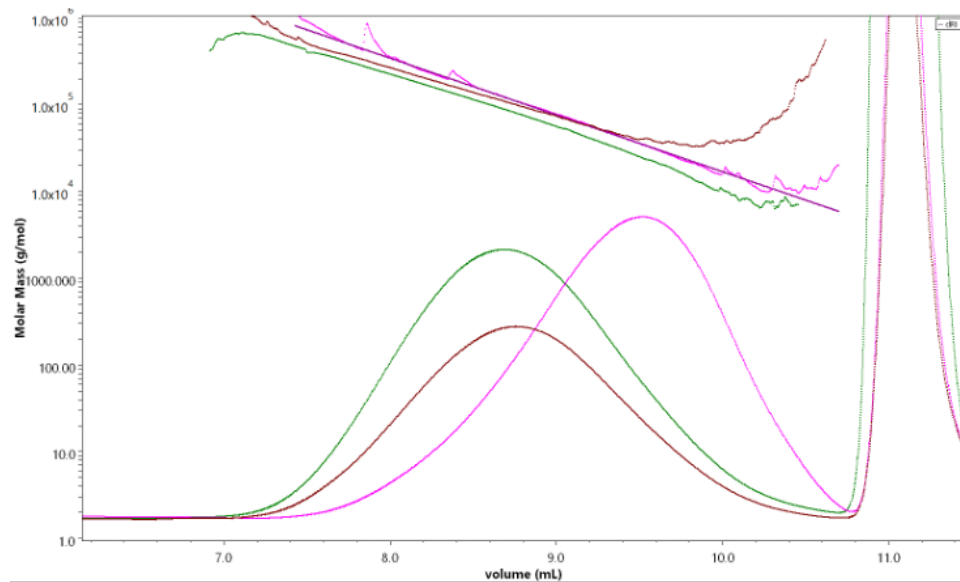


Figure B.1: Molecular weight averages and dispersity of the UPV-MVG alginate and LFS200S alginate after sulfation and LF10/60 alginate strand used as as standard. Green: LF10/60 Alginate standard, brown: UP-MVG sulfated and pink: LF200S sulfated.

## C Mechanical spectra for alginate-based gels

### C.1 Mechanical spectra for alginate gels in $\text{CaCl}_2$ -solution

Frequency sweep were performed on alginate gels stored in  $\text{Ca}^{2+}$ -solutions was performed at each set gap. Figure C.1 is the resulting mechanical spectra , when  $G'$ ,  $G''$  and  $\delta$  is at each set gap plotted against the frequency range.

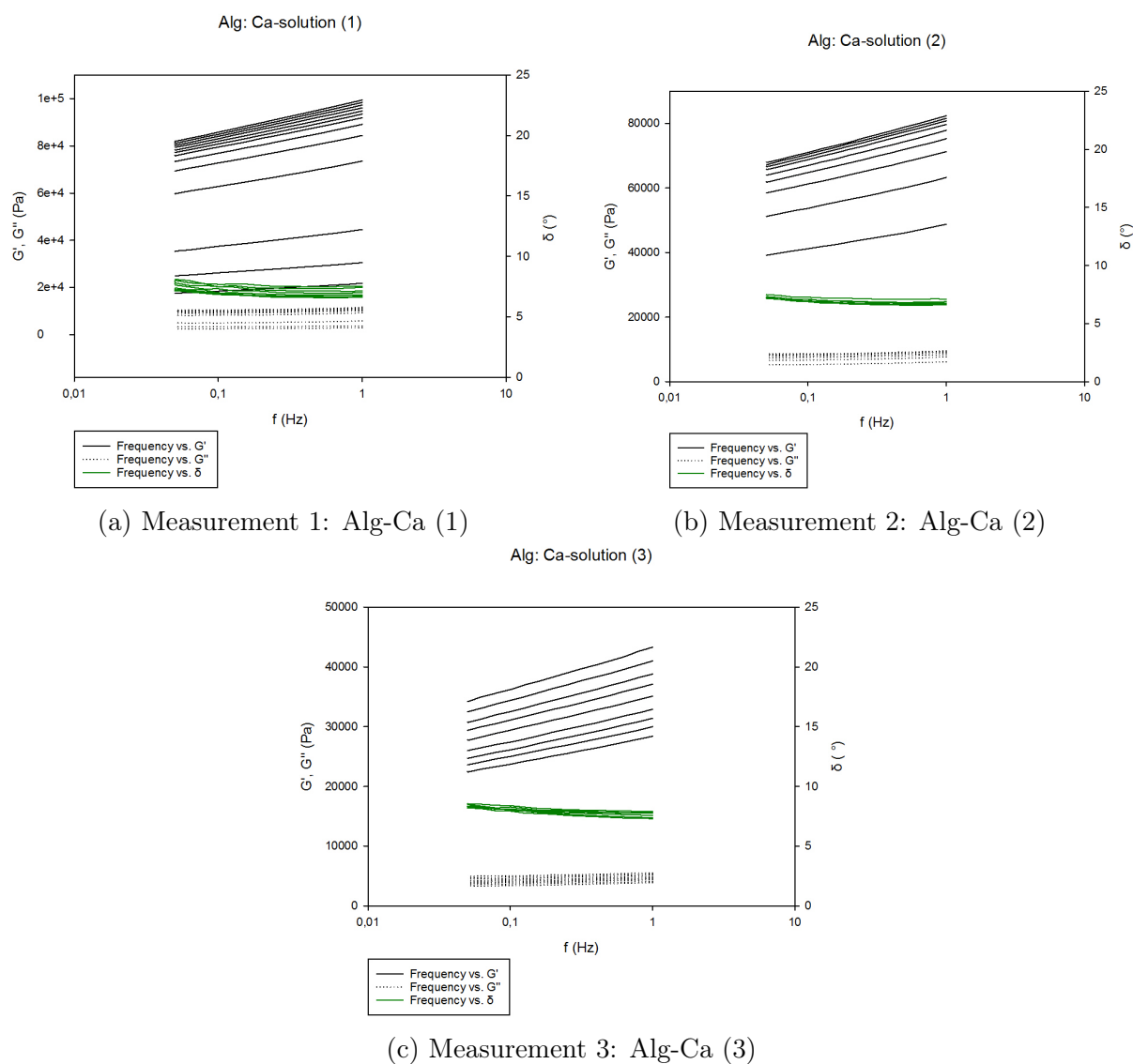
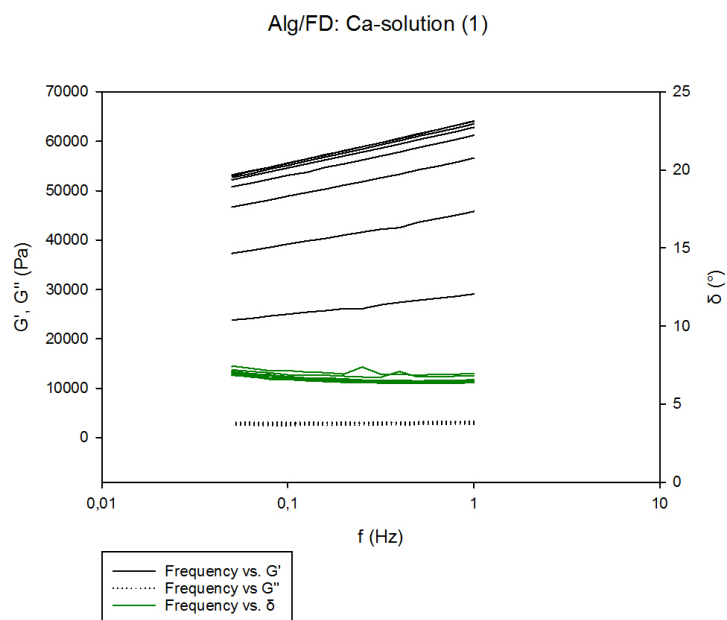
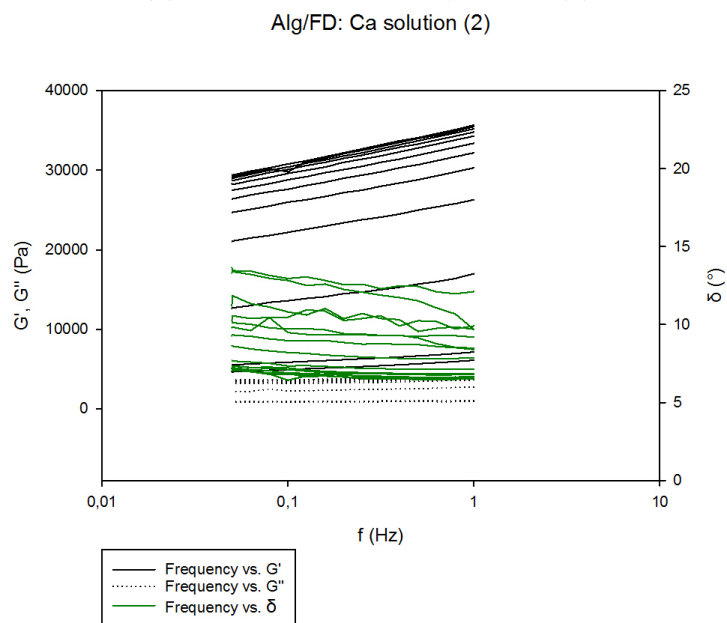


Figure C.1: Elastic modulus ( $G'$ ), viscous modulus ( $G''$ ) and phase angle ( $\delta$ ) values for 1.8 % (w/v) alginate solution gelled with  $\text{Ca}^{2+}$ -ions. Values were collected from frequency sweeps run at  $20^\circ\text{C}$  from 1-0.05 Hz frequency at 0.1 % constant shear rate with 10 samples per. decade.

## C.2 Mechanical spectra for Alginate/fucoidan gels in $\text{CaCl}_2$ -solution



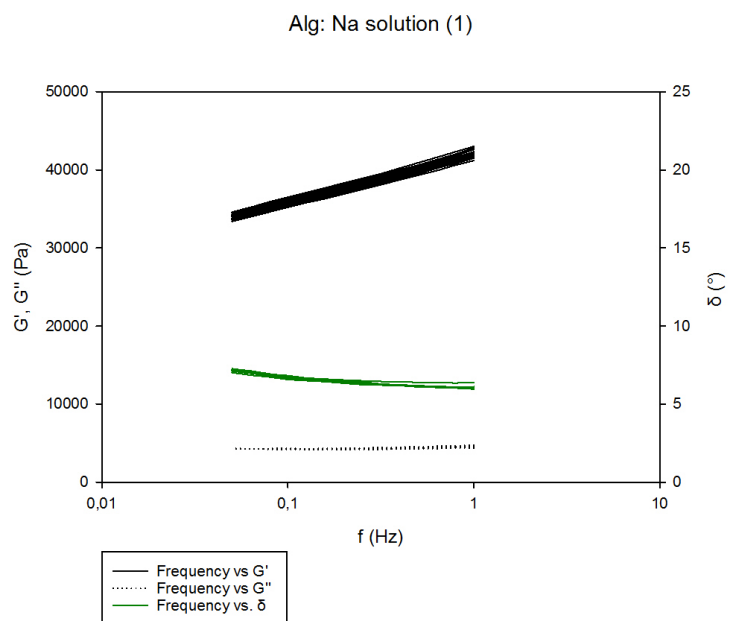
(a) Measurement 1: Alg/FD-Ca (1)



(b) Measurement 2: Alg/FD-Ca (2)

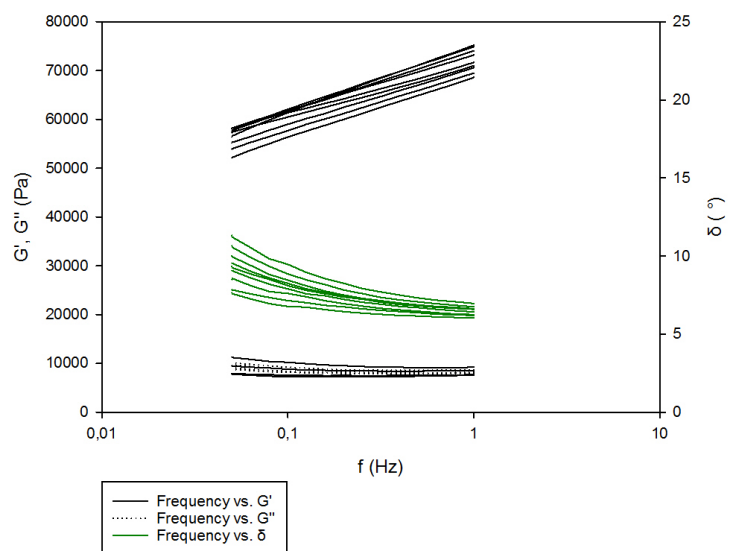
Figure C.2: Elastic modulus ( $G'$ ), viscous modulus ( $G''$ ) and phase angle ( $\delta$ ) values for 1.44 % (w/v) alginate and 0.36 % (w/v) fucoidan solutions gelled with  $\text{Ca}^{2+}$ -ions. Values were collected from frequency sweeps run at 20 ° C from 1-0.05 Hz frequency at 0.1 % constant shear rate with 10 samples per. decade. (d) The elastic modulus at 1 Hz (Pa) were plotted against the gap height (mm) for alginate/fucoidan gels.

### C.3 Mechanical spectra for alginate gels with alternative storing solution



(a) Alg-Na (1)

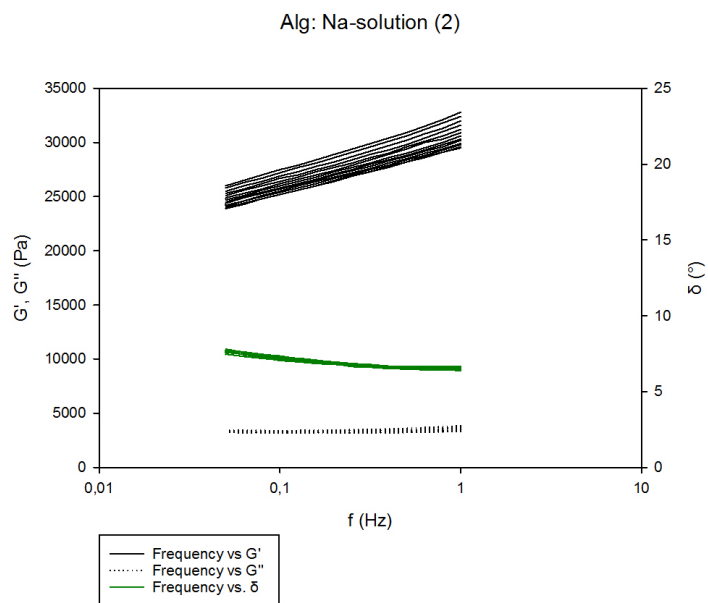
Alg: No solution



(b) Alg-No solution

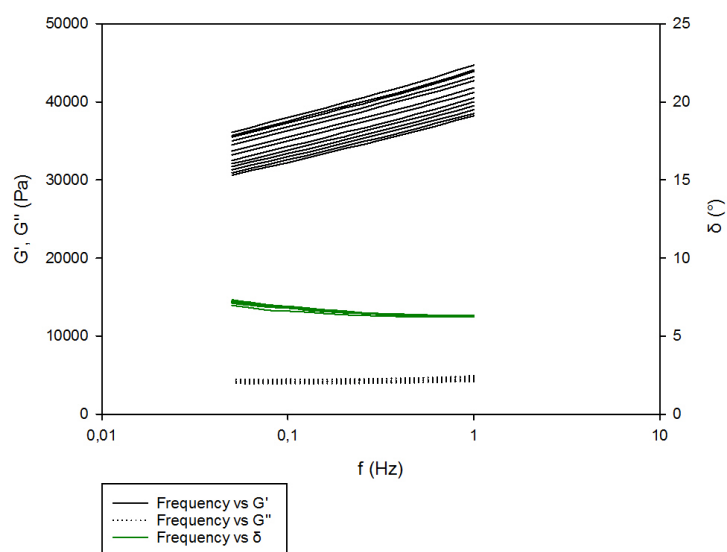
Figure C.3: Elastic modulus ( $G'$ ), viscous modulus ( $G''$ ) and phase angle ( $\delta$ ) values for 1.8 % (w/v) alginate solution gelled with  $\text{Ca}^{2+}$ -ions. (a) 1.8 % (w/v) Alginate solution ( $60 \mu\text{L}$ ) with 150 mM NaCl-solution (2mL). (b) 1.8 % (w/v) Alginate solution ( $60 \mu\text{L}$ ) with no storing solution, were collected from frequency sweeps run at  $20^\circ\text{C}$  from 1-0.05 Hz frequency at 0.1 % constant shear rate with 10 samples per. decade.

## C.4 Mechanical spectra for alginate gels in Na<sup>+</sup>-solution



(a) Alg-Na (2)

Alg: Na-solution (3)



(b) Alg-Na (3)

Figure C.4: Elastic modulus ( $G'$ ), viscous modulus ( $G''$ ) and phase angle ( $\delta$ ) values for 1.8 % (w/v) alginate solution gelled with Ca<sup>2+</sup>-ions. (a), (b) and (c): Values for 1.8 % (v/w) alginate solution gelled with CaCl<sub>2</sub> and stored with 150 mM NaCl (2mL) at 20 ° C were obtained by performing frequency sweeps from 1-0.05 Hz, at constant 0.1 % strain.

## C.5 Mechanical spectra for alginate/sulfated alginate gels in NaCl-solution

The 80/20 Alg/SA gels underwent frequency sweep to characterize the mechanical properties at each gap. The resulting  $G'$ ,  $G''$  and  $\delta$ -values were plotted against the frequency

for each gel to understand how the gels responds to the deformation applied. The results from these measurements are presented in Figure C.5.

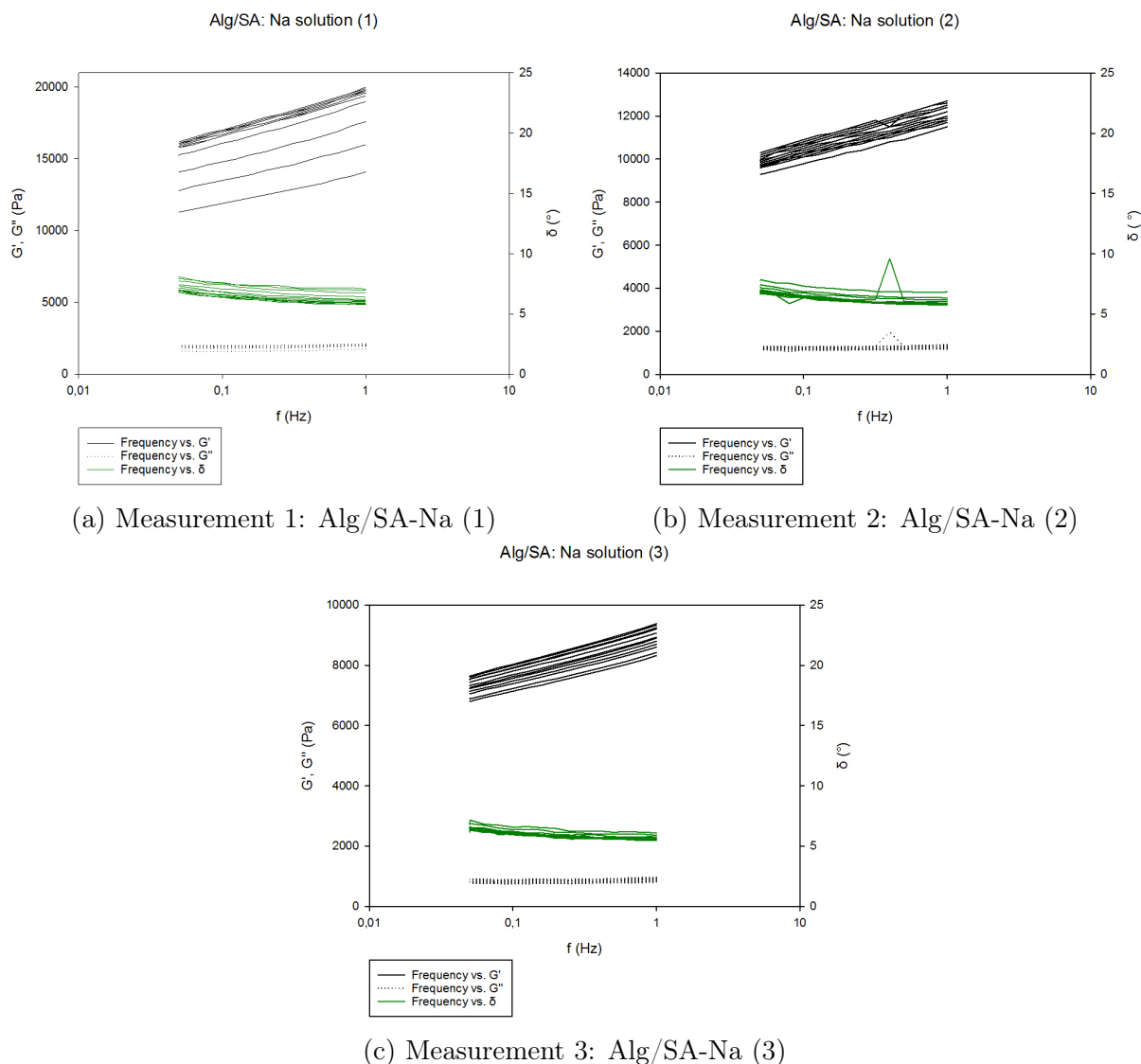
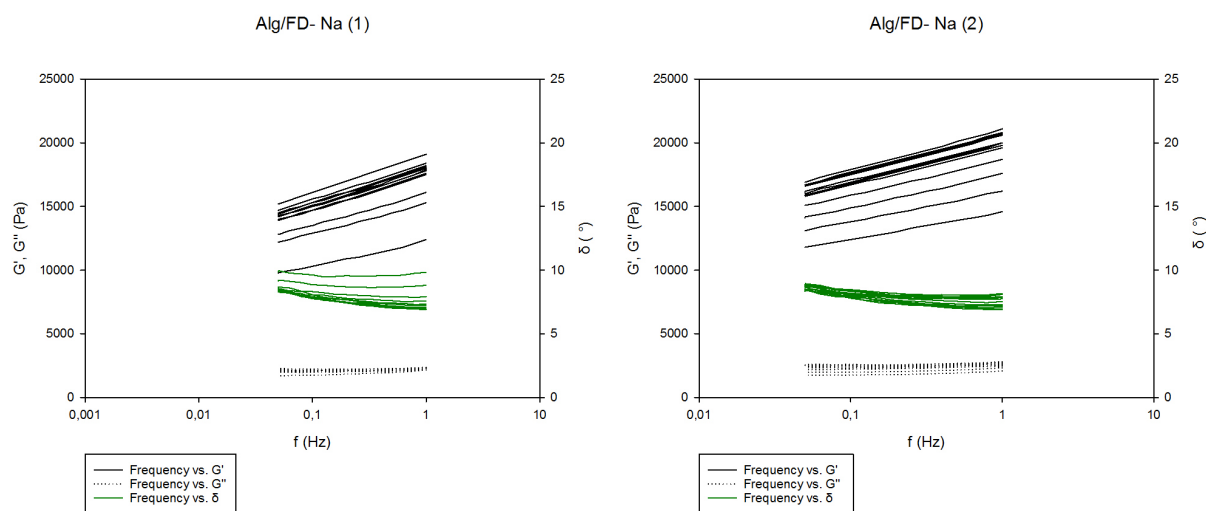


Figure C.5: Elastic modulus ( $G'$ ), viscous modulus ( $G''$ ) and phase angle ( $\delta$ ) values for 1.44 % (w/v) alginate and 0.36 % (v/w) solution gelled with  $\text{Ca}^{2+}$ -ions. (a), (b) and (c): Values for 1.8 % (v/w) alginate solution gelled with  $\text{CaCl}_2$  and stored with 150 mM NaCl (2mL) at 20 ° C were obtained by performing frequency sweeps from 1-0.05 Hz, at constant 0.1 % strain.



## C.6 Mechanical spectra for alginate/fucoidan gels in NaCl-solution

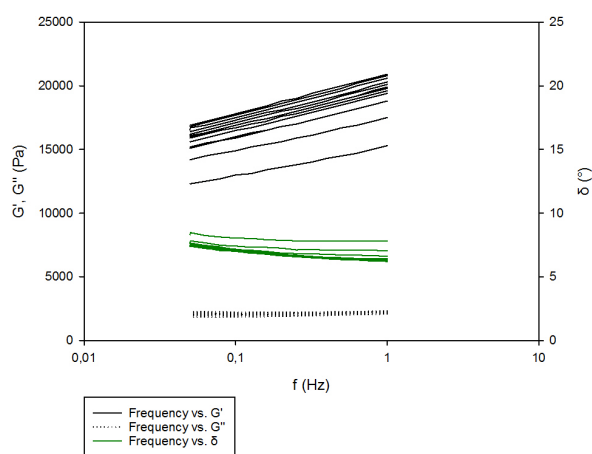
The elastic modulus ( $G'$ ), viscous modulus ( $G''$ ) and the phase angle ( $\delta$ ) were recorded at each set gap for alginate/fucoidan gels. Figure C.6 illustrates the mechanical spectra of  $G'$ ,  $G''$  and  $\delta$  plotted against logarithmically plotted frequency.



(a) Measurement 1: Alg/FD-Na (1)

(b) Measurement 2: Alg/FD-Na (2)

Alg/FD- Na (3)

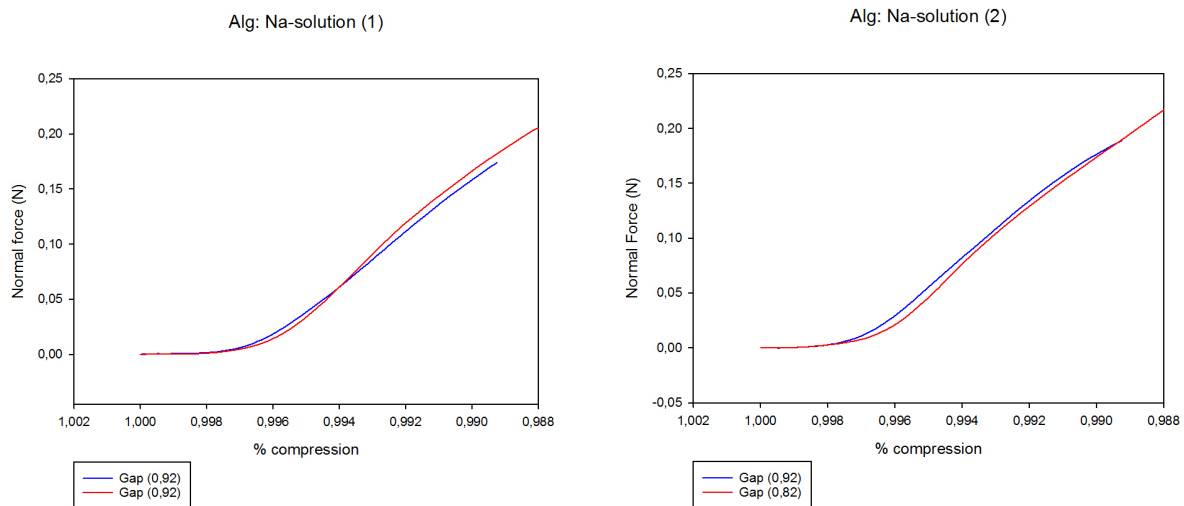


(c) Measurement 3: Alg/FD- Na(3)

Figure C.6: Elastic modulus ( $G'$ ), viscous modulus ( $G''$ ) and phase angle ( $\delta$ ) values for 1.44 % (w/v) alginate and 0.36 % (v/w) solution gelled with  $\text{Ca}^{2+}$ -ions. (a), (b) and (c): Values for 1.8 % (v/w) alginate solution gelled with  $\text{CaCl}_2$  and stored with 150 mM NaCl (2mL) at 20 ° C were obtained by performing frequency sweeps from 1-0.05 Hz, at constant 0.1 % strain.

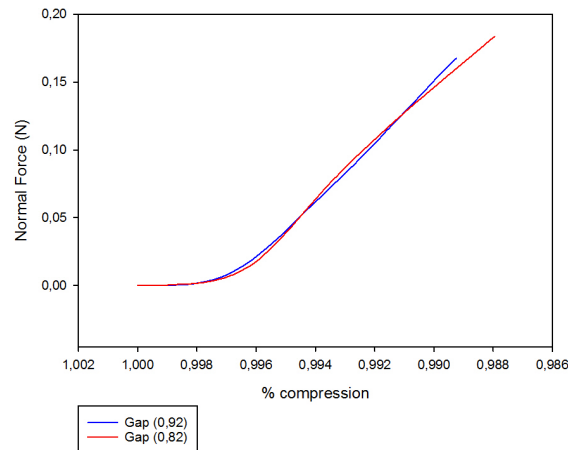
## D Microdamage in Alginate Gels Stored with NaCl-solution

Figure 4.5.5 shows that the elastic modulus is stabilizes after reaching a a plateau, this could indicate that microdamage in the gel could have occurred, as a consequence of increased compression. This was looked into by plotting the measured normal force for compression at 8 % gap redcuton and the values at 18 % gap reduction. The resulting plots are presented in Figure D.1.



(a) The change in normal force against % compression for Alg-Na (1)      (b) The change in normal force against % compression for Alg-Na (2)

Alg: Na-solution (3)



(c) The change in normal force against % compression for Alg-Na (3)

Figure D.1: Microdamage occurred in 1.8 % (w/v) alginate solution is indicated by plotting the change in normal force against % compression. The blue line is the change in normal force at 8 % compression, while the red line is at 18 % compression.

Indication of microdamage could be a observed as a reduction in normal force when the compression is increased. The normal force is expected to develop with increasing

compression. An indication of microdamage would be the normal force is not evolving. However, the resulting plots do not provide a conclusive result, therefore it is not possible to know whether this occurred or not.

## E Young's modulus

Young's modulus for each gel was calculated by determining the slope for the force/deformation curve when the gap was reduced from 0.95 mm to 0.94 mm. The slope was determined in the linear region. The stress-strain curve for Alg-Na (1h) is given in Figure E.1:

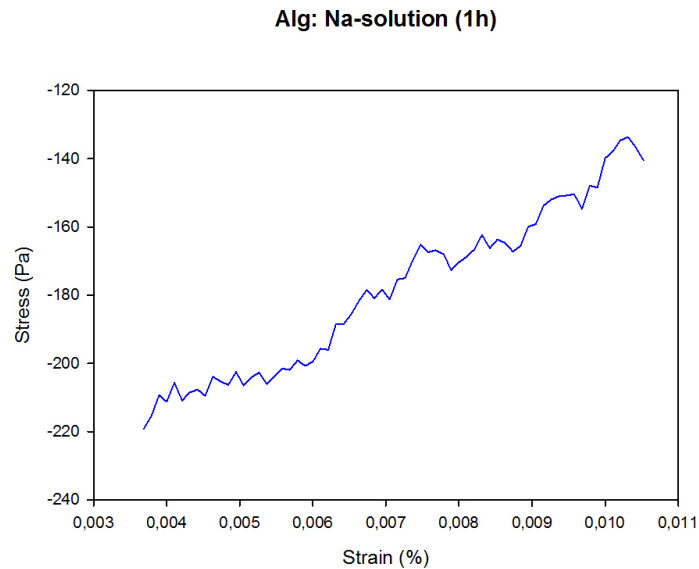


Figure E.1: Stress-strain curve for Alg-Na (1h) when the gap was reduced from 0.95 to 0.94. The stress (y-axis) is calculated by dividing the normal force/ area of the probe and is plotted against the strain (x-axis).

The stress-strain curve for Alg/SA-Na gels are given in Figure E.2.

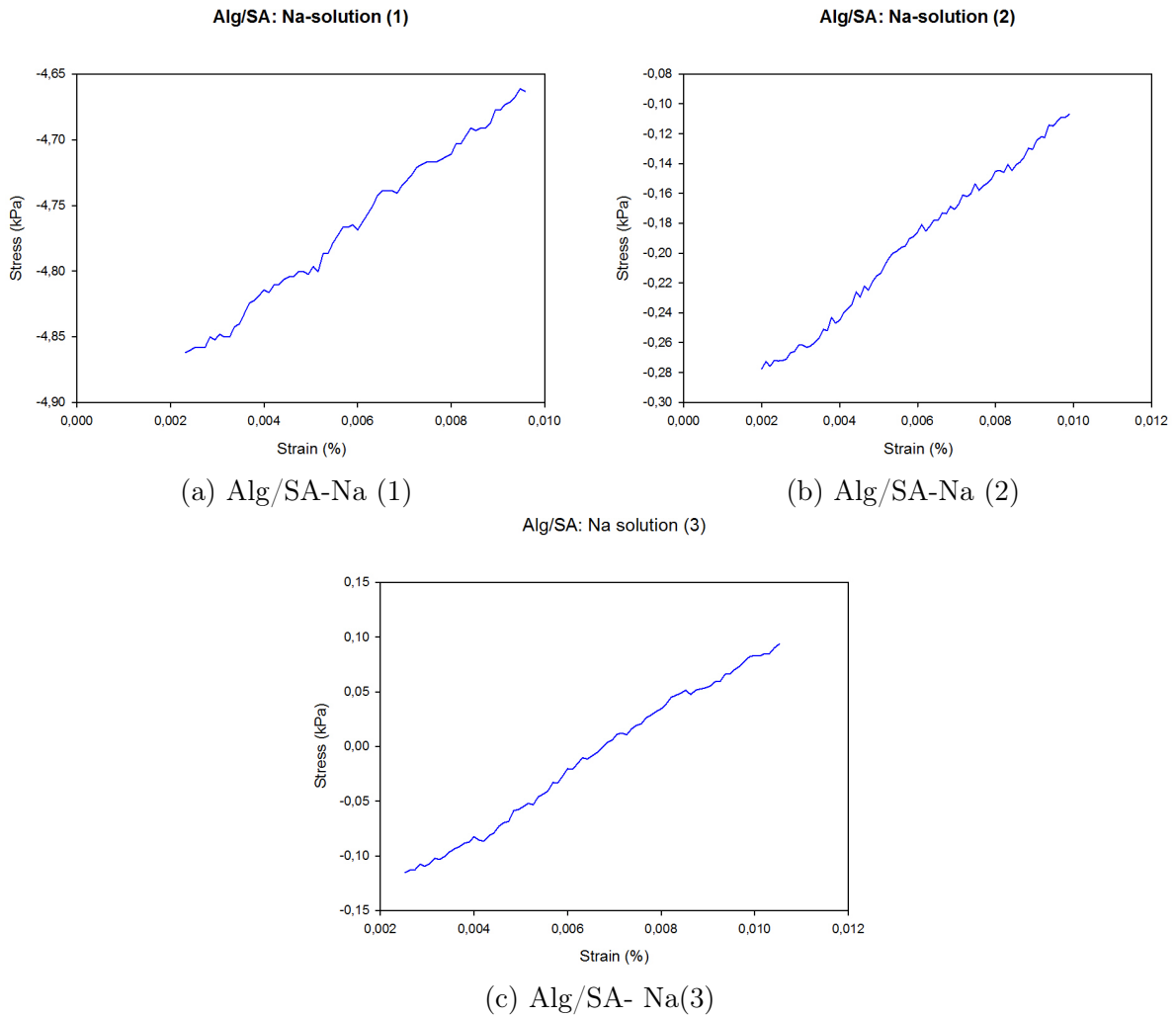


Figure E.2: Stress-strain curve for Alg/SA-Na gels when the gap was reduced from 0.95 to 0.94. The stress (y-axis) is calculated by dividing the normal force/ area of the probe and is plotted against the strain (x-axis).

The stress-strain curve for Alg/FD-Na gels are given in Figure E.3:

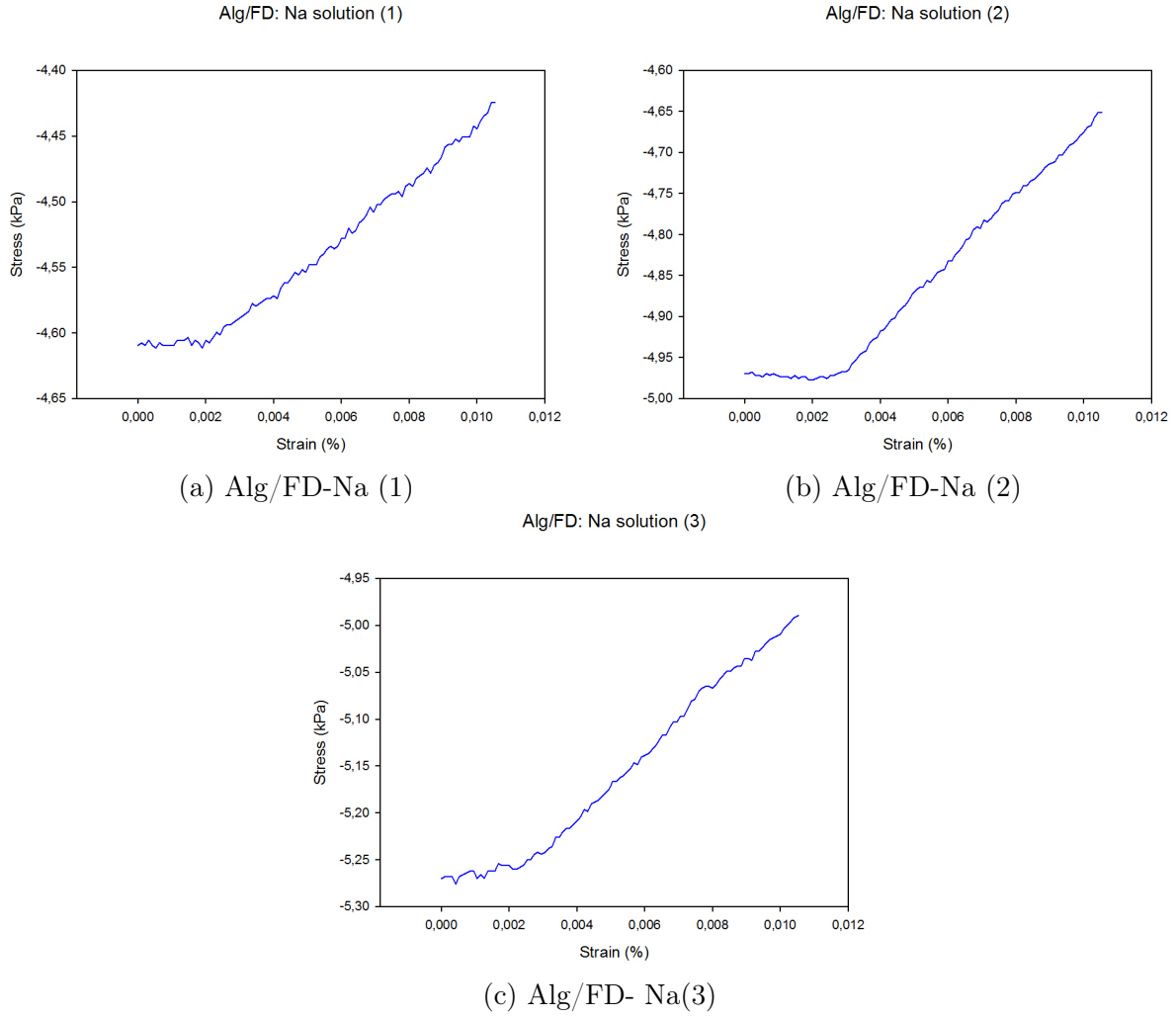


Figure E.3: Stress-strain curve for Alg/FD-Na gels when the gap was reduced from 0.95 to 0.94. The stress (y-axis) is calculated by dividing the normal force/ area of the probe and is plotted against the strain (x-axis).

The results from the linear regression for each gel is given in Table E.1:

Table E.1: Elastic modulus ( $G'$ ) obtained at 1 Hz by performing frequency sweep. In addition Young's modulus ( $E$ ) was obtained by plotting the stress-strain relationship at 5 % gap reduction.

Gel	Linear regression
Alg-Na (1h)	$11791x - 262,62$
Alg/SA-Na (1)	$28,468x - 4,934$
Alg/SA-Na (2)	$22,612x - 0,3281$
Alg/SA-Na (3)	$28,636x - 0,1968$
Alg/FD-Na (1)	$20,849x - 4,6524$
Alg/FD-Na (2)	$34,492x - 5,0328$
Alg/FD-Na (3)	$29,826x - 5,3106$

Further, the relation between storage modulus and Young's modulus can be deter-

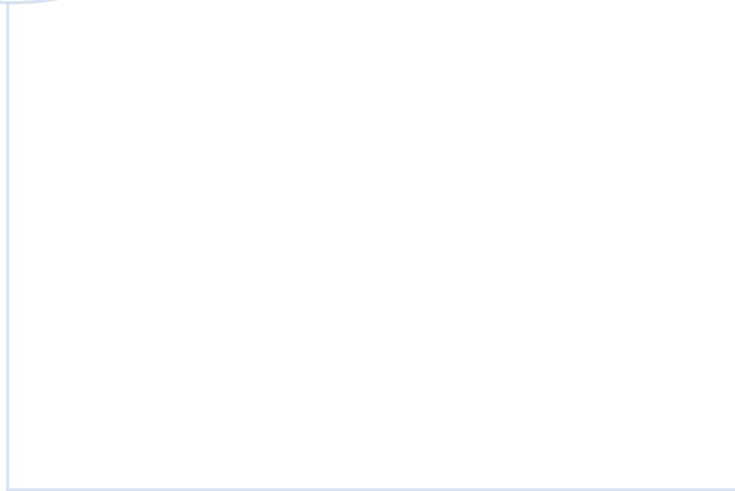
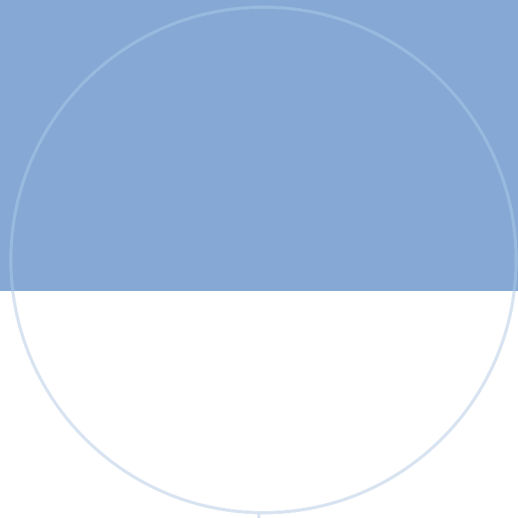
mined by equation 2 obtained from [71].

$$E = 2G(1 + \nu) \quad (2)$$

Where E is Young's modulus, G is storage modulus and  $\nu$  is the Poisson's ratio. Most hydrogels are assumed to have a Poisson's ratio of around 0.45-0.5, meaning that  $E \approx 3G$  [2]. This proportionality is only valid for ideal solid material, where compression in all three direction. The Young's modulus calculated through this relation yields the following values.

Table E.2: Elastic modulus ( $G'$ ) obtained at 1 Hz by performing frequency sweep. In addition Young's modulus (E) was obtained by plotting the stress-strain relationship at 5 % gap reduction.

Gel	E' [Pa]
Alg-Na (1h)	16323
Alg/SA-Na (1)	14907
Alg/SA-Na (2)	15108
Alg/SA-Na (3)	21327
Alg/FD-Na (1)	10113
Alg/FD-Na (2)	17292
Alg/FD-Na (3)	11421



 **NTNU**

Norwegian University of  
Science and Technology